UNIVERSITÀ
DEGLI STUDI
FIRENZE

DOTTORATO DI RICERCA IN NEUROSCIENZE

CICLO XXXVII

# Unveiling Hidden Dynamics: Neural Biomarkers for Psychiatric Disorders

Settore Scientifico Disciplinare
MED/26


Dottoranda
Dott.ssa Cinti Alessandra

Supervisore
Prof. Rossi Simone

Coordinatore
Prof.ssa Amato Maria Pia

*It is about simple awareness—awareness of what is so real and essential, so hidden in plain sight all around us, all the time, that we have to keep reminding ourselves, over and over: 'This is water. This is water'*

*DFW*

# Contents

# Abstract

This thesis delves into the neurophysiological mechanisms underlying psychiatric disorders, with a particular focus on mood disorders such as depression and bipolar disorder, as well as addictive behaviors. Through a series of studies, it explores how disruptions in brain oscillatory activity, as measured by electroencephalography (EEG), can serve as biomarkers to enhance diagnosis and inform treatment strategies.

The first study (described in Chapter 3) investigates EEG patterns in individuals with depression, highlighting disruptions in neural oscillations, particularly in the alpha and beta frequency bands. Depression is characterized by deficits in emotional regulation and cognitive processing, which are linked to an imbalance between excitatory and inhibitory (E/I) neural activity. The findings reveal that individuals with high depressive symptoms show increased beta and gamma power at baseline but, unlike healthy controls, fail to exhibit post-task increases in beta power. This lack of neural adaptability points to plasticity and energy regulation impairments, reflecting dysfunctions in key brain areas such as the prefrontal cortex and anterior cingulate cortex (ACC), essential for cognitive flexibility and emotional control.

Building on the insights from depression, the thesis also explores the effects of ketamine, a rapid-acting antidepressant, in individuals with bipolar disorder (Chapter 4). As an NMDA receptor antagonist, ketamine has shown effectiveness in alleviating depressive symptoms, particularly in cases where traditional treatments have failed. This study examines the acute neurophysiological changes induced by ketamine, using EEG to monitor shifts in brain oscillatory patterns. The results suggest ketamine's impact on neural circuits involves distinct alterations in rhythmic and arrhythmic brain activity. The study identifies endophenotypic differences, as early and late responders exhibit different EEG patterns. This suggests that neurophysiological profiles could be used to tailor ketamine treatment, optimizing dosage and duration for individual patients.

The final study (illustrated in Chapter 5) focuses on the neurocircuitry of addiction, analyzing how disruptions in dopamine signaling contribute to reward processing deficits, impulsivity, and executive dysfunction. Addiction is marked by dysregulation in dopamine receptors, particularly the D2, D3, and D4 subtypes, which play crucial roles in reward, motivation, and cognitive control. This research uses event-related spectral perturbation (ERSP) and resting-state EEG to examine theta, beta, and gamma oscillations during the Iowa Gambling Task. The results reveal significant disruptions in gamma activity and a flatter power-law exponent (PLE) in individuals with addiction, pointing to dysregulation in dopamine-driven reward circuits. These oscillatory abnormalities correlate with risky decision-making, suggesting that EEG markers could serve as reliable biomarkers for addiction.

Together, these studies illustrate the critical role of EEG in uncovering the neurophysiological underpinnings of psychiatric disorders. Across depression, bipolar disorder, and addiction, the consistent finding of disrupted neural oscillations emphasizes shared mechanisms of brain dysfunction. By identifying EEG biomarkers, this thesis offers potential diagnostic tools and paves the way for more personalized treatment strategies, ultimately advancing our understanding of brain disorders and improving clinical outcomes.

# Introduction

Mental health represents a significant public health challenge, with psychiatric disorders affecting millions of individuals worldwide. Among the most prevalent are mood disorders, such as depression and bipolar disorder, and addictive behaviors, such as substance use disorders (SUDs) and behavioral addictions. These conditions profoundly affect individuals' daily functioning and quality of life. According to the World Health Organization (*Mental Health Atlas 2020*, 2021; Moitra et al., 2022), over 280 million people worldwide suffer from depression, making it a leading cause of disability globally. Bipolar disorder affects an additional 45 million individuals, often resulting in severe functional impairment and heightened suicide risk. The burden of addictive behaviors, including SUDs and behavioral addictions such as gambling, also continues to grow, leading to devastating health and social consequences, particularly through the harmful use of alcohol and drugs, which account for millions of deaths each year (Geneva: World Health Organization, 2024).

The interplay between mood disorders and addiction complicates both diagnosis and treatment, with many individuals experiencing comorbidities. Comorbidity between mood disorders and SUDs often exacerbates symptoms and increases resistance to treatment, leading to worse outcomes (Quello et al., 2005). Understanding the neurobiological mechanisms that underlie these conditions is essential to developing effective interventions.

**Neural Dynamics and EEG Biomarkers in Psychiatry**

In recent years, advances in neuroimaging techniques, particularly electroencephalography (EEG), have deepened our understanding of the neural dynamics that underlie psychiatric disorders. With its high temporal resolution, EEG captures the brain's electrical oscillatory activity in real time, making it an invaluable tool for studying psychiatric conditions. By examining alterations in neural oscillations, researchers can identify potential biomarkers that reflect the dysregulated brain activity associated with depression, bipolar disorder, and addiction. These biomarkers hold promise for diagnosing psychiatric disorders and assessing treatment responses.

Dynamic network communication, as outlined by Voytek & Knight (2015), highlights the importance of synchronized large-scale networks for cognitive functions such as attention, memory, and emotional regulation (Voytek & Knight, 2015). In psychiatric conditions like depression and addiction, the efficient communication between these networks is disrupted and can be observed through altered EEG patterns. This framework emphasizes that healthy cognitive functions depend on flexible, well-coordinated brain networks, and disturbances in this communication might be at the core of many psychiatric symptoms.

EEG studies have revealed disruptions in neural oscillations across different frequency bands—such as delta (1-4 Hz), theta (4-8 Hz), alpha (8-12 Hz), beta (13-30 Hz), and gamma (30-100 Hz) —in individuals with psychiatric disorders. For example, individuals with depression exhibit altered prefrontal alpha asymmetry and elevated beta power (Thibodeau et al., 2006), both of which are linked to deficits in emotional regulation and cognitive processing. Similarly, surrogates of EEG analysis, as event-related potentials (ERPs), have provided insights into the timing and nature of neural responses, revealing that individuals with depression show altered P300 amplitudes associated with attentional and cognitive processing deficits (B. Hu et al., 2017).

**EEG Biomarkers in Depression**

A growing body of research supports the view that depression represents a disorder of neural plasticity, energy dysregulation, and disrupted excitatory/inhibitory (E/I) balance (Page & Coutellier, 2019). Depression is marked by disruptions in alpha and beta oscillatory patterns, contributing to cognitive rigidity and emotional dysregulation (Tian et al., 2022). This reflects broader network dysfunctions involving key brain regions such as the prefrontal cortex and anterior cingulate cortex (ACC), responsible for emotional regulation and executive function. Further, recent studies have highlighted the role of energy metabolism and synaptic plasticity in depression, pointing to dysfunctions in glutamatergic transmission and the GABAergic system (Cui et al., 2024).

Chapter 3 will explore these mechanisms by examining EEG spectral activity and phase-amplitude coupling (PAC) before and after a learning task. Individuals with high depressive symptoms exhibit increased beta and gamma power at baseline, but unlike controls, they do not show post-task increases in beta power. This lack of neural adaptability suggests plasticity and energy regulation impairments, which may stem from an inhibitory/excitatory imbalance in the brain's neural networks (Tatti et al., 2024).

Building on these findings, Chapter 4 will shift focus to the rapid-acting antidepressant effects of ketamine, an NMDA (N-Methyl-D-Aspartate) receptor antagonist, as a treatment for

depression in bipolar disorder. Here, we will provide comprehensive insights into the acute neurophysiological effects of ketamine in patients with bipolar disorder (BD) undergoing treatment for depression. The observed alterations across various rhythmic and arrhythmic components (this latter being a novel and emerging approach to the evaluation of EEG activity) of brain signals underscore the potential usefulness of EEG as a valuable tool for evaluating and monitoring the neurobiological effects of ketamine in real-world clinical settings. Additionally, the distinct responses observed between early and late responders emphasize the clinical significance of endophenotypic differences in response to psychoactive medications, reinforcing the need for further research in this area. If replicated, our findings could contribute to advancing clinical protocols for ketamine treatment by allowing for the stratification of patients based on their acute neurophysiological response to the drug. This would enable personalized treatment approaches, where ketamine therapy could be tailored to individual patient profiles, optimizing dosage and treatment duration (Agnorelli et al., 2025).

**Neurocircuitry of Addiction**

Addiction is increasingly understood as a disorder of reward processing, impulsivity, and executive dysfunction (Koob & Volkow, 2016), all of which can be measured using EEG.

The role of dopamine receptors, particularly the D2, D3, and D4 subtypes, is central to these neurophysiological changes in addiction, which significantly modulate reward, motivation, and cognitive flexibility (Missale et al., 1998). D2 and D3 receptors, primarily located in the limbic system, are key drivers of reward-seeking behaviors and impulsivity, and their dysregulation significantly contributes to addictive behaviors. In contrast, D4 receptors, predominantly found in the prefrontal cortex, regulate executive functions such as attention and cognitive flexibility, directly influencing decision-making processes in addiction (Furth et al., 2013).

D4 receptor dysregulation, in particular, has been linked to abnormal gamma oscillations, which are critical for synchronizing neural activity during cognitive tasks. Dysfunction in D4 receptors disrupts the balance between excitation and inhibition (E/I balance) in prefrontal circuits, leading to impaired neural synchronization and cognitive processing. This disruption manifests as abnormal gamma oscillations, which further exacerbate deficits in cognitive control and reward processing in individuals with addiction (FitzGerald et al., 2015; Furth et al., 2013). More recently, gamma alterations have also been described for many psychiatric conditions (Palmisano et al., 2024).

These neurophysiological abnormalities are particularly evident during tasks that require real-time decision-making under risk. Moreover, as detailed by Fitzgerald, dopamine signaling is crucial for modulating reward learning and prediction errors (Fitzgerald et al., 2015). In

individuals with addiction, altered dopamine function impairs the brain's precision in predicting rewards, which disrupts the integration of cognitive control mechanisms. This disruption, coupled with an imbalance in excitation and inhibition, is reflected in abnormal gamma activity and reduced theta power, indicating broader neural dysregulation. Such abnormalities signify cognitive dysfunction and contribute to compulsive decision-making, where individuals favor immediate gratification over long-term rewards (Ramey & Regier, 2019).

In this frame, chapter 5 will highlight the dysregulation of the reward circuit and dopamine-driven processes in individuals with addictive behaviors by using event-related spectral perturbation (ERSP) and resting-state EEG. Through the examination of theta, beta, and gamma oscillations, both pre- and post-decision, during the Iowa Gambling Task, the study uncovers disruptions in neural oscillations related to impulsivity and reward processing. Specifically, altered gamma activity and a flatter power-law exponent (PLE) may reflect dopamine dysregulation within the reward circuitry, providing potential biomarkers for risky decision-making and addiction.

To sum up, this series of papers underscores the critical role of EEG in elucidating the neurophysiological mechanisms underlying psychiatric disorders. Across depression, bipolar disorder, and addiction, the shared theme of altered brain dynamics and neural plasticity emerges, manifesting as disruptions in EEG spectral activity, phase-amplitude coupling, and event-related spectral perturbation. This body of work highlights potential diagnostic tools and avenues for personalized treatment strategies by identifying EEG biomarkers that reflect these changes, such as predicting responses to interventions like ketamine.

In conclusion, while the neurophysiological disruptions differ across conditions, the consistent findings of dysregulated neural oscillations and altered brain connectivity point to shared mechanisms of brain dysfunction in psychiatric disorders. As research continues to advance, EEG's role in identifying biomarkers for psychiatric disorders will be instrumental in developing targeted treatments that improve patient outcomes.

# Chapter 1: Mood Disorders and Addictive Behaviors - Definitions, Symptomatology, and Neurophysiology

## Mood Disorders

The *Diagnostic and Statistical Manual of Mental Disorders* (5th ed., text rev., DSM-5-TR) defines mood disorders as psychiatric conditions primarily characterized by disruptions in mood and emotional regulation (American Psychiatric Association, 2022). The two most prevalent forms of mood disorders are Major Depressive Disorder and Bipolar Disorder.

*Major Depressive Disorder (MDD)* involves persistent feelings of sadness, worthlessness, and lack of interest in daily activities, lasting for at least two weeks. According to the DSM-5, at least five symptoms must be present, including depressed mood, significant weight change, insomnia or hypersomnia, fatigue, cognitive difficulties, feelings of guilt, and recurrent thoughts of death or suicide. MDD is a leading cause of disability globally, with profound impacts on personal, social, and occupational functioning (*Mental Health Atlas 2020*, 2021).

*Bipolar Disorder (BD)* is defined by the presence of manic or hypomanic episodes, often alternating with depressive episodes. Bipolar I involves full-blown mania, which lasts for at least one week and can be severe enough to require hospitalization. Bipolar II, on the other hand, involves hypomania (less severe mania) but must also include at least one major depressive episode. Symptoms during manic episodes may include inflated self-esteem, reduced need for sleep, racing thoughts, increased talkativeness, and engagement in risky activities. BD often leads to significant disruptions in daily functioning, particularly during extreme mood swings.

## Addictive Behaviors

Addictive behaviors refer to both substance use disorders and behavioral addictions, such as Gambling Disorder and Internet Gaming Disorder, which are categorized in the DSM-5-TR. These conditions are characterized by a failure to control engagement in behaviors or substance use despite the resulting harm. Both SUDs and behavioral addictions share core features, including

impaired control, increased tolerance, withdrawal symptoms, and persistent engagement in the behavior despite negative consequences (American Psychiatric Association, 2022).

*Substance Use Disorder (SUD)* is defined by the problematic use of substances such as alcohol or drugs that leads to clinically significant impairment. The DSM-5-TR outlines criteria for SUD, which include increased tolerance, the presence of withdrawal symptoms, unsuccessful attempts to reduce substance use, and continued use despite negative consequences. These impairments often result in significant health complications, social dysfunction, and economic burden, with substances like alcohol contributing to millions of deaths annually.

Similarly, *Gambling Disorder* is included in the DSM-5-TR as a behavioral addiction. It is characterized by recurrent and persistent problematic gambling behavior leading to significant distress or impairment. Diagnostic criteria include a need to gamble with increasing amounts of money, repeated unsuccessful efforts to cut back on gambling, and continued gambling despite severe financial, social, or personal consequences. These behaviors mirror the compulsive engagement seen in SUD, particularly in how the brain's reward and impulse control systems are affected.

*Internet Gaming Disorder* is provisionally recognized in the DSM-5-TR under the category of behavioral addictions. It involves a pattern of excessive and compulsive gaming that significantly interferes with daily life. The diagnostic criteria for Internet Gaming Disorder include preoccupation with gaming, withdrawal symptoms when gaming is not possible, unsuccessful attempts to control gaming, a loss of interest in other activities, and continued gaming despite psychosocial or occupational impairment. While currently classified as a condition warranting further study, the DSM-5-TR highlights its similarity to other addictive behaviors in terms of its impact on reward circuitry and impulse control.

**Neurophysiology of Mood Disorders**

The neurophysiology of mood disorders like MDD and BD reveals distinct disruptions in brain networks and oscillatory patterns, often detectable through EEG.

MDD is characterized by abnormal patterns in brain oscillations, particularly in the alpha and beta frequency bands. Depressed individuals frequently show increased right-frontal alpha asymmetry, corresponding to hypoactivity in the left prefrontal cortex, a region associated with positive emotional states and cognitive control (Palmiero & Piccardi, 2017; Thibodeau et al., 2006). Elevated beta and gamma oscillations have also been noted, especially in the prefrontal cortex and parietal lobes, indicating increased baseline cortical arousal and impaired emotional regulation (Fingelkurts & Fingelkurts, 2015; Fitzgerald & Watson, 2018).

Disruptions in gamma oscillations may reflect impaired connectivity and coordination between brain networks, contributing to cognitive deficits and emotional dysregulation.

Bipolar Disorder, especially during manic episodes, exhibits heightened gamma activity, particularly in the prefrontal cortex and anterior cingulate cortex, areas involved in emotional regulation and decision-making (Ryu et al., 2021). During depressive episodes, BD shares similar EEG patterns with MDD, including alterations in alpha and beta oscillations, further suggesting impaired functional connectivity and neural plasticity across mood phases (Fitzgerald & Watson, 2018).

**Neurophysiology of Addictions**

Addictive behaviors, including substance use and behavioral addictions, involve profound neurophysiological changes, particularly in brain circuits associated with reward processing, impulse control, and stress regulation.

SUDs are primarily driven by changes in dopaminergic signaling within the brain's reward circuitry, specifically the basal ganglia, amygdala, and prefrontal cortex (Koob & Volkow, 2016). Chronic substance use leads to decreased dopamine D2 receptors in the striatum, resulting in reduced sensitivity to natural rewards and increased dependence on substance use for pleasure (Koob, 2013). EEG studies have demonstrated decreased P300 amplitude in the sons of alcoholic fathers during a monetary gambling task (MGT), which correlates with higher impulsiveness (Kamarajan et al., 2015). Moreover, high- and low-impulsive individuals' neural oscillatory responses during performance monitoring differ, particularly in the theta and beta bands (Barth et al., 2021).

Behavioral Addictions, such as Gambling Disorder, exhibit similar disruptions in brain networks as SUDs. Individuals with gambling addiction show decreased theta power and reduced frontal beta activity during risky decision-making tasks, indicating impairments in cognitive control and increased sensitivity to immediate rewards (Koob, 2013; Yau & Potenza, 2015). Neuroimaging studies have highlighted alterations in reward-related brain regions, such as the striatum and prefrontal cortex, which contribute to compulsive behaviors and poor decision-making (Volkow & Morales, 2015).

**Convergent Neurophysiology of Mood Disorders and Addictions**

Across both mood disorders and addictive behaviors, several neurophysiological themes emerge, indicating overlapping mechanisms of dysfunction:

*Synaptic Dysregulation and Neuroplasticity.* Both mood disorders and addictions involve long-lasting changes in synaptic plasticity, particularly in circuits related to reward processing,

cognitive control, and emotional regulation. Impaired glutamatergic and GABAergic signaling plays a central role in these disruptions, leading to altered excitatory/inhibitory (E/I) balance and reduced cognitive flexibility (Kauer & Malenka, 2007; Volkow et al., 2009). In depression, these changes manifest as rigid thought patterns and emotional dysregulation, while in addiction, they contribute to compulsive behavior and impaired decision-making (Fitzgerald & Watson, 2018a; Ramirez-Mahaluf et al., 2015). Both mood disorders and addictions are associated with altered late-stage neural responses, such as the Late Positive Potential (LPP), an ERP component reflecting sustained attention to emotional and salient stimuli. Dysregulated LPP responses suggest impairments in emotional processing and cognitive control, which are critical in mood disorders and addiction. In depression, reduced LPP amplitude correlates with difficulties in processing positive emotions (Hajcak et al., 2010), while in addiction, exaggerated LPPs are often linked to heightened sensitivity to reward cues and cravings (Luijten et al., 2016). These ERP alterations further underscore the shared neurophysiological basis of these disorders, particularly in terms of impaired regulatory mechanisms and maladaptive responses to emotional and rewarding stimuli.

*Energy Dysregulation.* In both conditions, there is evidence of metabolic dysfunction, particularly in key brain regions such as the prefrontal cortex and anterior cingulate cortex. These energy deficits, tied to mitochondrial dysfunction and impaired glucose metabolism, result in diminished neural communication and an inability to maintain neural oscillations, which are critical for normal cognitive and emotional functioning (Gu et al., 2021; M. Liu et al., 2022). Mitochondrial dysfunction, as indicated by elevated lactate levels, further exacerbates neural dysregulation, contributing to both depressive symptoms and addictive behaviors (Rezin et al., 2009; Scaglia, 2010).

*Reward Circuit Dysregulation.* Both mood disorders and addictions share a common disruption in the brain's reward system, particularly involving dopaminergic circuits in the nucleus accumbens and ventral tegmental area. In depression, this leads to anhedonia and reduced motivation (Russo & Nestler, 2013). At the same time, addiction results in hypersensitivity to substance-related cues and the compulsion to seek out immediate rewards despite negative consequences (Koob & Volkow, 2016).

This section highlights the shared neurophysiological underpinnings that link these seemingly disparate conditions. Both categories of disorders involve profound disruptions in neural plasticity, energy metabolism, and reward processing, with EEG playing a crucial role in uncovering these patterns. These insights offer potential biomarkers for treatment response and open pathways for personalized therapeutic strategies targeting the neural circuits implicated in both mood and addictive disorders. The following section will delve into EEG techniques in

greater detail, focusing on their utility in investigating the neurophysiological disruptions that underlie psychiatric conditions, from mood disorders to addictive behaviors.

Understanding the neurophysiological basis of mood disorders and addictions reveals how alterations in brain networks—ranging from synaptic plasticity to energy dysregulation—affect behavior and cognitive processes. However, to precisely capture these dynamic neural changes, non-invasive neuroimaging techniques like EEG offer valuable insights. EEG has proven especially powerful in identifying distinct oscillatory patterns that correspond to the neural dysfunctions observed in both depression and addiction. These real-time recordings of electrical activity enable researchers to delve deeper into the neural circuits involved in psychiatric conditions, providing crucial biomarkers for diagnosis, treatment response, and understanding the neuroplastic changes in the brain.

# Chapter 2: EEG in Psychiatric Research

**EEG as a Neuroimaging Tool**

Electroencephalography (EEG) is a noninvasive method for capturing the brain's electrical activity, providing invaluable insights into the neural mechanisms underlying psychiatric disorders. EEG measures voltage fluctuations produced by the synchronized activity of neural populations, particularly within the dendrites of pyramidal neurons. These signals reveal oscillatory activity across various frequency bands, each linked to different cognitive and emotional processes (Buzsáki et al., 2012).

The real-time nature of EEG, with the millisecond-level temporal resolution, allows researchers to capture fast neural responses, which is particularly valuable when studying disorders like depression and addiction. While EEG's spatial resolution is lower than other methods like fMRI, its ability to track brain dynamics during tasks or resting states compensates for this limitation. EEG analysis techniques like Power Spectral Density, event-related spectral perturbation (ERSP), and functional connectivity have deepened our understanding of how psychiatric conditions manifest as abnormalities in brain function.

**Spectral Power Analysis: Rhythmic Dynamics**

Spectral power analysis breaks down EEG signals into different frequency bands, each representing specific neural processes. In psychiatric disorders, deviations in these oscillations often reveal pathophysiological mechanisms:

Theta (4-8 Hz) and alpha (8-13 Hz) band oscillations are strongly tied to cognitive control and emotional regulation. For instance, depression is frequently characterized by alpha asymmetry, where increased right-frontal alpha power (linked to decreased activity) correlates with depressive symptoms, such as lack of motivation and emotional withdrawal (Thibodeau et al., 2006). Reduced theta power, particularly in the prefrontal cortex, reflects deficits in cognitive control, often observed during decision-making tasks (Cavanagh et al., 2010; Cooper et al., 2019).

Beta oscillations are often linked to sensorimotor functions and cognitive processing, and heightened baseline beta power in depression suggests impaired neuroplasticity and energy dysregulation (Fingelkurts & Fingelkurts, 2015). Similarly, gamma oscillations, critical for higher cognitive functions, are often dysregulated in both depression and addiction, indicating disrupted connectivity and impaired cognitive flexibility. (Fitzgerald & Watson, 2018; Palmisano et al., 2024)

The alterations in EEG metrics, such as decreased theta power and elevated beta and gamma oscillations, reflect the broader dysfunctions in network communication (Voytek & Knight, 2015). These disruptions impede the brain's ability to integrate information across regions involved in emotional and cognitive processing, contributing to the symptoms observed in mood disorders and addiction.

Studies examining the spectral power of individuals with depression often highlight an overabundance of beta power at rest, particularly over the frontal and parietal regions, which may suggest an energy imbalance, as reported by Gandal (2012) in schizophrenia disorder (Gandal et al., 2012; Newson & Thiagarajan, 2019; Olbrich & Arns, 2013). On the other hand, individuals with addictive behaviors exhibit reduced alpha and theta power during cognitive tasks, particularly those involving reward anticipation and decision-making, as seen in studies using gambling tasks. (Kamarajan et al., 2015; Mas-Herrero et al., 2015)

EEG oscillations are a direct reflection of rhythmic neural activity, and the analysis of these oscillations across different frequency bands has provided valuable insights into the neurophysiological underpinnings of psychiatric disorders. EEG rhythms are categorized into five main frequency bands, each associated with distinct cognitive functions and neurophysiological processes: delta, theta, alpha, beta, and gamma (Buzsáki et al., 2012).

*Delta rhythms* (1-4 Hz) are typically associated with deep sleep and some cognitive functions, particularly in states of reduced consciousness, such as under anesthesia or during non-REM (rapid eye movement) sleep. However, in mood disorders, increased delta power can indicate dysfunction in emotion regulation circuits, especially in MDD (Olbrich et al., 2015). This abnormal enhancement in slow-wave activity has been linked to deficits in emotional and cognitive processing, reflecting a reduced capacity for mental flexibility.

*Theta rhythms* (4-8 Hz) are closely linked to cognitive control and memory processes. Theta oscillations are predominantly generated in the hippocampus, with the prefrontal cortex playing a key role in modulating decision-making and executive functions. In depression, a reduction in theta power has been associated with impairments in cognitive control and executive dysfunction (Arns et al., 2015). Meanwhile, in addictive behaviors, deficits in prefrontal theta

oscillations have been observed during decision-making tasks, reflecting poor impulse control and risk assessment (Cavanagh & Shackman, 2015).

*Alpha rhythms* (8-12 Hz) are typically observed in states of resting wakefulness and are particularly pronounced in occipital regions when the eyes are closed. Alpha oscillations reflect cortical idling and are suppressed during cognitive tasks that require attention. In mood disorders, reduced alpha power is often found in frontal regions, reflecting increased cortical activation and emotional distress (Fingelkurts & Fingelkurts, 2015).

*Beta rhythms* (13-30 Hz) are generally associated with motor control, attention, and cognitive processing. Abnormal beta power has been consistently observed in psychiatric populations. In depression, increased frontal beta power has been associated with rumination and cognitive inflexibility, reflecting an overactive prefrontal cortex struggling to regulate emotions (Fitzgerald & Watson, 2018). In contrast, in addiction, beta oscillations are often dysregulated during tasks involving risk-taking and decision-making, indicating impairments in self-control and cognitive flexibility (Schmidt et al., 2019).

Gamma rhythms (30-100 Hz) are critical for higher-order cognitive functions, such as attention, working memory, and decision-making. In MDD, decreased gamma activity has been observed, particularly in regions associated with emotional regulation and cognitive control, such as the prefrontal cortex (Fitzgerald & Watson, 2018). In individuals with addiction, aberrant gamma oscillations have been linked to impulsivity and reward processing deficits, especially in tasks that involve risky choices (HajiHosseini et al., 2012).

By examining these frequency-specific oscillatory patterns, EEG spectral power analysis provides a window into the functional dysregulation present in psychiatric disorders. The differences in rhythmic oscillations between healthy individuals and those with depression or addiction highlight key disruptions in the brain's ability to synchronize and coordinate neural networks, further supporting the use of these EEG metrics as biomarkers for diagnosis and treatment evaluation.

**Spectral Power Analysis: Arhythmic Dynamics**

In addition to oscillatory activity, arrhythmic or non-rhythmic dynamics also play a crucial role in understanding brain function in psychiatric disorders. The arrhythmic component of EEG signals, evident in the scale-free (or fractal) properties of brain activity, reflects neural processes that do not adhere to a specific oscillatory frequency band but instead follow a 1/f power law relationship (E. J. He et al., 2008). Often regarded as background noise, these dynamics represent

essential brain activity functional properties related to cortical excitability and large-scale network coordination.

The scale-free (or fractal) component, characterized by a $1/f^{\beta}$ power-law relationship, is a key indicator of non-rhythmic activity. This descending linear trend in the log-log plot of EEG power vs. frequency reflects the self-organized criticality of brain networks (Beggs & Plenz, 2003). The balance between rhythmic and arrhythmic components is vital for maintaining healthy neural communication, and disruptions in this balance have been linked to psychiatric conditions like depression and addiction (Lendner et al., 2020).

Interestingly, it was shown that the PLE correlates with the subjective sense of selfhood, as measured via the self-consciousness scale. Muthukumaraswamy and Liley demonstrated that the PLE of the resting-state EEG signal is sensitive to various pharmacological manipulations, including ketamine (Wolff et al., 2019). In particular, sub-anesthetic doses of ketamine were shown to decrease the PLE exponent at frequencies between 5 and 100 Hz and decrease the PLE at lower frequencies in EEG recordings of non-human primates and healthy subjects (Muthukumaraswamy & Liley, 2018). To date, the relationship of the effect of ketamine on the $1/f^{\beta}$ power-law relationship with the subjective effects of the drug and therapeutic response in patients has not been investigated.

*Fractal dynamics in depression*: Individuals with depression often exhibit an altered PLE, which reflects deviations in their scale-free brain activity. A flatter slope of the $1/f^{\beta}$ power-law relationship has been observed in individuals with MDD, particularly in front-central regions, which may indicate heightened neural noise and impaired network efficiency (B. J. He, 2011a; M. Liu et al., 2022). This increased neural noise could result from dysregulated excitatory/inhibitory (E/I) balance, leading to inefficient signal transmission and reduced cognitive flexibility.

*Fractal dynamics in addiction:* Fractal dynamics in addiction remain largely unexplored, though a scale-free systems theory has been proposed. This theory suggests that addictive behaviors stem from dysregulation in hierarchical, scale-free neural systems governing motivation. Disruptions across multiple levels—from synaptic to behavioral—lead to impaired decision-making and compulsive behaviors. The model integrates neurobiological, psychological, and systems theory findings to explain how motivation and addiction are linked across various scales of brain function (Chambers et al., 2007a; Jones et al., 2023).

By understanding both rhythmic and arrhythmic components of EEG, researchers can gain a more comprehensive view of how brain networks function—and dysfunction—in psychiatric disorders. These findings emphasize the importance of focusing on specific frequency bands and considering the broader, scale-free dynamics that govern neural activity(B. J. He, 2011).

**Brain Signal Complexity**

Beyond rhythmic oscillations, non-linear brain dynamics and the complexity of neural signals offer critical insights into how brain function is disrupted in psychiatric conditions. Complexity refers to the variability and unpredictability of the brain's electrical signals, and it is considered a measure of the brain's capacity for processing information and adapting to environmental changes.

Lempel-Ziv complexity (LZc) is a commonly used measure of signal diversity, assessing how easily a signal can be compressed. The more diverse the signal, the greater the complexity. Increased LZc values indicate higher signal diversity, while lower values suggest a more predictable and less complex signal (M. M. Schartner et al., 2017). Studies have shown that LZc is significantly reduced in individuals with depression, reflecting cognitive inflexibility and rigidity in mental processes. These findings align with the idea that depression is characterized by a loss of neural variability, contributing to impaired emotional and cognitive responses.

The use of LZc has been increasingly incorporated into various pharmaco-EEG studies, including those involving ketamine and classic psychedelic drugs (M. M. Schartner et al., 2017). According to the "entropic brain hypothesis," the entropy of spontaneous brain activity reflects the informational richness of conscious states. This hypothesis is grounded in evidence showing reduced spontaneous brain complexity in states of reduced consciousness and increased complexity in altered states of consciousness induced by psychedelic drugs, correlating with the intensity of the subjective experience (Carhart-Harris, 2018).

A few studies have shown Increased EEG spontaneous signal complexity measured via LZc upon sub-anesthetic ketamine administration in healthy subjects (Farnes et al., 2020, 2020; D. Li & Mashour, 2019; M. M. Schartner et al., 2017). Notably, the intensity of the subjective experience induced by ketamine was found to correlate with LZc, particularly in relation to features such as of ego dissolution, complex imagery, elementary imagery, experience of unity, and anxiety. It is interesting to note that ketamine-induced increases in complexity appear to be limited to spontaneous EEG, with complexity following perturbation using transcranial magnetic brain stimulation (TMS) being unchanged (Farnes et al., 2020). Additionally, TMS-EEG evoked signal complexity was not reduced under ketamine anesthesia either, exhibiting a pattern close to wakefulness. Participants in this state reported long, vivid dreams unrelated to the external environment (Sarasso et al., 2015). Conversely, alternating low and high spontaneous complexity levels were observed during ketamine-induced anesthesia, stabilizing upon recovery [(D. Li & Mashour, 2019)]. Since evoked complexity metrics measure the general capacity of the brain to

sustain consciousness, these results suggest that ketamine mainly alters the content rather than the structuring of conscious experience (Casali et al., 2013). Regarding the effects of sub-anesthetic ketamine on LZc in depression and its relationship with treatment outcome, a recent study in a cohort of late-life treatment-resistant depression found that ketamine increased LZc. However, this increase did not correlate with antidepressant response (Murphy et al., 2023). While some evidence exists on the effects of sub-anesthetic doses of ketamine on brain signal complexity in healthy subjects, the characterization of such dynamics in the patient population is very limited. Also, the relationship of non-linear dynamics with subjective effects and therapeutic response to ketamine has not been investigated.

**Event-Related Spectral Perturbation (ERSP)**

Event-Related Spectral Perturbation (ERSP) provides insight into how brain oscillations change over time in response to tasks or stimuli. ERSP measures fluctuations in the power of different frequency bands during task engagement, reflecting how brain networks synchronize or desynchronize in response to cognitive demands (Delorme & Makeig, 2004)

ERSP has been widely applied in studies of decision-making and reward-related tasks, such as the Iowa Gambling Task (IGT) and the Balloon Analogue Risk Task (BART). In healthy subjects, ERSP analyses have shown reduced pre-choice theta and gamma power, which reflects cognitive control, and increased post-decision beta and gamma power, indicating sensitivity to reward or feedback (Cavanagh et al., 2010; Mas-Herrero et al., 2015).

ERSP's ability to track real-time changes in brain oscillations during cognitive tasks allows researchers to track dynamic changes in neural oscillations at specific moments during cognitive tasks. This temporal specificity enables ERSP to capture how different frequency bands of brain activity correspond to distinct behavioral events, such as decision-making or feedback processing, offering real-time insight into how the brain responds and adapts to various stimuli. ERSP bridges the gap between underlying brain activity and observable behavior with high temporal accuracy by aligning these neural responses with specific task phases.

**Functional Connectivity Measures**

Functional connectivity examines the interactions between different brain regions, offering insights into how these regions synchronize during cognitive processes. Phase-amplitude coupling (PAC), a key measure of functional connectivity, investigates how the phase of slower oscillations (like theta) modulates the amplitude of faster ones (like gamma), providing clues to the coordination of neural networks.

*PAC in Depression:* Phase-amplitude coupling is an important metric for studying MDD. Research shows that theta-gamma coupling in the prefrontal cortex is often disrupted in individuals with depression, reflecting failures in the integration of cognitive control and emotional regulation processes (Zhang et al., 2023). Elevated or diminished PAC can signal difficulties in shifting between cognitive states, which are central features of depression (Young et al., 2024). Studies suggest that PAC could serve as a biomarker for diagnosing and assessing the severity of depression, especially in treatment-resistant cases (X. Liu et al., 2022).

PAC analysis helps reveal how brain communication and coordination disruptions contribute to the cognitive and behavioral deficits observed in psychiatric disorders, making it a powerful tool for identifying neural biomarkers and therapeutic targets.

In conclusion, the critical neurophysiological mechanisms underpinning psychiatric disorders, focusing on mood disorders and addictive behaviors, have been outlined through the lens of EEG biomarkers and insights into neural oscillations, synaptic plasticity, and reward-processing circuitry. The common thread linking these disorders is the disruption of dynamic network communication, which underpins cognitive, emotional, and decision-making processes (Voytek & Knight, 2015). These shared neural dynamics are pivotal in understanding the mechanisms of psychiatric disorders and potential treatment strategies. The next chapters will delve into these topics in more detail.

In Chapter 3, we delve into the neural mechanisms of depression by examining EEG spectral activity and PAC before and after a learning task. Individuals with high depressive symptoms display increased beta and gamma power at baseline, yet unlike controls, they do not show post-task increases in beta power. This suggests impairments in neural plasticity and energy regulation, likely due to an excitatory/inhibitory imbalance in neural networks (Tatti et al., 2024).

Building on this, Chapter 4 shifts focus to the rapid-acting antidepressant effects of ketamine in treating depression within bipolar disorder. We provide insights into the acute neurophysiological effects of ketamine, highlighting EEG (and its non-rhythmic features) as a valuable tool for monitoring these effects in clinical settings. Differences in rhythmic and arrhythmic brain activity between early and late responders to ketamine underscore the importance of patient-specific neurophysiological profiles in treatment response. These findings, if replicated, could lead to personalized ketamine therapies, where treatment is tailored based on neurophysiological markers (Agnorelli et al., 2025).

Chapter 5 expands this exploration to individuals with addictive behaviors, focusing on the dysregulation of the reward circuitry and dopamine-driven processes. Using event-related spectral perturbation (ERSP) and resting-state EEG during the Iowa Gambling Task, we investigate theta, beta, and gamma oscillations pre- and post-decision. The findings reveal disruptions in neural oscillations linked to impulsivity and reward processing, with altered gamma activity and a flatter PLE suggesting dopamine dysregulation within the reward network. Together, these chapters highlight shared neurophysiological disruptions across mood disorders and addiction, offering potential biomarkers for more personalized interventions.

These chapters will provide a more detailed analysis of how EEG metrics can serve as valuable biomarkers for understanding the neurophysiological mechanisms behind these psychiatric disorders, ultimately aiding in the development of personalized treatment strategies.

# Chapter 3: Resting-State EEG Alterations of Practice-Related Spectral Activity and Connectivity Patterns in Depression

## Introduction

Depression and anxiety represent major mental health concerns, with their prevalence showing upward trends mostly in young subjects (Agyapong-Opoku et al., 2023; Grineski et al., 2024). Although clinical diagnosis remains the purview of mental health professionals, several approaches and instruments have been used to identify biomarkers and predictors of depression as well as its response to therapies. Electroencephalography (EEG) recorded at rest is a particularly cost-effective and widely accessible method for functional brain imaging. Power analysis of EEG frequency bands in individuals with depression can yield insightful results by disclosing alterations that occur in specific bands, and that may be associated with neural mechanisms underlying depressive symptoms. Notably, a debated EEG correlate of major depression is the frontal asymmetry in the alpha range, that is, the unequal activation of the two hemispheres (Thibodeau et al., 2006) often associated with altered emotional processing and regulation. Moreover, different degrees and patterns of alterations in beta (Fingelkurts & Fingelkurts, 2015) and gamma (Fitzgerald & Watson, 2018) bands have been reported in depression.

A series of works now supports the hypothesis that depression can be described as a network disorder with particular emphasis on metabolic regulation, synaptic plasticity, and excitatory/inhibitory balance (Gu et al., 2021; Z. Li et al., 2021; Ramirez-Mahaluf et al., 2017). In this respect, there is accumulating evidence that depression is characterized by (i) an imbalance of excitation and inhibition processes (Y.-T. Hu et al., 2023; Narayan et al., 2022; Sarawagi et al., 2021), (ii) plasticity alterations (Fuchs et al., 2004; B. Liu et al., 2017; W. Liu et al., 2017), and (iii) dysregulation of energy mechanisms (Gu et al., 2021), a dysfunction that has direct effects on both excitation/inhibition balance and plasticity. The impaired energy balance in depression has been substantiated by findings of brain lactate increases in these patients (Drevets, 2002; Pizzagalli, 2011) and by the fact that lactate increases are coupled with mitochondrial dysfunction (Raza et

al., 2015; Scaglia, 2010b; Stork & Renshaw, 2005; Tobe, 2013). Direct evidence of elevated lactate levels in depressed patients has been reported in the ventricular CSF (Bradley et al., 2016; Shungu et al., 2012) and the anterior cingulate (Ernst et al., 2017) using magnetic resonance spectroscopy (MRS). However, MRS's limited availability and high costs preclude its use for extended studies and clinical application in depression.

Recent evidence suggests that the EEG beta frequency band may have a metabolic meaning, as its power magnitude directly correlates with high levels of cerebral lactate concentration (Grønli et al., 2016)(Ghilardi et al., 2021) as well as with the energy mechanisms involved in long-term potentiation (LTP) processes. Indeed, we found in normal subjects that local levels of beta power during resting wake increase immediately after a visuomotor learning task over the areas previously involved in the learning activity (Nelson et al., 2021). Importantly, such beta power increases vanish after either quiet wake or sleep (Nelson et al., 2021; Tatti et al., 2020), in agreement with the animal findings of lactate concentration decreases during quiet wake (Grønli et al., 2016). Further support for the association between energy dysregulation and beta power comes from studies in patients with Parkinson's disease, showing that the levels of beta power are greater than in normal controls and do not increase with practice in a motor adaptation task (Nelson et al., 2017). Parkinson's disease is a disorder that often presents with depressive symptomatology and is characterized by impaired LTP processes and energy dysregulation (Chahine et al., 2021; Hang & Lim, 2020; Kempster & Perju-Dumbrava, 2021), similarly to depression. Therefore, we hypothesize that the EEG during resting states will show greater beta power in subjects with depression than normal controls and display significant increases in beta power following practice of a task in controls but not in subjects with depression.

In this study, we took advantage of a publicly available dataset of EEG recorded during quiet wake in two groups of college students, one with normal Beck Depression Inventory (BDI) (Beck et al., 2011) scores and the other with high BDI scores (Cavanagh et al., 2011, 2019).

The BDI comprises 21 items, each rated on a 4-point scale, with higher scores reflecting greater severity of depressive symptoms. The total score ranges from 0 to 63, where a score below 10 indicates no depression, 11–16 suggests mild depression, 17–20 indicates borderline clinical depression, 21–30 represents moderate depression, 31–40 corresponds to severe depression, and scores above 40 signify extreme depression. We analyzed the EEG recordings collected before and after performance in a probabilistic learning task.

## Materials and Methods

### *Subjects, Task, and Experimental Design*

The dataset used for this study was retrieved from the open-access data archive OpenNeuro (https://openneuro.org/datasets/ds003478/versions/1.1.0, accessed on 3 March 2023) and included clinical data and raw resting EEG recordings from 122 college students (Cavanagh et al., 2011, 2019). Participants were recruited based on a mass survey with BDI (Beck et al., 1961) conducted at the University of Arizona. General criteria to enter the study were: (i) age between 18 and 25 years; (ii) no history of seizures or head trauma; and (iii) no current use of medications with psychoactive effects. Before the experimental procedure, subjects were clinically reassessed with the electronic mini-international neuropsychological interview and were classified as belonging to one of two groups. Participants without a history of major depressive disorders, BDI scores < 7 at both the initial and subsequent assessments, and without symptoms suggesting an Axis I disorder were included in the control group (CTL, N = 75, mean age: 19 ± 1.21; 40 women). Individuals with high BDI scores (>13) at the two testing points were included in the high BDI (hBDI) group (N = 46, mean age: 19 ± 1.14, 34 women). In addition to BDI, all participants completed the Spielberger Trait Anxiety Inventory (TAI) (Spielberger, 1983) and the Behavioral Inhibition Scale/Behavioral Activation Scale (BIS/BAS), a measure of reward and punishment reactivity (Carver & White, 1994). The STAI (State-Trait Anxiety Inventory) by Spielberger (1983) consists of 40 items, each rated on a 4-point Likert scale, designed to measure both state anxiety (items 1–20) and trait anxiety (items 21–40). Higher scores indicate greater levels of anxiety, with the total score ranging from 20 to 80. In this study, only the Trait Anxiety Inventory (TAI) was administered and analyzed. The BIS/BAS scales comprise 24 items rated on a 4-point scale, assessing individual sensitivity to punishment (BIS) and reward (BAS). Higher BIS scores reflect greater sensitivity to negative outcomes, while higher BAS scores indicate stronger responsiveness to reward. The BAS is further divided into three subscales: Reward Responsiveness, Drive, and Fun Seeking, with higher scores on these subscales indicating greater tendencies toward these specific behavioral aspects.

EEG recordings were acquired at rest before and after a probabilistic learning task (Cavanagh et al., 2011, 2019). Cavanagh and colleagues fully describe the probabilistic learning task (Cavanagh et al., 2011, 2019). After the baseline EEG recording, participants completed two runs of a compulsory choice probabilistic learning task training and a testing phase (Frank et al., 2004). During the training, three pairs of Japanese Hiragana characters were displayed; each pair of stimuli was linked to a probability of receiving a “Correct” or “Incorrect” feedback of 80/20%, 70/30%, or 60/40%. Each presentation lasted from 4300 to 4700 ms, and the stimuli

disappeared upon the participant's response. Feedback was provided 50 to 100 ms after the response during this training phase but not during the test. During the test phase, all possible combinations of stimuli pairs were presented eight times for a total of 120 trials.

As reported by Cavanagh and colleagues (Cavanagh et al., 2011, 2019), the local IRB approved the project and the consent forms. Each participant provided written informed consent before entering the study.

### *EEG Data Acquisition and Preprocessing*

Scalp EEG recordings were recorded for 6 min (3 min eyes open, EO, and 3 min eyes closed) using a Synamps2 system with 64 Ag/AgCl electrodes (band-pass filter: 0.5–100 Hz, sampling rate: 500 Hz, impedances < 10 kΩ). The online reference was a single electrode placed between Cz and CPz) (Cavanagh et al., 2011). EEG recordings were performed before and after the training and testing of probabilistic tasks. After downloading the publicly available raw data, we preprocessed the EEG signal only for the eyes open condition using the public MATLAB toolbox EEGLAB (version 2022) (Delorme & Makeig, 2004). The continuous EEG signal was filtered using a finite impulse response (FIR) filter from 1 to 90 Hz and notch filtered from 56 to 64 Hz to remove power line noise (*pop_eegfiltnew*). The signal was then visually inspected to remove channels with poor signal quality. Independent component analysis (ICA) was run using the Infomax algorithm to identify eye blinks and horizontal eye movements, high-frequency muscular activity, heartbeat, and other periodic EEG artifacts (*pop_runica*). Component rejection was performed automatically using the EEGLAB toolbox IC Label, which automatically provides a proportion (in %) of independent components identified in EEG data that are classified into specific categories based on their characteristics (Pion-Tonachini et al., 2019). Components labeled as Muscle (50–100%), Eye (80–100%), Heart (80–100%), and Line noise (80–100%) were rejected from the signal, resulting in an average of 36 ± 13.32 components kept per subject. Electrodes with bad signal quality were reconstructed using spherical spline interpolation (*pop_eeg_interp*), and the signal was re-referenced on the average channel activity (*pop_reref*). Subsequent analyses were carried out using custom data analysis scripts using the MATLAB-based Fieldtrip Toolbox (version 20220104) (Oostenveld et al., 2011).

### *Spectral Current Density Analyses*

The preprocessed data was transformed by applying the Fieldtrip current source density (CSD) algorithm (*ft_scalpcurrentdensity*) to estimate the current flow underlying an EEG topography and reduce the impact of volume conduction on scalp-recorded data. After spatial filtering, the spectral profile for both the pre-task and post-task activity was estimated via fast-

Fourier transform (multi-taper FFT with Hanning window) (from 1 to 90 Hz, 0.5 Hz bins, *ft_freqanalysis*). In addition to the "original" spectral power, we determined the distinct contributions of the oscillatory and fractal components. We thus decomposed the signal using irregular-resampled auto-spectral analysis (IRASA) (Wen & Liu, 2016). This technique allows for the analysis of the "fractal background" (i.e., 1/f distribution of a time series) that reflects the background overall brain activity without specific rhythmic patterns. For the "original", fractal, and oscillatory signals, statistical analyses were conducted on the theta (4–8 Hz), alpha (8.5–13 Hz), beta (13.5–25.5 Hz), gamma (30–90 Hz), low gamma (30–55 Hz), and high gamma (65–90 Hz) frequency ranges. We further parametrized the fractal, scale-free, and signal components by computing the power-law exponent (PLE). For each participant, the fractal component was thus transformed in log-log coordinates, and the distribution slope was computed for each channel using the MATLAB linear regression function *fitlm*, resulting in a single beta coefficient per channel.

***Phase–Amplitude Coupling***

In addition to the analysis of brain oscillatory activity and the distinct contributions of periodic and scale-free signals, we explored differences in functional connectivity to better understand how low-frequency and high-frequency oscillatory activity coordinate information processing in the brain. We first analyzed phase–amplitude coupling (PAC) between the phase of theta and the amplitudes of beta and gamma oscillations (*ft_crossfrequencyanalysis*) and computed the modulation index (MI) (Tort et al., 2010). The selected bandwidth for both beta (11.5 Hz, ranging from 13.5 to 25 Hz) and gamma amplitude estimation (50 Hz, ranging from 30 to 80 Hz) exceeds the highest frequency within the theta phase band (4–8 Hz). This ensures a robust detection of PAC according to the criteria that the amplitude bandwidth should at least match the peak phase frequency. PAC estimation first involved filtering the signal using a two-way Butterworth filter and then its Hilbert transformation. As described by Tort and colleagues (Tort et al., 2010), we assessed PAC by dividing the phase (0–360°) into 18 segments and calculating the average amplitude for each segment, adjusted by the mean amplitude across all segments. As displayed in the formula below, the MI is derived by contrasting the observed amplitude-phase distribution (P) with a theoretical uniform PAC distribution (Q) using the Kullback–Leibler distance (D) grounded in the principles of Shannon's entropy.

$$MI = D(P, Q)/log\ (Nbins)$$

PAC values were computed individually for each subject, trial, and channel, and subsequently averaged to derive a single Modulation Index (MI) value per amplitude and phase for each channel.

### *Statistical Analyses*

#### *Clinical Measures*

We used the following clinical outcome measures: BDI scores, including its anhedonia and melancholia subscales; STAI scores; BIS scores with the reward, fun-seeking, and drive subscales; and BAS scores. Differences between the hBDI and CTL groups were assessed with non-parametric independent samples using Mann–Whitney tests. Spearman correlation analyses were used to explore possible relationships between clinical scores, demographic variables, and EEG-derived measures. Finally, logistic regression analysis was performed to investigate whether BIS/BAS domains could serve as predictors of depressive symptomatology.

#### *Task Performance Accuracy*

We obtained the task performance data from the first author of the original studies (Cavanagh et al., 2011, 2019). We averaged the mean accuracy for the two runs of the training and test phases to check for group differences with Mann–Whitney tests. Spearman correlation analyses were run for task accuracy and changes in resting-state EEG activity.

#### *Spectral Current Density*

We first examined pre-task resting-state EEG activity to identify baseline differences between the two groups. Then, we conducted a similar comparison of post-task activity between the two groups. Finally, we investigated the impact of probabilistic learning practice on post-task activity in the two groups separately (post-task vs. pre-task). In all cases, we assessed whether significant differences were present from the original, periodic, and fractal components of the signal.

Statistical analyses on the original (or mixed) spectral power, the oscillatory, the scale-free components, and the extracted PLE values were computed using the non-parametric Monte Carlo-based permutation procedure as implemented in Fieldtrip (Maris & Oostenveld, 2007). At the first level of analysis, the null hypothesis that the two groups are equal (hBDI vs. CTL, independent *t*-test) was tested using a critical alpha of 0.05 and a minimum number of two neighboring electrodes to form a cluster. The second-level cluster-level statistic was computed using the sum of the t values within each cluster of electrodes. The maximum statistical value from the cluster-level analysis was finally compared using the Monte Carlo method with a distribution of maximum cluster values obtained after 10,000 permutations.

*Phase–Amplitude Coupling*

Differences in theta–beta MI and theta–gamma MI strength between the hBDI and CTL groups, as well as changes with learning practice, were assessed using non-parametric cluster-based permutation testing (10,000 permutations, alpha = 0.05). As for the spectral analyses, initial comparisons were made between pre-task MI values across the two groups. Then, practice-related changes in functional connectivity (post vs. pre-task) within each group were evaluated, and subsequent comparisons examined post-task changes between the two groups.

## Results

Age and test scores for the two groups are summarized in Table 1. As noted in the Methods, the hBDI group, which included a higher percentage of women (34 women out of 46 participants, 74%) than the CTL group (40 out of 75, 54%), had greater scores for BDI, TAI, and BIS. No significant group differences were observed for all BAS scores. We found no difference between men and women for all the clinical test scores.

| | **CTL** **Mean (SD)** | **hBDI** **Mean (SD)** | ***U*** | ***p*-value** |
|---|---|---|---|---|
| Age (yrs) | 18.97 (1.22) | 18.74 (1.14) | 1.30 | 0.25 |
| BDI | **1.73 (1.65)** | **22.22 (4.9)** | **85.90** | **<0.001*** ** |
| TAI | **31.05 (5.49)** | **55.76 (7.08)** | **83.49** | **<0.001*** ** |
| BIS | **19.44 (3.05)** | **22.72 (3.07)** | **26.38** | **<0.001*** ** |
| BAStot | 40.45 (4.94) | 39.17 (5.68) | 1.07 | 0.30 |
| BASrew | 17.67 (1.71) | 17.13 (2.15) | 1.52 | 0.22 |
| BASfun | 11.88 (2.17) | 11.52 (2.93) | 0.07 | 0.79 |
| BASdrv | 10.89 (2.15) | 10.52 (2.79) | 0.03 | 0.86 |

*Table 1. Mean of age and scores of neuropsychological tests of the control (CTL) and depressed (hBDI) groups. In parentheses, we report the standard deviation (SD). The values of U Mann-Whitney tests comparing the two groups are reported with p-values. Significant group differences are reported in bold. (BDI: Beck Depression Inventory; TAI: Trait Anxiety Inventory; BIS: Behavioral Inhibition System; BAS: Behavioral Activation System; BAStot: BAS total score; BASrew: BAS reward score; BASfun: BAS fun-seeking score; BASdrv: BAS drive score). Asterisks refer to significance level.*

BDI scores displayed a very strong positive correlation with TAI ($\rho = 0.83$, $p < 0.001$; confidence intervals (CI): 0.87, 0.75) and a moderate correlation with BIS scores ($\rho = 0.49$, $p < 0.001$; CI: 0.63, 0.32). TAI scores positively correlated with BIS scores ($\rho = 0.61$, $p < 0.001$; CI: 0.71, 0.48) and, to a lesser extent, negatively correlated with BAS scores ($\rho = -0.18$, $p = 0.047$; CI: −0.00083, −0.35).

Logistic regression analysis showed that the BIS score was a good predictor of acute depressive symptomatology ($X^2 = 27.51$, $p < 0.001$; Wald stat = 20.24, $p < 0.001$; AUC = 0.77;

Accuracy = 0.75; Sensitivity = 0.56; Specificity = 0.87), with greater sensitivity when the analysis was restricted to women (CTL: N = 39; hBDI: N = 33; $X^2$ = 18.65, $p$ < 0.001; $W$= 13.49, $p$ = 0.0002; AUC = 0.77; Accuracy = 0.74; Sensitivity = 0.70; Specificity = 0.77).

***At Baseline, hBDI Displays Greater Beta and Gamma Oscillatory Activity than CTL***

We first analyzed the EEG collected at baseline before the probabilistic learning task. Cluster-based permutation statistics on the "original" spectral activity highlighted significant differences between the two groups in both beta and gamma frequency ranges (Figure 1, first column, see also Supplementary Figures S1 and S2A). Specifically, compared to the CTL, the hBDI group displayed greater beta power in a cluster of electrodes located over the frontal region (Cluster $t$ = 25.81, $p$ = 0.028) and greater gamma power in two clusters, one over the central midline (Cluster $t$ = 23.70, $p$ = 0.021) and the other one over the occipital region (Cluster $t$ = 21.14, $p$ = 0.023). No significant group differences were observed for the other frequency ranges. Analyses of the individual beta and gamma frequency peaks in the significant clusters were similar in the two groups (beta, hBDI: 16.53 ± 3.51 Hz, CTL: 16.84 ± 3.30 Hz; $W$ = 1753, $p$ = 0.45; gamma, hBDI: 31.98 ± 5.53 Hz, CTL: 32.83 ± 7.89 Hz, $W$ = 1823, $p$ = 0.23), suggesting that the greater beta and gamma activity we found in hBDI is not due to a shift in frequency peaks.

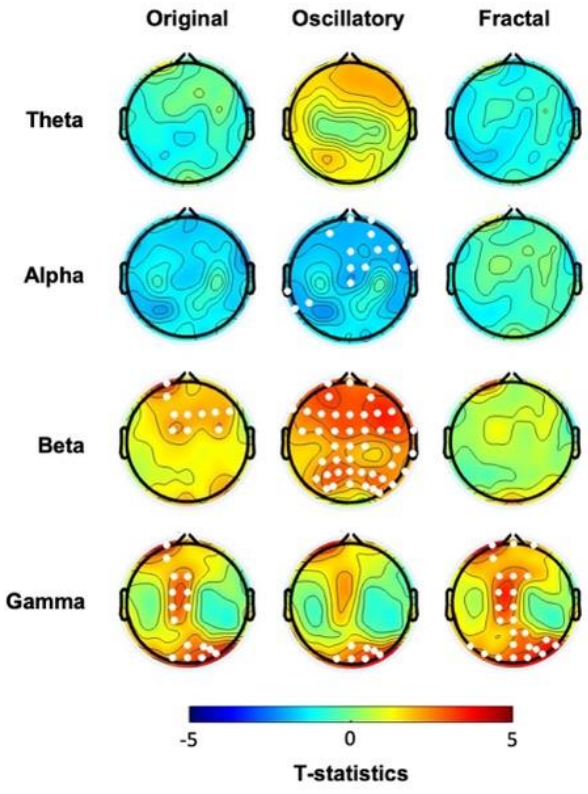

*Figure 1. Scalp topographies displaying the t-values for group comparisons (hBDI vs. CLT) before the task, at baseline for the original, oscillatory, and fractal components for each frequency band. White dots indicate electrodes with significant group differences after cluster correction for multiple comparisons.*

We then focused on the two EEG components obtained with IRASA. The analysis of the pure oscillatory component isolated from the fractal (Figure 1, second column, see also Supplementary Figures S1 and S2B) confirmed greater beta oscillatory activity over fronto-parietal areas in the hBDI group (Cluster $t$ = 125.41, $p$ = 0.004), as well as greater gamma activity over the right parieto-occipital region (Cluster $t$ = 19.98, $p$ = 0.023). Furthermore, the hBDI group displayed lower alpha activity in a cluster of electrodes over the right frontal (Cluster $t$= −27.76, $p$ = 0.016) and left temporal (Cluster 2: $t$ = −6.31, $p$ = 0.040) scalp regions.

Regarding the fractal component, group differences were found only in the gamma range (Cluster $t$ = 74.22, $p$ = 0.003), with greater values for the hBDI group in midline and parieto-occipital electrodes (Figure 1, third column, see also Supplementary Figures S1 and S2C). Cluster-based analysis of the PLE index highlighted a significant group difference bilaterally over the parieto-occipital area (Cluster $t$ = 24.18, $p$ = 0.03), with hBDI having a reduced slope compared to the CTL (Figure 2A).

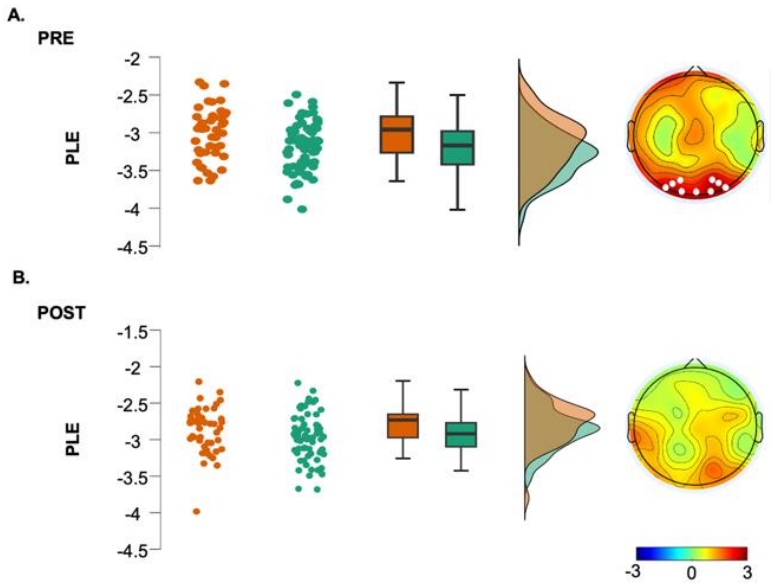


*Figure 2. EEG Power-Law Exponent (PLE) for the hBDI group (orange) and CTL group (green) before (A) and after task (B), with individual data points, box plots, and density plots to visualize data distribution. Topographic plots depict the t-values of cluster-based permutation statistics (right). Electrodes within significant clusters are represented as white dots.*

In summary, we found that the baseline EEG of the hBDI group was characterized by greater activity in the high-frequency ranges (beta and gamma) than the CTL's, mostly over fronto-parietal regions, with minor discrepancies between the original oscillatory, pure oscillatory, and fractal components. We did not find any significant correlation between original, oscillatory, and fractal components and the clinical measures for each of the two groups.

### *The hBDI Group Displayed Greater Theta-Beta and Theta-Gamma PAC*

We then analyzed PAC for theta–beta and theta–gamma by extracting the corresponding MI in the baseline EEG recordings. Non-parametric permutation analyses demonstrated increased theta–beta coupling mostly over a centro-parietal cluster ($t$ = 23.16; $p$ = 0.0175) (Figure 3A, first line) and greater theta–gamma coupling over the right occipital areas ($t$ = 10.12; $p$ = 0.048) in the hBDI group compared to the CTL group (Figure 3B, first line).

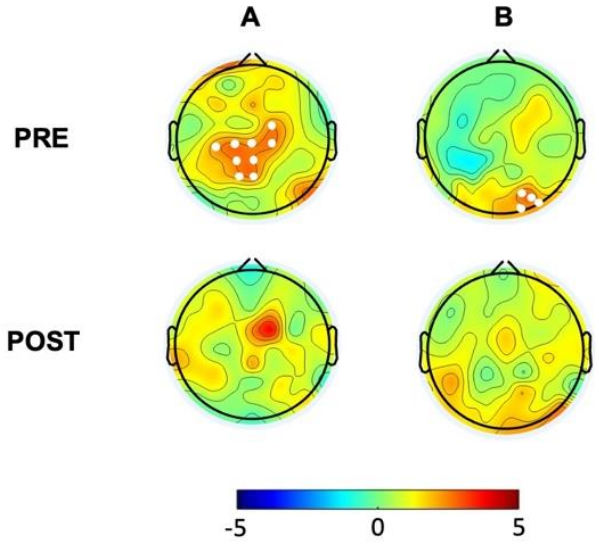


*Figure 3. Group differences (hBDI vs. CTL) for theta–beta (A) and theta–gamma (B) PAC. Topographic plots depict the results of cluster-based permutation t-statistics. In the top line, PRE represents the group comparison at baseline before task performance. POST (bottom line) refers to group comparison after the task execution. White dots represent electrodes within significant clusters.*

### *EEG Activity at Rest Changes after One-Hour Task Practice*

After the baseline EEG, all subjects underwent two blocks of training and testing in a probabilistic learning task. The performance of the two groups was similar in both the training (CTL: mean ± SD: 68 + 9%; hBDI: 68 ± 10%; Mann-Whitney $U$ = 1755, $p$ = 0.87) and the test (CTL: 65 ± 9%; hBDI: 67 ± 10%; $U$ = 1776, $p$ = 0.79).

Cluster-based analysis of the "original" spectral activity following the task revealed lower power values in the low-frequency ranges, i.e., theta and alpha in hBDI compared to CTL (Figure 4, first column, see also Supplementary Figures S3 and S4A). The post-task result differs from the pre-task finding of local increases in the hBDI group for the higher frequency ranges, i.e., beta and gamma (see Figure 1, first column). Specifically, in the post-task recordings, compared to CTL, the hBDI group showed less theta range activity over a centro-parietal region (Cluster $t$ = −12.87, $p$ = 0.028) and in alpha range in a cluster of electrodes over the frontal region (Cluster $t$ = −16.72, $p$ = 0.025) (Figure 4, first column). There was no group difference for the peak frequency of theta

(CTL: 5.82 ± 1.48 Hz; hBDI: 5.83 ± 1.44 Hz; $W$ = 1568, $p$ = 0.863) and alpha (CTL: 9.98 ± 1.01 Hz; hBDI: 10.33 ± 1.18Hz; $W$ = 1288, $p$ = 0.077) for the electrodes included in the clusters.

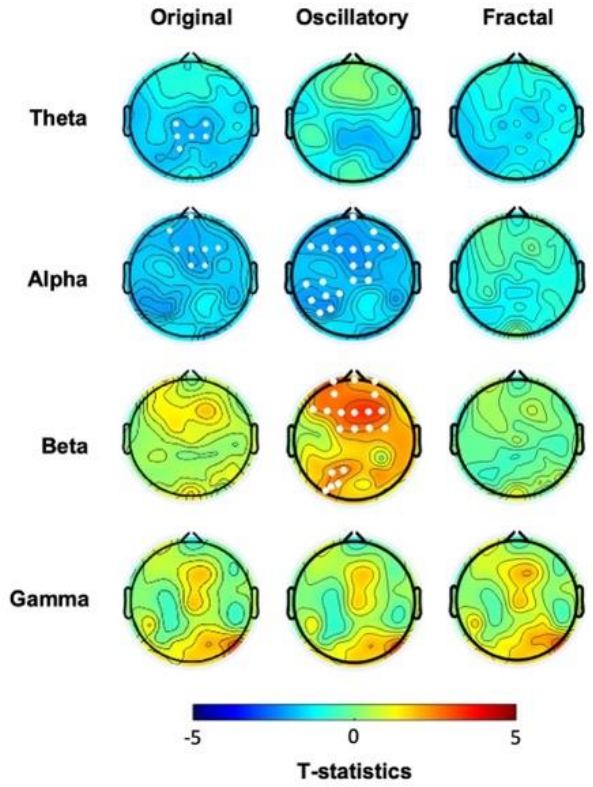


*Figure 4. Scalp topographical t-maps of group comparisons (hBDI vs. CLT) in the post-task resting-state EEG for the original, oscillatory, and fractal components. White dots indicate electrodes with significant group differences after cluster correction for multiple comparisons.*

We then ascertained whether this change of pattern was present for the oscillatory and fractal components in the post-task recordings. While we found no significant group differences for the fractal component (Figure 4, third column, see also Supplementary Figures S3C and S4C) or for the PLE (Figure 2B), the analysis of the oscillatory component confirmed that the hBDI group showed lower alpha power in a cluster of electrodes over the frontal region extending to the left parietal area (Cluster $t$ = −46.49, $p$ = 0.014) (Figure 4, second column, see also Supplementary Figures S3 and S4B). Nevertheless, the hBDI group showed greater beta power in electrodes over the frontal region (Cluster $t$ = 40.28, $p$ = 0.017) and, to a smaller extent, over the left parieto-occipital area (Cluster $t$ = 12.53, $p$ = 0.0497) (Figure 4, second column).

Altogether, the analyses of the post-task original and the pure oscillatory components produced results diverging from the pre-task findings in terms of group differences. Specifically, for the original oscillatory component, visual inspection of the pre- and post-task group differences (Figures 1 and 4, see Table 2) suggests that task practice generated a more substantial power increase in the CTL than the hBDI group for all frequencies. For the pure oscillatory

component, the group difference for the beta range fell in the post-task EEG in terms of both power amplitude and cluster magnitude (first columns of both Figures 1 and 4) with the opposite effect for alpha frequency. Together with the absence of group differences in the gamma range in the post-task recordings, these findings support the hypothesis that, despite similar performance accuracy, the task activity induced different patterns of oscillatory changes in the two groups. To verify this hypothesis, we thus searched for post-pre task EEG changes in each of the two groups separately.

| | **Pre-task: hBDI > CTL** | **Post-task: hBDI > CTL** |
|---|---|---|
| Theta | ORIG: *none*<br>OSCIL: *none*<br>FRACT: *none* | **ORIG:** *centro-parietal*<br>OSCIL: *none*<br>FRACT: *none* |
| Alpha | ORIG: *none*<br>**OSCIL:** *R frontal & L temporal*<br>FRACT: *none* | **ORIG:** *frontal*<br>**OSCIL:** *from frontal to L parietal*<br>FRACT: *none* |
| Beta | **ORIG:** *frontal*<br>**OSCIL:** *fronto-parietal*<br>FRACT: *none* | **ORIG:** *frontal*<br>**OSCIL:** *fronto-parietal*<br>FRACT: *none* |
| Gamma | **ORIG**: *central midline & occipital*<br>**OSCIL**: *R parieto-occipital*<br>**FRACT**: *midline & parieto-occipital* | **ORIG**: *central midline & occipital*<br>**OSCIL**: *R parieto-occipital*<br>FRACT: *none* |

*Table 2. Summary of group differences (hBDI > CLT) of the original (ORIG), pure oscillatory (OSCIL), and fractal (FRACT) activity for theta (4–8 Hz), alpha (8.5–13 Hz), beta (13.5–25.5 Hz), and gamma (30–90 Hz) before (Pre-task) and after (Post-task) the learning task. In red, we report results where the hBDI group exhibited significantly greater activity than CTL. In blue, we report results where CTL displayed significant activity. "None" refers to no significant group differences. R = right; L = left.*

Cluster-based analyses of the original spectral activity in the CTL group confirmed that significant post-pre task increases occurred in all frequency ranges (Figure 5A, first column). Specifically, we found increased activity in (i) theta band: in two clusters of electrodes over frontal (Cluster $t$ = 59.375, $p$ = 0.003) and occipital areas (Cluster $t$ = 50.32, $p$ = 0.003); (ii) alpha band: in two clusters over the frontal (Cluster $t$ = 64.04, $p$ = 0.003) and right parietal areas (Cluster $t$ = 19.44, $p$ = 0.017); (iii) beta band: in a cluster of electrodes extending from the prefrontal to the occipital areas (Cluster $t$ = 95.83, $p$ = 0.0005); and (iv) gamma band: in two clusters over frontal (Cluster $t$ = 45.63, $p$ = 0.0006) and occipital areas (Cluster $t$ = −65.73, $p$ = 0.0004).

The same comparison in the hBDI group displayed a different pattern with increases that affected only the theta and gamma ranges (Figure 5B, first column). Indeed, following the task, increased oscillatory was present for theta in a cluster of electrodes over the frontal region

(Cluster $t$ = 15.30, $p$ = 0.019) and a smaller one over the occipital region (Cluster $t$ = 7.70, $p$ = 0.050) and for gamma in two clusters over the centro-parietal areas (right: Cluster $t$ = 11.22, $p$ = 0.023; left: Cluster $t$ = 18.076, $p$ = 0.010).

Post-pre task comparison of the pure oscillatory component (Figure 5A, second column) showed that, following task practice, the CTL group exhibited increased alpha activity in two clusters of electrodes, one over the frontal area (Cluster $t$ = 28.38, $p$ = 0.015) and the other over the right parieto-occipital region (Cluster $t$ = 13.50, $p$ = 0.034). Increased power was also found in the beta range over the central region (Cluster $t$ = 13.20, $p$ = 0.026) and in the gamma range in two clusters of electrodes, one over the frontal area (Cluster $t$ = 39.73, $p$ = 0.0006) and the other over the occipital region (Cluster $t$ = 49.28, $p$ = 0.0006). The same analyses performed in the hBDI group (Figure 5B, second column) revealed a different pattern of changes. Following the task, beta power decreased in a cluster of electrodes over the right parieto-occipital region (Cluster $t$ = −20.87, $p$ = 0.003) and gamma power increased in two clusters of electrodes over the fronto-centro-temporal areas (left: Cluster $t$ = 15.68, $p$ = 0.014; right: Cluster $t$ = 12.92, $p$ = 0.018).

For the fractal component, compared to pre-task EEG, CTL post-task recordings demonstrated a general power increase for all frequency ranges in almost all electrodes (Figure 5A, third column). Namely, increases were found in a big cluster involving most of the electrodes for theta (Cluster $t$ = 130.57, $p$ = 0.00001), alpha (Cluster $t$ = 148.82, $p$ = 0.00001), and gamma (Cluster $t$ = 142.28, $p$ = 0.00001), with beta power increasing in both a frontal (Cluster $t$ = 72.91, $p$ = 0.0024) and an occipital (Cluster $t$ = 66.98, $p$ = 0.0026) cluster. A significant post-pre difference in the PLE was found for all electrodes (Cluster $t$ = 267.79, $p$ < 0.0001). Post-task increases of the fractal component were less evident in the hBDI group (Figure 5B, third column) and did not involve the beta range. Theta increases were present in two small clusters of electrodes, one over the frontal area (Cluster t= 24.88, $p$ = 0.00001) and another over the left occipital area (Cluster $t$ = 8.32; $p$ = 0.042); Alpha power increased in a small right frontal cluster (Cluster $t$ = 14.56, $p$ = 0.026) and gamma over the left centro-parietal area (Cluster $t$ = 14.74, $p$ = 0.014) and the right fronto-central (Cluster $t$ = 11.40, $p$ = 0.024) region. As for the CTL group, PLE increased significantly for all electrodes (Cluster $t$ = 218.57, $p$ < 0.0001).

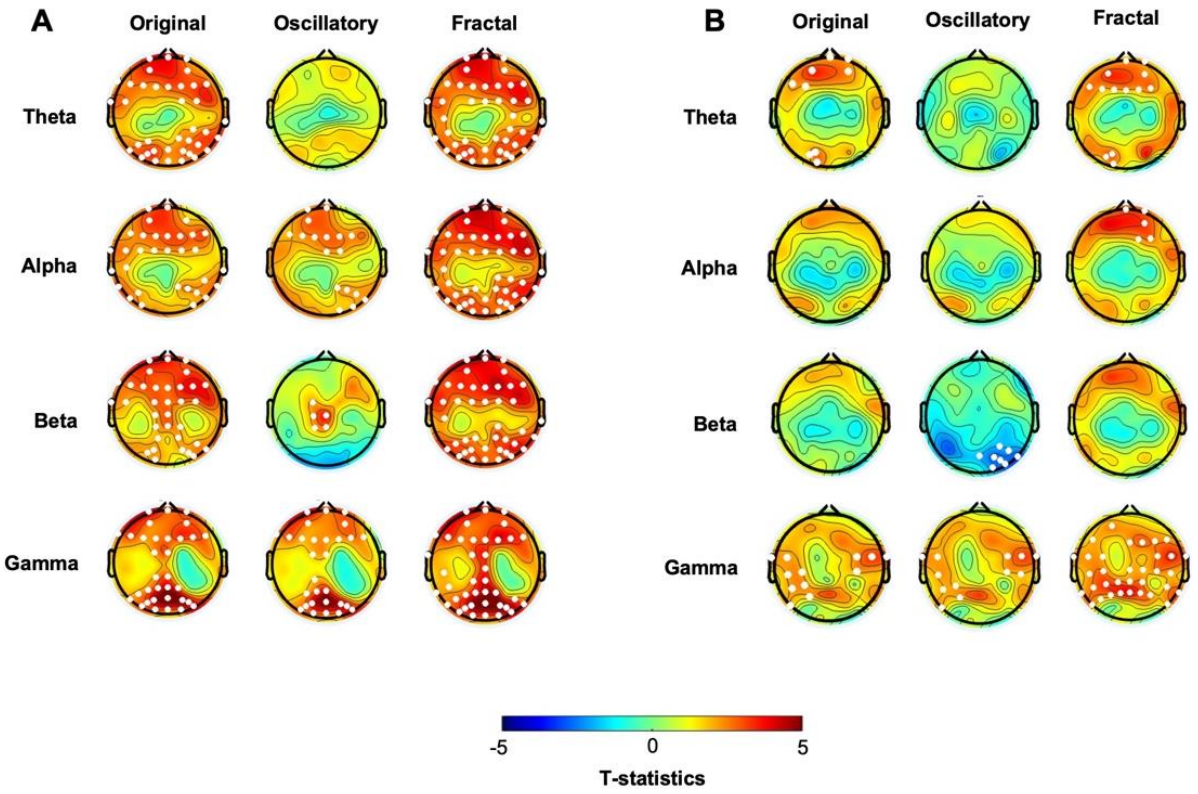


*Figure 5. Scalp topographical t-values maps for post-pre task comparisons (post-task vs. pre-task EEG) in the CTL (A) and hBDI (B) groups. Results for the original, oscillatory, and fractal components are presented for each frequency band. White dots indicate electrodes with significant group differences after cluster correction for multiple comparisons.*

In summary, the separate comparisons of the post-task and pre-task recordings in each group (Table 3) confirmed that practice in a probabilistic learning task induced a different pattern of EEG changes in both the CTL and hBDI, even though the two groups performed the task with similar accuracy. These last analyses highlighted that post-task changes involved increases in all frequency ranges for the CTL group but not for the hBDI group. Indeed, beta power increase was found only in CTL, while the hBDI displayed either no changes or even some power decrements of the pure oscillatory component.

| | **CTL: Post-task > Pre-task** | **hBDI: Post-task > Pre-task** |
|---|---|---|
| Theta | **ORIG:** *frontal & occipital*<br>OSCIL: *none*<br>**FRACT**: *most all electrodes* | **ORIG:** *frontal & occipital*<br>OSCIL: *none*<br>**FRACT**: *frontal & occipital* |
| Alpha | **ORIG:** *frontal & R parietal*<br>**OSCIL:** *frontal & R occipital*<br>**FRACT**: *most all electrodes* | ORIG: *none*<br>OSCIL: *none*<br>**FRACT**: *frontal* |
| Beta | **ORIG:** *from frontal to occipital*<br>**OSCIL:** *central*<br>**FRACT**: *frontal & occipital* | ORIG:*none*<br>**OSCIL:** *R parieto-occipital*<br>FRACT: *none* |
| Gamma | **ORIG:** *frontal & occipital*<br>**OSCIL**: *frontal & occipital*<br>**FRACT**: *most all electrodes* | **ORIG:** *L & R centro-parietal*<br>**OSCIL**: *fronto-centro-parietal*<br>**FRACT**: *L centro-parietal & R fronto-central* |

*Table 3. Summary of the differences between post-task and pre-task for the original (ORIG), pure oscillatory (OSCIL), fractal (FRACT) EEG activity in the CTL and the hBDI groups for theta (4–8 Hz), alpha (8.5–13 Hz), beta (13.5–25.5 Hz), and gamma (30–90 Hz). In red, we report results where post-task values were significantly greater than pre-task. In blue, we report results where pre-task values were greater than post-task. "None" refers to no significant differences between the two-time points.*

### *Phase–Amplitude Coupling Is Greater in hBDI Only at Baseline*

Lastly, we analyzed group differences for theta–beta and theta–gamma PAC in the post-task recordings. Non-parametric permutation analyses demonstrated that, differently from the pre-task recordings, there were no group differences for theta–beta and theta–gamma MI in the post-task recordings (Figure 3B). Thus, in line with the results of post-task original and oscillatory components, these results suggest that task activity had differential effects on the MI of the two groups, despite similar performance rates. Indeed, separate group analyses (Figure 6) revealed that in the post-task compared to the pre-task recordings, theta–beta MI of the CTL group increased in electrodes over a right frontocentral region (Cluster $t$ = 22.63, $p$ = 0.0018, SD: 0.0004, CI: 0.0008) and the left central area (Cluster $t$ = 11.63, $p$ = 0.014, SD: 0.0012, CI: 0.0023) (Figure 6A, first line). Theta–gamma PAC increased in most electrodes (Cluster $t$ = 114.74, $p$ = 0.00001, SD: 0.0012, CI: 0.0023) (Figure 6B, first line). The same comparisons in the hBDI group did not show any significant change for theta–beta PAC (Figure 6A, bottom line), while theta–gamma MI increased over an extended area on both hemispheres without involvement of the mid-frontal electrodes (Cluster $t$ = 80.56, $p$ = 0.0005, SD: 0.0002, CI: 0.0004) (Figure 6B, bottom line). These findings suggest that substantial and extensive increases of both theta–beta and theta–gamma PAC occurred post-task in CTL, while no changes were noted in hBDI for theta–beta PAC.

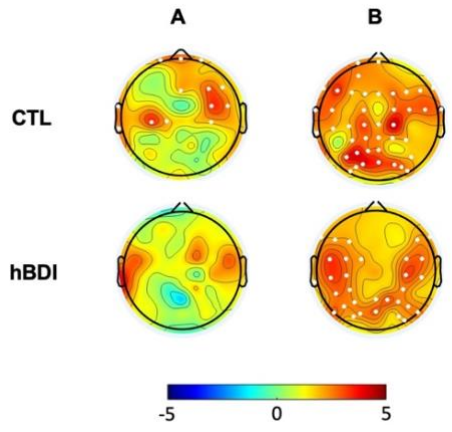


*Figure 6. Post-task/pre-task differences for theta–beta (A) and theta–gamma (B) PAC in the CTL (first line) and hBDI (bottom line) groups. Topographic plots depict the results of cluster-based permutation t-statistics. White dots represent electrodes within significant clusters.*

## Discussion

To our knowledge, this study is the first to highlight that, in individuals with depression, practicing a learning task fails to elicit the same increases in higher-frequency oscillatory activity during resting-state EEG as observed in healthy individuals. This deficit likely indicates disruptions in plasticity-related mechanisms and brain energy metabolism. we analyzed EEG results recorded during resting states before and after the performance of a learning task in a large cohort of young college students who were tested for depression and anxiety. As summarized in Table 2, we found that, compared to CTL, subjects with high BDI scores showed greater power in the high-frequency range, beta and gamma, mostly over fronto-parietal regions. However, after performing a learning task with similar accuracy, such differences either disappeared or diminished (see Tables 2 and 3). Specifically, post-task EEG changes showed substantial increases in all frequency ranges (with a notable increase in beta) for the CTL group but not for the hBDI group. Further analyses focused on the pure oscillatory and fractal components as well as on theta–beta and theta–gamma PAC revealed additional differences between the two groups, both before and after the learning task. In the following paragraphs, we will first discuss the characteristics of our study population and then explore the potential implications and meanings of the EEG differences (in terms of oscillatory and fractal components) observed between the CTL and hBDI groups at baseline and their changes following the learning task. We will then comment on our findings about theta–beta and theta–gamma PAC at baseline and following the task.

### *Over-Sensitive Behavioral Inhibition System Is Linked to Depression and Anxiety*

The demographic characteristics of the hBDI group were similar to those reported in the 2021 NSDUH Annual National Report at https://www.samhsa.gov/data/report/2021-nsduh-annual-national-report (accessed on 12 April 2024). In fact, compared to CTL, our depressed cohort included more women than men and had higher levels of trait anxiety, sensitivity to punishment, and withdrawal from aversive or unfamiliar stimuli. BAS displayed a weak negative correlation to trait anxiety scores but not to the BDI scores. The association of anxiety with depression and the correlations between clinical tests suggest that all these psychological constructs are linked (Choi et al., 2020; Hopwood, 2023; Kessler et al., 2015; Zhou et al., 2017). These findings are in line with Gray's reinforcement sensitivity theory about the role of personality in the genesis of mood and anxiety disorders (Masuyama et al., 2022; Takahashi et al., 2021; Toyoshima et al., 2022). Indeed, increased behavioral inhibition sensitivity may be a risk factor for affective disorders, with higher BIS scores linked to elevated levels of trait anxiety and depression (Sun et al., 2020). Despite the relatively small sample, our results are in agreement

with previous accounts (Kasch et al., 2002; Quilty et al., 2014) that depression may be associated with an overactive inhibitory system and a hypoactive activation system. At the same time, anxiety may be more related to heightened inhibitory sensitivity and avoidance behavior (Takahashi et al., 2021). The results of our logistic regression model showing that BIS accurately identified 70% of individuals with high BDI scores further strengthens the value of BIS as a good predictor of an ongoing depressive status.

### *Depression Is Characterized by Greater Beta Power during Resting-State EEG before the Task*

In line with previous reports (Fingelkurts & Fingelkurts, 2015), the group with depressive symptoms displayed greater beta oscillatory activity compared to CTL over the fronto-parietal regions in the resting-state EEG results recorded before the task. Frontal beta activity has been associated with top-down control of attention-related mechanisms and emotional processing (Kavanaugh et al., 2023; Y. Li et al., 2017). Studies in normal and depressed subjects have reported that beta power over frontal areas increases with attention and working memory (Palacios-García et al., 2021; Spitzer & Haegens, 2017), stress (Ehrhardt et al., 2022, p. 202; Palacios-García et al., 2021), and anxiety (Sporn et al., n.d., p. 202) and decreases with inattention (Roh et al., 2016). Executive dysfunction and attentional deficits, such as impaired concentration and decision-making abilities, are indeed common in depression (Cotrena et al., 2016; Gohier et al., 2009; Snyder, 2013; Stordal et al., 2004). The role of beta in executive functioning is also supported by analyses of phase synchronization (D. L. Clark et al., 2016; Y. Li et al., 2017) and theta–beta ratio (an index reflecting attentional control, top-down inhibition, and cognitive processing (D. L. Clark et al., 2016; Morillas-Romero et al., 2015)).

What is the meaning of greater frontal beta power in depression? As shown by functional MRI studies (Harvey et al., 2005; Rose et al., 2006), the frontal areas may be particularly active in depressed subjects in an attempt to maintain a normal level of performance during working memory tasks. Accordingly, the frontal enhancement of beta oscillations in the hBDI group could be interpreted in the frame of compensatory mechanisms to increase the efficiency of attentional control and maintain cognitive and emotional functioning. On the other hand, it may reflect hyperarousal linked to anxiety and stress (Hein & Herrojo Ruiz, 2022). While plausible, these conclusions remain, at least for the moment, hypotheses to be tested in ad-hoc studies, as the database we used did not include cognitive functioning assessment.

The observed beta power increase could also be linked to power decrements in the lower frequency ranges, such as the lower alpha oscillatory activity we found over the right frontal and left temporal areas. Decreased frontal alpha activity is a well-documented finding in depression (Davidson et al., 2002; Thibodeau et al., 2006). Frontal alpha asymmetry in depressive disorders

was first described in 1983 (Schaffer et al., 1983), with the left frontal area displaying higher alpha band power than the right one (Allen & Cohen, 2010; Davidson, 1992; Davidson et al., 2002; Schaffer et al., 1983; van der Vinne et al., 2019). Although some publications have now questioned it, frontal alpha asymmetry has been mainly linked to emotional dysregulation and other factors such as motivation and positive affect (for a review, see: (Reznik & Allen, 2018; Thibodeau et al., 2006); with reduced right frontal alpha reflecting negative emotional states and withdrawal (Davidson et al., 1990, 2002; Thibodeau et al., 2006).

Another interesting finding is that increased beta power over the frontal area and the reduced alpha power in hBDI compared to controls were present only for the signal's mixed and pure periodic component but not for the fractal component. Previously discarded as "1/f noise", the scale-free dynamics are thought to be generated by mechanisms that differ from those ruling periodic oscillatory activity and have been hypothesized to reflect neural complexity (Stam, 2005a; Wen & Liu, 2016a; Werner, 2010). Thus, the sole increase in the oscillatory component we observed in the hBDI group indicates that such changes likely reflect localized brain functions, such as heightened cognitive or emotional processing, that rely on a specific, state-dependent, rhythmic activity.

***Gamma Power at Rest Is Greater in Depression***

Subjects in the hBDI group also displayed greater parieto-occipital gamma power, a finding that could further support the association between depression and altered attentional processes. Lately proposed as a putative biomarker of depression, studies on the role of gamma oscillatory activity in depression have yielded mixed results, with some of them reporting reductions and others reporting increases in gamma activity (Fitzgerald & Watson, 2018). These discrepant results may stem from differences in pharmacological treatments: serotonergic drugs (e.g., fluoxetine) lower gamma activity, while noradrenergic drugs (e.g., reboxetine) increase it (Cape & Jones, 1998; Fitzgerald & Watson, 2018a; Hajós et al., 2003). In this line, other investigations have suggested that the combination of increased cortical levels of glutamate and reduced GABAergic activity is a biomarker of trait vulnerability to depression rather than a correlate of mood alterations (Bhagwagar et al., 2007; Sanacora et al., 2004), although such excitatory and inhibitory imbalances have been often associated with depression (Bhagwagar et al., 2007; Hashimoto et al., 2007; Y.-T. Hu et al., 2023; Sanacora et al., 2004, 2012). The link between increased glutamatergic activity and high-frequency oscillatory activity has been further confirmed by a model showing that slowing down glutamate decay increases both beta and gamma oscillatory activity (Ramirez-Mahaluf et al., 2017). Therefore, our increased high-frequency oscillatory activity results could reflect altered glutamatergic signaling (Lally et al., 2014).

It should be noted that the power increase in the gamma range in the hBDI group also involved the fractal component, suggesting a different or disrupted dynamic complexity in the hBDI group. Moreover, our finding of a flatter broadband power-law decay (PLE) over the parieto-occipital areas in hBDI parallels previous findings of reduced slope in individuals with trait anxiety (Tolkunov et al., 2010). Similar results have also been reported during cognitive performance (Ciuciu et al., 2012; B. J. He, 2011) as well as in aging and dementia (Smits et al., 2016), further supporting associations between depression, altered cognitive processes, and abnormal power-law scaling. As a steeper broadband spectral slope suggests more efficient information processing (B. J. He, 2014), the flatter slope observed in our hBDI sample may be interpreted as a biomarker of increased neural noise and dysregulated brain function. While additional studies are needed to confirm our interpretations, these findings underscore the importance of examining both periodic and aperiodic components in brain activity to get a comprehensive picture of the neural alterations that occur in and can predict depression.

***Phase–Amplitude Coupling Is Greater in hBDI Only before the Task***

We found increased theta–beta PAC over the parietal region and theta–gamma coupling over the right occipital area in our hBDI subjects. From a behavioral point of view, increased PAC, particularly between theta and gamma oscillations, has been linked to various cognitive processes, such as working memory, attention, and cognitive flexibility, abnormalities often found in depression. Previous studies on depression have reported conflicting results about PAC, with some showing increased coupling (Young et al., 2024b; Zhang et al., 2023), as in our case, and others showing decreased coupling in different frequency ranges (X. Liu et al., 2022b; Noda et al., 2017). Such contrasting results might be due to differences in study designs and conditions tested, patient sample characteristics, specific brain regions examined, and other factors, including testing time. For example, intracranial recordings in epileptic patients showed that low/middle to high-frequency PAC was increased in clinically depressed subjects with epilepsy compared to subjects with epilepsy only, with greater PAC values found in the evening/night than during the daytime (Young et al., 2024). Also, a study of untreated patients during their first depressive episode found greater resting theta–gamma PAC in depressed patients compared to controls (Zhang et al., 2023). In that case, recordings were performed at rest and during an auditory test with alternating baseline and stimulation periods.

An important finding of the present work was that, after the task, the hBDI group showed some increase only in the theta–gamma PAC, while the control group displayed a substantial increase in both theta–beta and theta–gamma PAC. As a result, the group difference found at baseline for both theta–beta and theta–gamma PAC basically vanished following the learning task. While from a behavioral point of view, it may underlie cognitive aspects, low-high frequency PAC

may be, at the system level, a measure of information processing and facilitation within and between cortical networks (Van Der Meij et al., 2012) that depends on a proper balance of excitatory and inhibition mechanisms at the cellular level (Fries et al., 2007; Huerta & Lisman, 1995; Lakatos et al., 2005, 2008; Large & Kolen, 1994; Zheng & Zhang, 2015). Consequently, PAC plays an important role in long- and short-term potentiation processes, as shown also by studies in animal models of depression (Zheng & Zhang, 2015). Thus, the lack of substantial PAC increase in the hBDI group after the task may be an expression of decreased plasticity, a finding previously described in depression (W. Liu et al., 2017). In turn, altered plasticity may be linked to brain energy dysregulation that has been reported in this disease (Głombik et al., 2020; Gu et al., 2021; Østergaard et al., 2018; Shaffer et al., 2022) as discussed at the end of next section.

***Oscillatory Activity Increases after Task Practice in CTL but Not in hBDI***

The analyses of the EEG recordings after the task revealed a different pattern of changes in the two groups despite almost identical performance scores in the task. In general, the post-task resting-state EEG of the CTL group was characterized by broadband power increases in alpha, beta, and gamma ranges of both the pure oscillatory and fractal components and in theta range for the fractal component only. These changes in the oscillatory component are in line with our previous findings that after practicing learning tasks, the resting-state EEG of healthy subjects displays local increases of power, mostly in beta and theta ranges (Nelson et al., 2021) and also in gamma (Ricci et al., 2021), that occur mostly over the areas previously engaged in the task. Conversely, in the present hBDI group, we found a decrement of beta power in a few electrodes over the parieto-occipital area and a modest increase in gamma power involving fewer electrodes than the CTL group. The greater baseline oscillatory activity of the hBDI group may impede further growth because the power may have reached saturation levels. In previous work, we suggested that power increases found after task performance may represent the electrical signature of metabolic processes related to short and long-term potentiation induced by learning and practice (Ghilardi et al., 2021; Nelson et al., 2021; Ricci et al., 2021). We thus speculate that the lack of substantial EEG changes following task practice in the hBDI group, together with our findings on theta–beta PAC (see previous section), may reflect a defective engagement of plasticity-related processes that include excitatory/inhibition balance and energy regulation. Three sets of considerations support this conclusion: 1. plasticity-related processes, excitatory/inhibition balance, and energy regulation are impaired in depression (Cai et al., 2024; Głombik et al., 2020); 2. the changes in beta may signal lactate availability needed to produce fast energy resources for brain activity (Ghilardi et al., 2021; Grønli et al., 2016), and the changes in gamma may be related to mitochondrial activity (Bas-Orth et al., 2020); 3. there is direct evidence of mitochondrial dysfunction and increased lactate levels in the brains of depressed patients

(Bradley et al., 2016; Ernst et al., 2017; Shungu et al., 2012) and that lactate increases are coupled with mitochondrial dysfunction (Raza et al., 2015; Scaglia, 2010b; Stork & Renshaw, 2005; Tobe, 2013). Indeed, we acknowledge the need for targeted studies to prove our hypothesis that practice-related beta and gamma power changes can be biomarkers of energy dysregulation in depression. Such investigations would be rather important, especially in light of recent studies proposing the use of lactate as an antidepressant drug (Cai et al., 2024).

***Limitations***

The present study has several limitations. A good number of them are related to the dataset we chose because of the great advantage of EEG recordings before and after a task in subjects with high and low BDI scores. Specifically, this dataset did not provide information about the socioeconomic status of the participants, did not include participants with a BDI score between 7 and 16 (thus precluding analysis with continuous BDI scores), and only included clinical scores of BDI, STAI, BIS, and BAS. Such scores were largely intercorrelated; individuals of the hBDI groups also displayed greater trait anxiety compared to CTL, making it very difficult to disentangle the contribution of anxiety to EEG abnormalities without additional clinical measures. Most importantly, the dataset did not offer a comprehensive assessment and testing of aspects related to cognition and plasticity mechanisms that may be part of depression.

Despite the clear group differences in EEG-derived measures, we did not find significant correlations between them and the clinical scores, suggesting that other psychological and cognitive factors might explain the observed spectral and connectivity differences. Among them, attentional and working memory abnormalities, stress, and sleep quality are important factors for plasticity and often accompany depression. The lack of this type of information severely curtails the interpretation of our EEG findings, especially as biomarkers of specific factors associated with depression.

Another limitation of this investigation is that the subjects were all college students within a narrow age range. This aspect likely decreased variability but makes it critical to validate the present results for other age ranges and populations with stressors other than those related to specific life experiences. Therefore, caution should be exercised in extending these results to older people or to populations from different socioeconomic and cultural backgrounds, and future investigations are needed to address these issues. Moreover, it would be important to replicate the present findings using other types of tasks, which may induce different topographical patterns, to assess the generalizability of our conclusions in terms of frequency changes. Finally, among other limitations, there is a lack of information about previous antidepressant treatments and major depression episodes. As discussed in the previous

paragraphs, these factors may influence brain inhibition/excitatory balance and, thus, EEG results.

***Conclusions***

This is the first study demonstrating that in depressed subjects, a period of practice in a learning task does not induce the same increases observed in healthy individuals of higher frequency oscillatory activity recorded during resting-state EEG. This deficit likely reflects alterations of plasticity-related mechanisms and brain energetic metabolism. However, only future EEG studies coupled with techniques specifically exploring brain metabolism, such as MRS, will provide a comprehensive picture of the dysfunction underlying depression and its symptoms. These studies, in turn, will help foster the development of novel and targeted therapies based on pharmacological and non-pharmacological approaches.

# Chapter 4: Neurophysiological correlates of ketamine-induced dissociative state in bipolar disorder

## Introduction

Ketamine, a versatile compound with various applications spanning anesthesia, antidepressant treatment, recreational use, and abuse, has recently taken center stage in neuropsychiatric research. Several clinical trials have validated ketamine's therapeutic properties in a variety of psychiatric conditions, demonstrating high efficacy against treatment-resistant depression (TRD), especially for suicidal ideation, and promising results for bipolar disorder (BD), post-traumatic stress disorder, and substance use disorders (R. M. Berman et al., 2000; Dakwar et al., 2018; Feder et al., 2014; Grabski et al., 2022; Kryst et al., 2020; Zarate et al., 2006). This bears huge importance, given the growing prevalence of mood disorders and the limitations of conventional antidepressants (Trivedi et al., 2006). At subanesthetic doses, ketamine triggers an altered state of consciousness that some authors describe as dissociation, similar to symptoms seen in dissociative disorders (Acevedo-Diaz et al., 2020). In contrast, others liken it to a psychedelic experience (Studerus et al., 2011; Vollenweider & Kometer, 2010). In the hour following ketamine's administration as a treatment for depression, patients commonly report unusual bodily sensations, a sense of peace, disinhibition, and altered perception (van Schalkwyk et al., 2018). A systematic review investigating the link between ketamine-induced subjective effects and antidepressant response produced mixed findings. Of all the studies analyzed, only three reported a significant correlation between antidepressant response and scores on the Clinician-Administered Dissociative States Scale (CADSS) or the Brief Psychotic Rating Scale (BPRS) (Ballard & Zarate, 2020). Using the altered states of consciousness questionnaire (ASCQ), one study demonstrated that a stronger antidepressant response to ketamine was associated with experiences of unity, spirituality, and insight (Sumner et al., 2021). However, another study found that non-responders scored higher on dread of ego dissolution (Aust et al., 2019). In patients with substance-use disorder, the mystical-type effects of ketamine, measured via the Hood Mysticism

Scale (HMS), were found to mediate the reduction in patients' cocaine use and craving (Dakwar et al., 2018).

Indeed, the subjective effects of ketamine appear to be highly variable, influenced significantly by factors such as dosage, individual differences, the setting of administration, and the instrument employed to assess the experience. This variability underscores the need to identify reliable biomarkers of acute neurophenomenology of ketamine in diverse patient populations and contexts.

Electroencephalography (EEG) is one of the most appropriate neuroimaging methods to flexibly investigate the neural dynamics of psychoactive drugs due to its high temporal resolution and non-invasiveness. The neural signal recorded by EEG displays a diverse combination of rhythmic and arrhythmic patterns (Buzsáki et al., 2012). Rhythmic patterns emerge from oscillatory network activity with a characteristic time scale (Buzsáki & Draguhn, 2004), while arrhythmic patterns lack confinement to any specific scale, reflecting nonlinear dynamics (B. J. He et al., 2010). In both healthy subjects and patients with depression, a single continuous infusion of a subanesthetic dose of ketamine modulates brain rhythmic activity by decreasing spectral power in the low frequencies, such as δ (de la Salle et al., 2016; A. E. M. Forsyth et al., 2021; V. J. Knott et al., 2011; McMillan et al., 2019; Shaw et al., 2015; Vlisides et al., 2018; Zacharias et al., 2020) and θ (de la Salle et al., 2016; Vlisides et al., 2017, 2018; Zacharias et al., 2020), and also in the α (de la Salle et al., 2016; A. E. M. Forsyth et al., 2021; V. J. Knott et al., 2011; McMillan et al., 2019; Shaw et al., 2015; Vlisides et al., 2018; Zacharias et al., 2020) and β (A. Forsyth et al., 2018; V. Knott et al., 2006; McMillan et al., 2019; Muthukumaraswamy et al., 2015; Rivolta et al., 2015; Vlisides et al., 2017) bands, while increasing γ (de la Salle et al., 2016; A. Forsyth et al., 2018; McMillan et al., 2019; Muthukumaraswamy et al., 2015; Rivolta et al., 2015; Vlisides et al., 2017, 2018; Zacharias et al., 2020) frequency.

In one study, the reduction of α power induced by ketamine was found to correlate with depersonalization scores of the CADSS (de la Salle et al., 2016) and alterations of elementary imagery of the ASCQ by another (Vlisides et al., 2018). In patients with TRD, frequency-specific EEG changes induced by ketamine were predictive of decreases in depressive symptoms (i.e., θ, α, γ) and suicidal ideation (i.e., α) (de la Salle et al., 2022; Lijffijt et al., 2022), but not consistently across studies (McMillan et al., 2020). In recent years, the arrhythmic and non-linear dynamics of the neural signal have progressively been studied and characterized (Stam, 2005). One such property is the scale-free (also termed fractal) activity, which adheres to a 1/f power-law relationship, expressing the property of brain signal to show an inverse relationship between power and frequency (Buzsáki & Draguhn, 2004). While the physiological mechanisms by which power-law scaling is generated in the brain are poorly understood, and their significance remains

controversial (Buzsáki et al., 2012), its alteration in various neuropsychiatric conditions underscores the potential functional importance of power-law scaling in the brain (Lai et al., 2010; Maxim et al., 2005; Wei et al., 2013). Muthukumaraswamy and Liley demonstrated that the Power Law Exponent (PLE) of the brain signal recorded at rest is sensitive to various pharmacological interventions, including ketamine. In particular, a subanesthetic dose of ketamine was found to decrease the PLE exponent at frequencies between 5 and 100 Hz in healthy subjects (Muthukumaraswamy & Liley, 2018). To date, the effect of ketamine on PLE and its relationship with the subjective effects of the drug and therapeutic response in patients has not been investigated. In addition to scale-free properties, the high temporal resolution provided by the EEG signal makes it ideal for determining measures of complexity and entropy of brain activity. One such measure is the Lempel-Ziv complexity (LZc), which assesses the level of compressibility and diversity of a signal (M. Schartner et al., 2015). Ketamine was observed to consistently increase spontaneous brain complexity (Cortes-Briones et al., 2015; Sarasso et al., 2015; M. Schartner et al., 2015; M. M. Schartner et al., 2017), with one study reporting a correlation with the intensity of the subjective experience (M. Schartner et al., 2015). There is very limited research on the characterization of complexity in patient populations and its association with therapeutic response, with only one investigation in a cohort of late-life TRD patients (Murphy et al., 2023).

In summary, while some evidence suggests the potential utility of EEG metrics as biomarkers for ketamine-induced altered states of consciousness and therapeutic effects, further investigation is required. Data concerning the impact of ketamine on non-linear brain dynamics, their interaction with rhythmic neural activity, and their phenomenological and clinical implications are currently lacking. Critically, the escalating use of ketamine within psychiatry raises the crucial issue of identifying robust biomarkers of ketamine's mechanism of action (Wilkinson et al., 2017). Moreover, limited evidence exists regarding ketamine response in complex patient populations with diverse demographics and often undergoing poly-pharmacological treatments in real-world hospital settings. Large-scale studies and clinical observations have consistently highlighted significant variability in patients' neural therapeutic response to ketamine and its brain-based correlates, with response rates oscillating between 35% and 60% (Medeiros et al., 2023). Notably, while some patients experience rapid antidepressant effects after a single infusion, a substantial proportion of individuals require multiple infusions to achieve a clinically meaningful response (d'Andrea et al., 2024; Martinotti et al., 2022).

In this study, we employed a portable 32-channel EEG headset to 1) characterize the neurophysiological underpinnings of the dissociative state induced by a subanesthetic dose of ketamine in BD patients in a clinical, real-world setting and 2) to explore the relationship of such

markers with the dissociative subjective effects and treatment response induced by ketamine. More specifically, based on real-world observations of ketamine therapy, we hypothesized that endophenotypic differences in therapeutic response would correspond to distinct neurophysiological patterns in response to the treatment.

## Materials and Methods

### *Patient population*

The study included a total of 30 patients (Mean age = 51 ± 13, Females = 12; Table 4) with TR-BP type 2 with a history of failure of at least 2 conventional antidepressant treatments and currently undergoing a depressive episode requiring hospitalization. The severity of depression at inclusion was assessed with the Montgomery–Åsberg Depression Rating Scale (MADRS) and a semi-structured interview by the study psychiatrist. The criteria for inclusion were: having between 18 and 70 years of age, a diagnosis of BP type 2 in accordance with the DSM-5 criteria (American Psychiatric Association & American Psychiatric Association, 2013), an ongoing TR depressive episode defined as history of failure of at least 2 conventional antidepressants, and a MADRAS score at inclusion above 30 (i.e., moderate to severe depression). Acute suicidal ideation, presence of psychotic symptoms, current dependence on alcohol and other substances of abuse, and presence of other severe medical conditions were grounds for exclusion. Comorbidity with other minor psychiatric conditions was allowed. All participants in the study were undergoing concomitant psychotropic medications during the study (Table 4). To be included, all patients were required to be in treatment with a psychiatrist at the moment of study enrolment.

All patients provided informed consent to participate in the study, which was collected by the researcher and study psychiatrist. The study was approved by the research ethics committee of the University Hospital of Siena. All inclusion and experimental procedures were performed in the psychiatry unit within the Department of Mental Health of the University Hospital of Siena, Italy.

### *Study design*

The patients included in this experiment were recruited from a cohort of in-patients with TR-BP undergoing off-label ketamine therapy for a current major depressive episode. The treatment involved 30 minutes long i.v. continuous infusions of sub-anesthetic doses of racemic ketamine (1:1 mixture of the S-ketamine and R-ketamine enantiomers) twice a week for a month, following which the treatment was adjusted based on individual needs. The treatment started at dosages lower than 0.5 mg/kg and was titrated based on individual tolerability and clinical

response to a maximum of 1 mg/kg. Depressive symptomatology was monitored at baseline and weekly by the administration of the MADRS until the end of treatment by the study psychiatrist.

For each patient, the EEG signal was measured once during one of the ketamine administrations with a dosage between 0.5 and 1 mg/kg, known to reliably produce acute subjective effects (Lavender et al., 2020). All EEG recordings were performed at least 1 week after the beginning of treatment. Hence, each participant had a variable dose and number of prior exposures to ketamine at the time of the EEG recording. To quantify the intensity and phenomenology of the subjective experience induced by ketamine on the day of the EEG, the CADSS was administered immediately after the infusion. This scale was chosen as being the most commonly used in previous literature (van Schalkwyk et al., 2018).

The EEG recording consisted of 6 minutes of baseline resting state before the start of ketamine infusion. The 6 minutes of baseline EEG recording were subdivided into 3 minutes of eyes open (Pre-OP) and 3 minutes of eyes closed (Pre-EC) conditions. Then, EEG was recorded throughout the 30 minutes of continuous i.v. infusion of a sub-anesthetic dose of ketamine (0.5-1 mg/kg). Immediately after the infusion, EEG recording continued for an additional 6 minutes, subdivided into 3 minutes of eyes open (Post-EO) and 3 minutes of eyes closed (Post-EC) conditions. A summary of the study design is shown in Figure 7 A. Continuous i.v. infusion of a sub-anesthetic dose of ketamine (0.5-1 mg/kg) of 30 minutes has been shown to have an elimination half-life of 2-3 hours, with dissociative/psychedelic-like effects lasting around 1-2 hours. Thus, our post-ketamine EEG condition captured the acute phase of the ketamine state.

***CADSS***

To quantify the intensity and character of the subjective experience induced by ketamine, the 25-item version of the CADSS was administered. The items were adapted to the Italian language. The scale was scored according to Bremner et al. (1998), resulting in the 3 factors of dissociation: depersonalization, derealization, and amnesia (Bremner et al., 1998).

***MADRS***

To assess the clinical trajectory of the patients, the MADRS was administered by the study psychiatrist on a weekly basis from the start until the end of treatment. The time points of MADRS administration relevant to the current investigation were the time of recruitment (T0), 1 week after the beginning of the treatment (T1), and before the ketamine infusion with concurrent EEG recording (T2) (Figure 7 A). At the session where EEG recordings were made (T2), all patients had responded to the prior treatments, with all participants exhibiting MADRS scores below 19. Patients who showed a 50% reduction of MADRS after the first week of treatment were classified

as early responders (ER), while the other portion of patients were classified as late responders (LR).

***EEG setup***

The EEG recording was performed with a Wireless, 32-channel Starstim device (Neuroelectrics®, Barcelona, Spain). The montage included 32 Ag+/ Ag+Cl– passive electrodes (10-20 international EEG system). This portable and quick to setup EEG headset was chosen as it offers enough channel density to reliably measure good quality electrophysiological signal across the scalp with minimal invasiveness and distress for the patient, making it suitable for ecologically valid recording in an hospitalized population. The acquisition sampling rate was 500 Hz. Two reference electrodes were placed on the left mastoid. Data were acquired with the Neuroelectrics® Instrument Controller (NIC2) software.

***EEG pre-processing***

The continuous EEG signal was pre-processed off-line, retaining the sampling resolution of 500 Hz. The pre-processing steps followed a standard procedure. First, the data were baseline corrected, and a 1 to 80 Hz band-pass filter was applied, with a notch filter at 50 Hz. Then, a semi-automatic artifact removal approach was applied. The process involved the automatic detection of portions of signal showing a standardized score of deviation from the mean above a pre-specified threshold. Then, the data were visualized for manually removing artifacts associated with movements, jaw clenches, and noisy channels. Then, independent component analysis (ICA), using the "runica" algorithm, was applied to remove from the signal EEG components of muscle activity, blinks, ocular movement, and cardiac activity. Removed channels were then interpolated using the weighted average of neighboring electrodes. Lastly, the data were re-referenced to the average of all electrodes. A comparable amount of channels (Pre-ketamine: M = 2, SD =2; Post-ketamine: M = 3, SD =2) and ICA components (Pre-ketamine: M = 6, SD =2; Post-ketamine: M = 8, SD =3) was removed before and after ketamine. Also, the different conditions had similar data lengths after pre-processing: Pre-EO (M = 182 s, SD = 7), Pre-EC (M = 177 s, SD = 7), Post-EO (M = 184 s, SD = 11), and Post-EC (M = 175 s, SD = 13). All pre-processing steps were implemented in MATLAB (*MATLAB R2023a*, MathWorks Inc., Natick, MA) using the open-source toolbox FieldTrip (Oostenveld et al., 2011).

***EEG analysis***

All analyses were performed on EEG data recordings of the 3-minute eye open and 3-minute eye closed conditions before and immediately following ketamine infusion. Prior to all analysis,

the continuous pre-processed EEG data were subdivided into non-overlapping epochs of 2 seconds.

For the power spectral density (PSD) analysis, data were Fast-Fourier transformed using a conventional single taper (e.g., Hanning) for frequencies between 1 and 30 Hz and using the multiple tapers based on discrete prolate spheroidal sequences (DPSS) for frequencies between 30 and 80 Hz. To determine the separate contribution of oscillatory and fractal components to the original spectral power, the signal was decomposed using the Irregularly Resampled Auto Spectral Analysis (IRASA) algorithm, as described by Wen and Liu (Wen & Liu, 2016). The technique virtually compresses and expands the time-domain data with a set of non-integer resampling factors prior to FFT-based spectral decomposition. As a result, oscillatory components in the power spectrum are redistributed while the fractal 1/f contribution is left intact. Taking the median of the resulting auto-spectral distributions extracts the power-spectral fractal component, and the subsequent removal of the fractal component from the original power spectrum offers a power-spectral estimate of oscillatory content alone. Original, fractal, and oscillatory spectral power densities were divided into the following canonical frequency bands for statistical analysis: delta (1-4Hz), theta (4-8 Hz), alpha (8-13 Hz), low beta (13-20 Hz), high beta (20-30 Hz), low gamma (30-45 Hz), high gamma (55-80 Hz), and broadband (1-80 Hz).

In order to estimate the power law exponents (PLE) of the power spectrum, the fractal component $1/f^{\beta}$ was transformed to log-log coordinates. Taking the log brings the β down from the exponent, turning the relation into a linear one: $\log(1/f^{\beta}) = \beta \log(1/f)$. Then, a linear regression was performed to extract the β coefficient. Finally, taking the negative of the β coefficient turns $f^{\beta}$ to $1/f^{\beta}$ (i.e., PLE). To avoid biasing regression estimates towards the higher frequencies, where more sampling points exist in logarithmic space, frequency estimates are resampled to be evenly spaced in logarithmic coordinates prior to the computation of the regression. Also, visual inspection of the log-log distribution of the fractal power showed a "knee" frequency at 20 Hz, where the spectrum's slope (i.e., β coefficient or PLE) showed a significant change. Thus, data were separated into frequency bands "by eye" into two spectral regions, a high-frequency region (20-80 Hz) for which we defined parameter PLEhf and a lower frequency range (1-20 Hz) for which we defined PLElf, following a similar approach to the one of Muthukumaraswamy and Liley (Muthukumaraswamy & Liley, 2018).

For the quantification of LZc, the pre-processed data were first binarized by comparing each data point for epoch and channel to the mean value of that channel and epoch, with values above the mean transformed into 1s and values below into 0s. Then, the LZ76 algorithm was applied to compute the number of distinct "patterns" (or substrings) in each binarized epoch and channel and then normalized the resulting number for data length by a factor $N/\log_2(N)$, where N is the

data length in samples. Then, the normalized values were averaged over epochs to measure brain entropy estimate (here referred to as LZc). Regular signals are characterized by a few patterns and hence have low LZc, while irregular signals contain many different patterns and hence have a high LZc. The analysis followed the original method described by Lempel and Ziv (Kaspar & Schuster, 1987)and was applied to EEG data.

For the quantification of the complexity contribution of each frequency band, the novel estimator called Complexity via State-space Entropy Rate (CSER) was computed. The CSER is a spectrally and temporally resolved estimation of neural signal diversity, recently introduced by Mediano et al (Mediano et al., 2023). Compared to LZc, CSER does not require the signal to be discretized, allowing it to fully exploit continuous signals and avoiding potential artifacts introduced by the discretization procedure. Also, CSER has the unique advantage of allowing for complexity analysis within spectral frequency bands. First, the pre-processed data were down-sampled to 160 Hz. Then, data were normalized via z-scoring, subtracting the mean and dividing by the standard deviation in each channel. The CSER was applied to the z-scored data to obtain a CSER measure for each frequency band, adding to a total CSER. The frequency-specific CSER was compounded on 2 Hz broadband windows and then averaged within the frequency bands of interest. We compared the LZ76 analysis with the same down-sampled and normalized data, showing comparable results to the LZ76 computed on the 500 Hz resolution data (data not shown). All analyses were performed in MATLAB software using the open-source toolbox FieldTrip (Oostenveld et al., 2011) for the EEG spectral analysis and the EntRate package for the LZ76 and CSER analysis (Mediano et al., 2023).

***Statistical Analysis***

The analysis of the original, fractal, and oscillatory power spectral density (divided in the main frequency of interest), as well as the PLE and LZc measures of the EEG, involved group-level channel-specific comparisons between the eyes open closed conditions before and immediately after ketamine infusion ended. For each EEG metric and channel, a cluster-level permutation test was computed between conditions, an approach shown to be the most efficient in addressing the multiple comparisons problem (Maris & Oostenveld, 2007). For every channel, the experimental conditions are compared through a t-value. All samples are selected whose t-value is larger than a cluster alpha value of 0.05. Then, selected samples are clustered in connected sets based on temporal, spatial, and spectral adjacency. Cluster-level statistics are calculated by taking the sum of the t-values within every cluster, and the maximum of the cluster-level statistics is taken. The significance probability is calculated by means of the so-called Monte Carlo method. The method collects the trials of the different experimental conditions in a single set and randomly draws as

many trials from this combined data set as there were trials in condition 1 and places them into subset 1. The remaining trials are put in subset 2. On this randomized set, the test statistic is computed as described above (i.e., the maximum of the cluster-level summed t-values). These steps were repeated for 1000 random permutations to obtain a distribution of test statistics, from which the proportion of random partitions that resulted in a larger test statistic than the observed one is computed. If the probability value (i.e., p-value) is smaller than the critical alpha level of 0.025 (one tail for positive and one for negative clusters), then we concluded that the data in the two experimental conditions were significantly different.

To analyze changes in CSER, an average CSER value across channels was obtained for each frequency and broadband data. A linear mixed-effect model was used to calculate the pre- vs. post-ketamine difference in CSER, using a random slope for each subject to account for the within-subject design. This analysis was performed using the open-source programming language R.

For correlations between EEG metrics and between EEG metrics with dose, scores on the CADSS, and MADRS scores at T2, the electrodes belonging to statistically significant clusters computed with the permutation tests were extracted for each comparison and metric. Then, the difference (i.e., Δ value) between post- to pre-ketamine values was computed for those electrodes only. Both the raw and relative (corrected for the baseline value) differences were computed. For each contrast, non-parametric Spearman correlation tests were performed between EEG metrics, total, depersonalization, derealization, and amnesia CADSS scores, MADRS scores at T2 (EEG day, before ketamine administration), and ketamine dosage. For the correlation with the CADSS scores only, the analysis was repeated with the exclusion of one patient who reported an abnormally high CADSS score compared to the others. The outlier was identified by analyzing the quantile distribution using Tukey's rule (Tukey, 1977). Outliers were defined as data points laying 1.5 times the Interquartile range above the third quartile (75% of the distribution) or below the first quartile (25% of the distribution). To account for family-wise false discovery rate (FDR) inflation due to multiple comparisons, the p-values resulting from Spearman tests were adjusted independently using the Benjamini-Hochberg adjustment (Benjamini & Hochberg, 1995). The results of the FDR correction are reported as "p adj." in the main text.

Patients were stratified based on the difference in MADRS scores between the T0 and T1 for the analysis of early versus late responders. Patients who showed a reduction of MADRS scores of more than 50 % between the 2 time points were considered ER, while the others were classified as LR. The significance analysis for comparing baseline EEG metrics between groups was performed with cluster-based permutation statistics with a between-subject design. For comparing EEG changes induced by ketamine between groups, cluster-based permutation statistics with a mixed within-between subject design was employed. First, condition differences

were computed for each EEG metric and contrasts (i.e., post-EO vs pre-EO; post-EC vs pre-EC). Then, the difference between conditions was compared between groups (i.e., ER vs LR). For CSER and the inclusion of dosage as a covariate, the analysis was implemented with a linear mixed-effects model, using the channel-averaged EEG metrics as the dependent variable, group, and condition as independent variables, plus their interaction, dose as a covariate, and a random effect for each subject.

## Results

### *Demographics, Drugs, and Psychometric measures*

| | **TRD-BP (N = 30)** | **ER (N = 18)** | **LR (N = 12)** |
|---|---|---|---|
| ***Sex*** | M = 18, F = 12 | M = 11, F = 7 | M = 7, F = 5 |
| ***Age*** | 51 ± 13 | 52 ± 11 | 48 ± 15 |
| ***SSRI (T0)*** | 77 % | 78 % | 75 % |
| ***SNRI (T0)*** | 17 % | 11 % | 25 % |
| ***Lithium (T0)*** | 80 % | 72 % | 92 % |
| ***Valproate (T0)*** | 43 % | 50 % | 33 % |
| ***Antipsychotic (T0)*** | 73 % | 72 % | 75 % |
| ***Antiepileptic (T0)*** | 47 % | 50 % | 42 % |
| ***Benzodiazepines (T0)*** | 47 % | 44 % | 50 % |
| ***Bupropion (T0)*** | 13 % | 17 % | 8 % |
| ***Other medications (T0)*** | 43 % | 39 % | 50 % |
| ***MADRS (T0)*** | 38 ± 5 | 38 ± 5 | 38 ± 4 |
| ***MADRS (T1)*** | 21 ± 6 | 17 ± 3 | 27 ± 5 |
| ***MADRS (T2)*** | 13 ± 3 | 14 ± 3 | 12 ± 4 |
| ***Ketamine dose mg/kg (T2)*** | 0.7 ± 0.2 | 0.6 ± 0.1 | 0.9 ± 0.09 |
| ***CADSS Tot (T2)*** | 26 ± 15 | 29 ± 17 | 22 ± 13 |
| ***CADSS Depersonalization (T2)*** | 8 ± 3 | 9 ± 5 | 7 ± 5 |
| ***CADSS Derealization (T2)*** | 14 ± 8 | 15 ± 8 | 12 ± 6 |
| ***CADSS Amnesia (T2)*** | 2 ± 2 | 3 ± 2 | 1 ± 1 |
| ***N° of previous ketamine administrations (T0-T2)*** | 9 ± 8 | 7 ± 8 | 11 ± 7 |

*Table 4. Demographics, Drugs, and Psychometric Measures. TRD-BP = Treatment-Resistant Depression in Bipolar Disorder; ER = Early Responders; LR = Late Responders; SSRI = Selective Serotonin Reuptake Inhibitor; SNRI = Serotonin-Norepinephrine Reuptake Inhibitor; MADRS = Montgomery-Åsberg Depression Rating Scale; CADSS = Clinician-*

*Administered Dissociative States Scale; T0 = the time of recruitment; T1 = 1 week after the beginning of the treatment; T2 = before the ketamine infusion with concurrent EEG recording (T2).*

All patients reported a clinically meaningful experience of dissociation during the EEG-recorded ketamine administration, defined by a CADSS total score above 4 (based on previously reported normative scores in healthy participants according to Bremner et al. (Bremner et al., 1998)). No significant correlations between dose and CADSS total or CADSS sub-dimensions were observed. Also, there was no correlation between MADRS scores before ketamine administration and CADSS scores after ketamine infusion.

### *EEG metrics*

The analysis of the acute neurophysiological changes induced by a single continuous infusion of ketamine (i.v., 0.5-1 mg/kg, 40 minutes) involved comparing rhythmic and arrhythmic components of the resting-state EEG signal. All EEG metrics were computed as averages within each of the 3-minute-long conditions, namely the pre-ketamine eyes open condition (Pre-EO), pre-ketamine eyes closed condition (Pre-EC), post-ketamine eyes open condition (Post-EO), and post-ketamine eyes closed condition (Post-EC). The main experimental contrasts were between the Pre-EO and Post-EO conditions and between the Pre-EC and Post-EC conditions. A plot of the power spectra and its oscillatory and fractal components is shown in Figure 7 (B-D).

*Power Spectral Density (PSD)*

The analysis of the PSD for the Pre-EO vs Post-EO contrast revealed a significant reduction in broadband (i.e., 1 to 80 Hz) PSD during ketamine exposure (Cluster-based stats = -53.80.41; $p = 0.002$; CI = 0.004). Frequency-specific analysis showed a reduction in the delta (Cluster-based stats = -43.33; $p < 0.001$; CI = 0.002), theta (Cluster-based stats = -108.08; $p < 0.001$; CI = 0.002), alpha (Cluster-based stats = -191.30; $p < 0.001$; CI = 0.002), low beta (Cluster-based stats = -153.62; $p < 0.001$; CI = 0.002), and high beta (Cluster-based stats = -15.72; $p= 0.016$; CI = 0.008) bands. No statistically significant differences were observed for low and high gamma (All data are shown in Figure 8 A). Similarly, for the Pre-EC vs Post EC contrast there was a broadband reduction of PSD during ketamine administration (Cluster-based stats = -74.76; $p < 0.001$; CI = 0.002), with reduction in delta (Cluster-based stats = -67.92; $p = 0.002$; CI = 0.003), theta (Cluster-based stats = -151.57; $p < 0.001$; CI = 0.002), alpha (Cluster-based stats = - 221.26; $p < 0.001$; CI = 0.002), and low beta (Cluster-based stats = -152.81; $p < 0.001$; CI = 0.002). Consistent with the EO condition, no differences were found in high beta, low, and high gamma power (All data are shown in Figure 8 B).

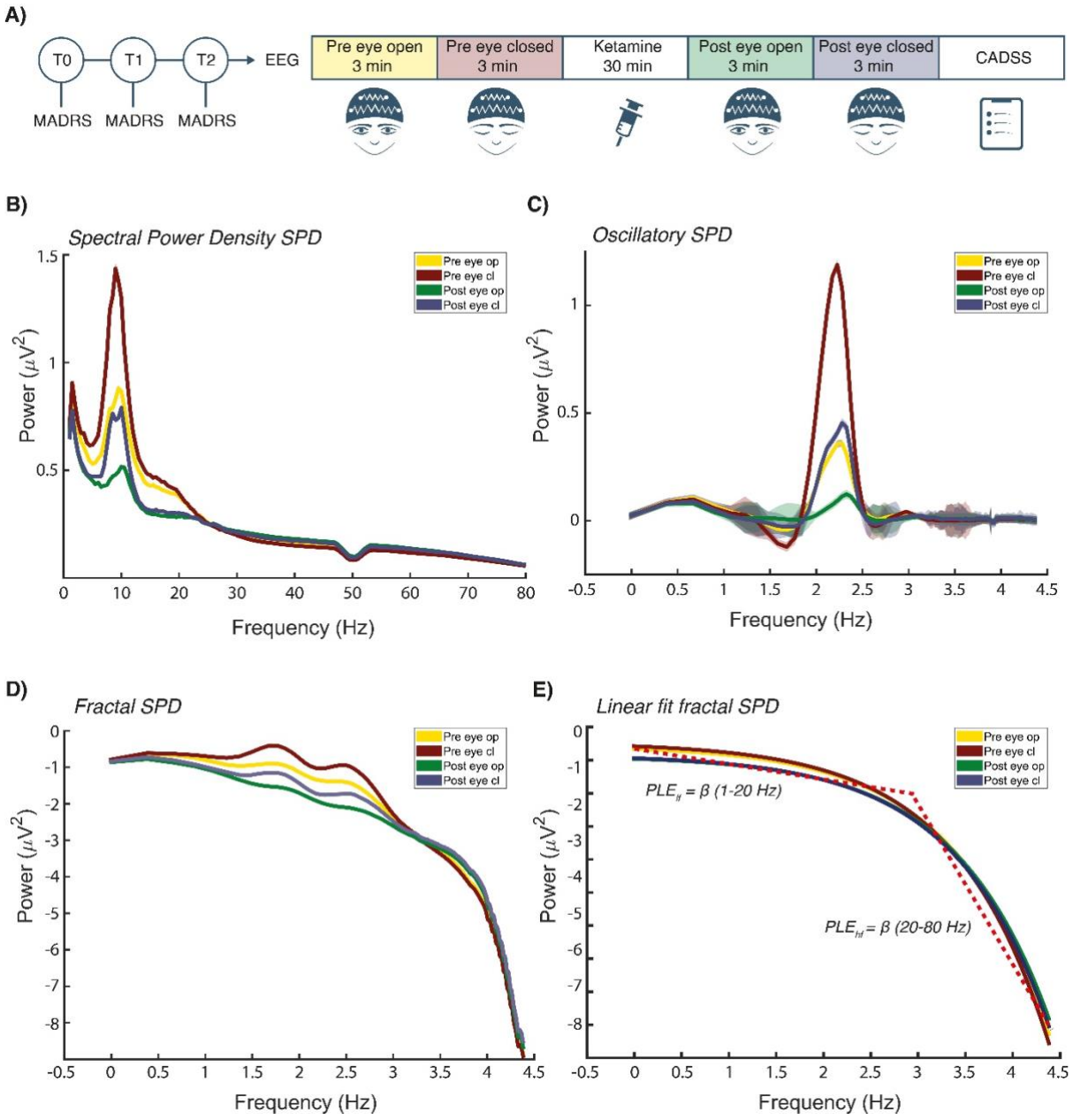


*Figure 7. Study design and power spectra. A) The illustration shows the timeline and structure of the experiment (see materials and methods). B) The frequency/power plot of the power spectral density (PSD). C) The logarithm of the frequency is plotted over the oscillatory component of the power spectra. D) the log-log plot of the power spectra's fractal (scale-free) component. E) The log-log plot of the linear fit of the fractal component of the power spectra. The dashed lines show the interpolated regression lines used to estimate the power-law exponent (PLE) for the low (1- 20 Hz) and high frequencies (20-80 Hz).*

### *Irregular Resampling Auto-Spectral Analysis (IRASA)*

The original PSD was decomposed using the IRASA method into its oscillatory and fractal components. As for the original PSD, the analysis of the oscillatory component of the spectral power for the Pre-EO vs Post-EO contrast showed a significant broadband reduction following ketamine administration (Cluster-based stats = -80.66; $p < 0.001$; CI = 0.002). However, frequency-specific oscillatory power showed significant reductions only for the alpha (Cluster-

based stats = -137.01; p < 0.001; CI = 0.002) and low beta (Cluster-based stats = -73.77; p < 0.001; CI = 0.002) frequencies, while an increase was observed for the low gamma (Cluster-based stats = 64.73; p < 0.001; CI = 0.002) oscillatory power. No differences were observed for delta, theta, high beta, and high gamma (All data are shown in Figure 8 A). A similar reduction of broadband (Cluster-based stats = -119.30; p < 0.001; CI = 0.002), alpha (Cluster-based stats = -162.71; p < 0.001; CI = 0.002), and low beta (Cluster-based stats =-26.54; p = 0.014; CI = 0.007) and increase in low gamma (Cluster-based stats = 53.98; p < 0.001; CI = 0.002) oscillatory power was present for Pre-EC vs Post EC contrast. Interestingly, there was also a reduction of theta (Cluster-based stats = -47.72; p = 0.005; CI = 0.004) as well. No differences were observed for delta, high beta, and high gamma power (All data are shown in Figure 8 B).

The analysis of the fractal component of the spectral power for the Pre-EO vs Post-EO contrast showed a broadband (Cluster-based stats = -66.56; p < 0.001; CI = 0.002) reduction during ketamine, with reductions within the delta (Cluster-based stats = -11.90; p = 0.017; CI = 0.008), theta (Cluster-based stats = -105.12; p < 0.001; CI = 0.002), alpha (Cluster-based stats = -125.30; p < 0.001; CI = 0.002), low beta (Cluster-based stats = -99.45; p < 0.001; CI = 0.002), and high beta (Cluster-based stats = -17.38; p = 0.020; CI = 0.009) bands. No statistically significant differences were observed for low and high gamma fractal power (All data are shown in Figure 8 A). In the Pre-EC vs Post-EC contrast, there was a significant broadband reduction of fractal power (Cluster-based stats = -85.42; p < 0.001; CI = 0.002), with similar decreases in the delta (Cluster-based stats = -37.82; p = 0.002; CI = 0.004), theta (Cluster-based stats = -135.60; p < 0.001; CI = 0.002), alpha (Cluster-based stats = -145.82; p < 0.001; CI = 0.002), low beta (Cluster-based stats = -108.32; p = 0.002; CI = 0.003) and high beta (Cluster-based stats = -9.93; p = 0.021; CI = 0.009) bands, as observed in the other contrast. There were no differences in low and high gamma (All data are shown in Figure 8 B).

***Power-law Exponent (PLE)***

The analysis of the slope of the fractal component of the EEG signal was performed by estimating the PLE for all frequencies (i.e., 1-80 Hz, $PLE_{tot}$), as well as for low frequencies (i.e., 1-20 Hz, $PLE_{lf}$) and high frequencies (20-80 Hz, $PLE_{hf}$) separately (Shown in Figure 7 E). A statistically significant reduction of the $PLE_{tot}$ was observed following ketamine exposure for both the Pre-EO vs Post-EO (Cluster-based stats = -170.15; p < 0.001; CI = 0.002, Figure 9 A) and Pre-EC vs Post-EC contrasts (Cluster-based stats = -166.76; p < 0.001; CI = 0.002, Figure 9 B). Signifying a reduction in the steepness of the 1/f fractal distribution. In particular, there was no difference in the $PLE_{lf}$ and a significant decrease in the $PLE_{hf}$ in Pre-EO vs Post-EO (Cluster-based stats = - 139.88; p < 0.001; CI = 0.002, Figure 9 A) and Pre-EC vs Post-EC

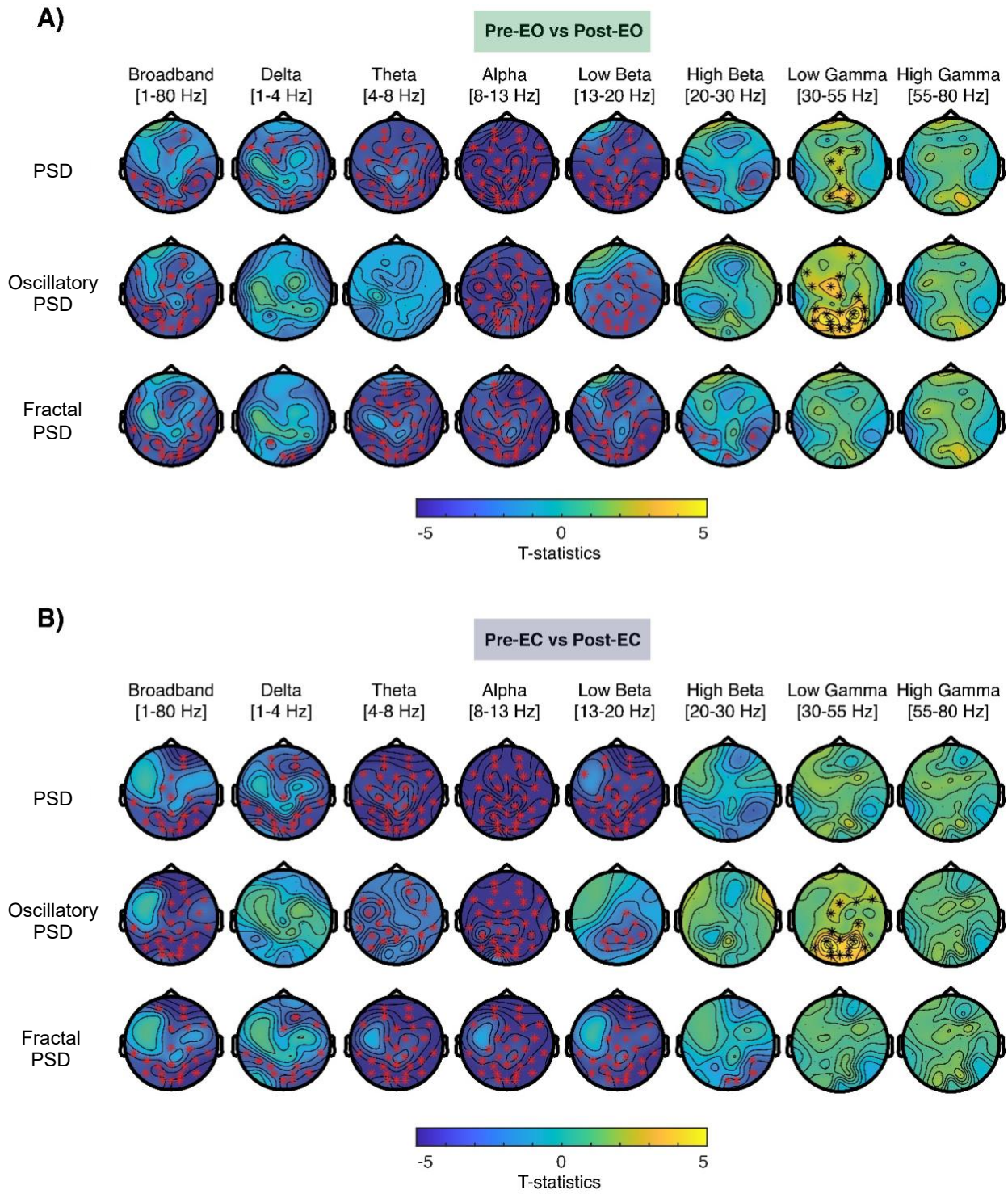


*Figure 8. The rhythmic features of the EEG signal. A) The topoplots of the original, oscillatory, and fractal components of the Power Spectral Density (PSD) for the eyes open condition divided by frequency. B) The topoplots of the original, oscillatory, and fractal components of the PSD for the eyes closed condition divided by frequency. The values in the topoplots correspond to the results of the cluster-based permutation T-statistics. Electrodes belonging to significant clusters are marked in red, if there was a decrease from pre- to post-ketamine, and in black if there was an increase from pre- to post-ketamine. Clusters were considered statistically significant with an α value < 0.025.*

(Cluster-based stats = -127.16; $p < 0.001$; CI = 0.002, Figure 9 B) contrasts. Further analysis of the $PLE_{hf}$ showed that the change in slope was confined within the high beta (20-30 Hz) frequency band in both the Pre-EO vs Post-EO (Cluster-based stats = -179.71; $p < 0.001$; CI = 0.002) and Pre-EC vs Post-EC contrasts (Cluster-based stats = -201.75; $p < 0.001$; CI = 0.002). Therefore, the change in PLE within the high beta ($PLE_{beta}$) was later used for the correlation with the other EEG and behavioral metrics.

*Lempel–Ziv Complexity (LZc)*

Analysis of the broadband entropy of the EEG signal was performed via LZc computation. Both the Pre-EO vs Post-EO (Cluster-based stats = 165.68; $p < 0.001$; CI = 0.002, Figure 9 A) and Pre-EC vs Post-EC contrast (Cluster-based stats = 203.35; $p < 0.001$; CI = 0.002, Figure 9 B) showed a marked increase in LZc following ketamine administration.

*Complexity via State-space Entropy Rate (CSER)*

Analysis of the broadband entropy of the EEG signal averaged across channels performed via CSER, showing an increase in both the Pre-EO vs Post-EO ($\chi^2 = 49.63p < 0.001$; d = 1.29, Figure 9 A) and Pre-EC vs Post-EC ($\chi^2 = 71.92$; $p < 0.001$; d = 1.55, Figure 9 B) contrasts. The results of CSER were consistent with what was observed for LZc averaged across channels (both pre-processed at 160 Hz and 500 Hz sampling rates, data not shown). Frequency-decomposed CSER showed an increase within the delta ($\chi^2 = 9.06$; $p = 0.003$; d = 0.55), high beta ($\chi^2 = 38.24$; $p < 0.001$; d = 1.13), low gamma ($\chi^2 = 81.33$; $p < 0.001$; d = 1.65), and high gamma ($\chi^2 = 46.40$; $p < 0.001$; d = 1.24) bands but a decrease within alpha ($\chi^2 = 38.79$; $p < 0.001$;d = - 1.14) and low beta ($\chi^2 = 13.09$; $p < 0.001$; d = -0.66) bands for the Pre-EO vs Post-EO contrast (Figure 9 A). Similar results were obtained for the Pre-EC vs Post-EC contrast (Figure 9 B), with the exception of no significant differences for low beta; delta ($\chi^2 = 15.53$; $p < 0.001$; d = 0.72), theta (ns), alpha ($\chi^2 = 26.18$; $p < 0.001$; d = -0.93), high beta ($\chi^2 = 78.56$; $p < 0.001$; d = 1.62), low gamma ($\chi^2 = 96.20$; $p < 0.001$; d 1.79), high gamma ($\chi^2 = 56.70$; $p < 0.001$; d = 1.37).

***Correlation between EEG metrics***

There was a statistically significant negative correlation between relative change in broadband CSER and $PLE_{\beta}$ in the EC contrasts (p adj. = 0.012). Within the α band, the change in CSER and $PLE_{\beta}$ correlated positively (EO, p adj. < 0.001; EC, p adj. = 0.011), as did the change in oscillatory power with $PLE_{\beta}$ in both contrasts (EO, p adj. < 0.001; EC, p adj. = 0.017). In the low γ band, there was a negative correlation between changes in CSER and $PLE_{\beta}$ in the EC contrast (p adj. = 0.019). All data are shown in Table 5.

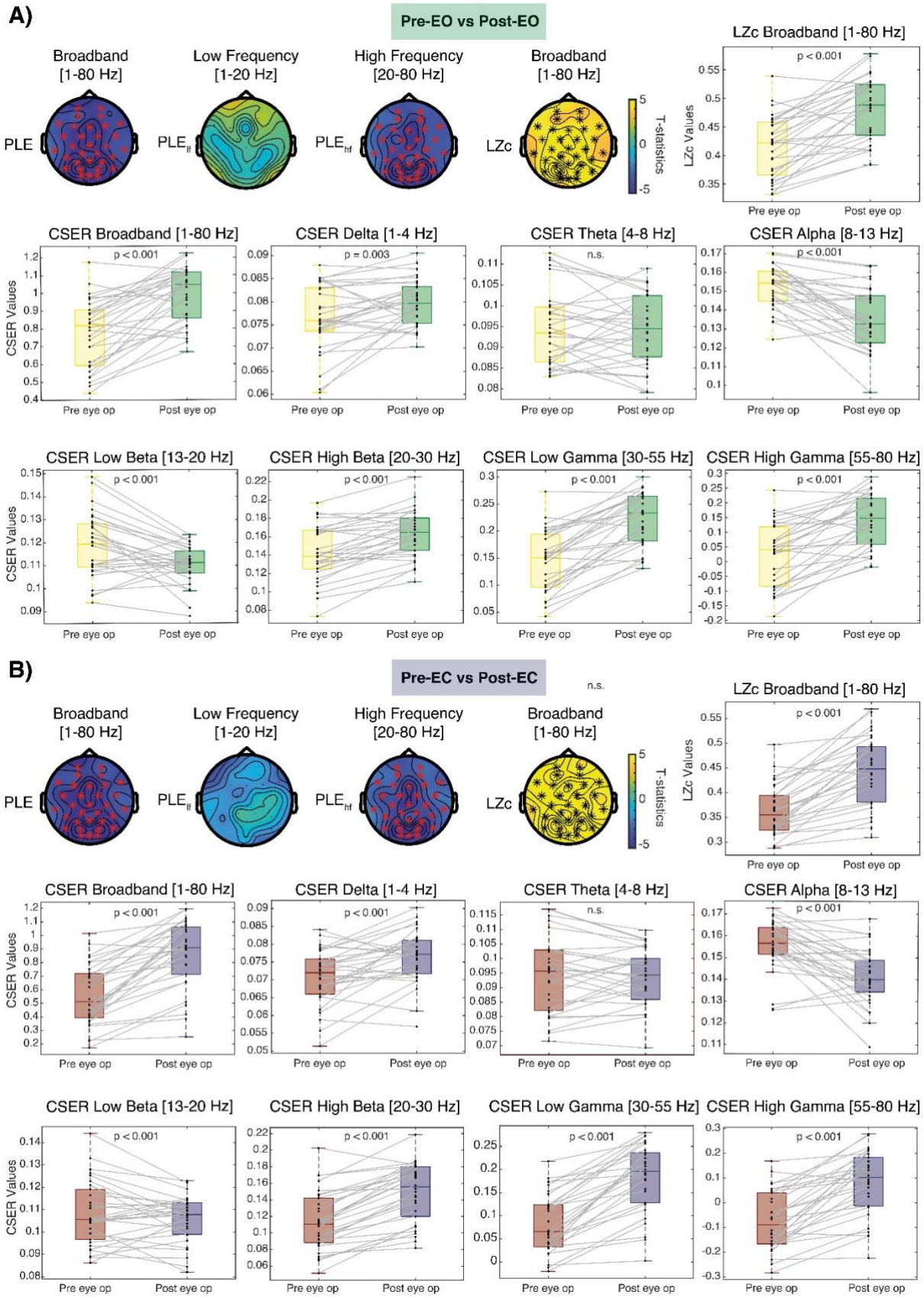


*Figure 9. The arrhythmic features of the EEG signal. A) The difference in arrhythmic features of the EEG signal in the eyes open condition. B) The difference in arrhythmic features of the EEG signal in the eyes closed condition. Those include the topoplots of the power-law exponent (PLE) for low frequencies (PLElf) and high frequencies (PLEhf), the topoplot of the*

*normalized Lempel-ziv Complexity (LZc), and the channel average of the LZc as well as broadband and frequency-decomposed Complexity via State-space Entropy Rate (CSER). The values in the topoplots correspond to the results of the cluster-based permutation T-statistics. Electrodes belonging to significant clusters are marked in red, if there was decrease from pre- to post-ketamine, and in black if there was an increase from pre- to post-ketamine. Clusters were considered statistically significant with an α value < 0.025.*

| Condition | EEG Metric 1 | EEG metric 2 | ρ coefficient | p value | p adj |
|---|---|---|---|---|---|
| **Pre-EO vs Post-EO** | oscillatory α | $PLE_{\beta}$ | 0.69 | < 0.001*** | < 0.001*** |
| | oscillatory α | CSER α | 0.36 | 0.05* | 0.315 |
| | oscillatory low β | $PLE_{\beta}$ | 0.29 | 0.117 | 0.328 |
| | oscillatory low β | CSER low β | -0.01 | 0.957 | 0.957 |
| | oscillatory low γ | $PLE_{\beta}$ | 0.11 | 0.545 | 0.647 |
| | oscillatory low γ | CSER low γ | 0.07 | 0.714 | 0.798 |
| | oscillatory low γ | $PLE_{\beta}$ | -0.34 | 0.071 | 0.328 |
| | oscillatory low γ | CSER low γ | -0.19 | 0.311 | 0.423 |
| | oscillatory broadband | $PLE_{\beta}$ | 0.05 | 0.774 | 0.817 |
| | oscillatory broadband | CSER tot | 0.21 | 0.26 | 0.414 |
| | $PLE_{\beta}$ | CSER tot | -0.30 | 0.112 | 0.328 |
| | $PLE_{\beta}$ | CSER δ | -0.19 | 0.301 | 0.423 |
| | $PLE_{\beta}$ | CSER θ | 0.23 | 0.226 | 0.414 |
| | $PLE_{\beta}$ | CSER α | 0.68 | < 0.001*** | < 0.001*** |
| | $PLE_{\beta}$ | CSER β | -0.21 | 0.262 | 0.414 |
| | $PLE_{\beta}$ | CSER low β | 0.16 | 0.402 | 0.509 |
| | $PLE_{\beta}$ | CSER high β | -0.29 | 0.121 | 0.328 |
| | $PLE_{\beta}$ | CSER low γ | -0.24 | 0.202 | 0.414 |
| | $PLE_{\beta}$ | CSER high γ | -0.22 | 0.249 | 0.414 |
| **Pre-EC vs Post-EC** | oscillatory θ | CSER high β | 0.20 | 0.279 | 0.456 |
| | oscillatory θ | CSER θ | -0.13 | 0.483 | 0.655 |
| | oscillatory α | $PLE_{\beta}$ | 0.52 | 0.004** | 0.017* |
| | oscillatory α | CSER α | 0.67 | < 0.001*** | 0.001*** |
| | oscillatory low β | $PLE_{\beta}$ | -0.20 | 0.288 | 0.456 |
| | oscillatory low β | CSER low β | 0.09 | 0.652 | 0.774 |
| | oscillatory low γ | $PLE_{\beta}$ | -0.30 | 0.112 | 0.236 |
| | oscillatory low γ | CSER low γ | -0.05 | 0.805 | 0.805 |
| | oscillatory broadband | $PLE_{\beta}$ | -0.43 | 0.018* | 0.056 |
| | oscillatory broadband | CSER tot | 0.18 | 0.334 | 0.488 |
| | $PLE_{\beta}$ | CSER tot | -0.55 | 0.002** | 0.012* |
| | $PLE_{\beta}$ | CSER δ | -0.10 | 0.587 | 0.743 |
| | $PLE_{\beta}$ | CSER θ | 0.06 | 0.739 | 0.805 |
| | $PLE_{\beta}$ | CSER α | 0.57 | 0.001** | 0.011* |

| | | | | | |
|---|---|---|---|---|---|
| | $PLE_{\beta}$ | CSER low β | -0.06 | 0.769 | 0.805 |
| | $PLE_{\beta}$ | CSER high β | -0.27 | 0.155 | 0.295 |
| | $PLE_{\beta}$ | CSER low γ | -0.50 | 0.005** | 0.019* |
| | $PLE_{\beta}$ | CSER high γ | 0.33 | 0.076 | 0.206 |

*Table 5. Correlation between EEG metrics. The results of pairwise Spearman correlations between relative changes in EEG metrics after ketamine. The p values were adjusted for multiple comparisons using the using the Benjamini-Hochberg adjustment (p adj.). * Statistically significant results at α-level ≤ 0.05; ** Statistically significant results at α-level ≤ 0.01; *** Statistically significant results at α-level ≤ 0.001.*

### *Correlation between EEG metrics and ketamine dose*

*Power Spectral Density (PSD)*

Analysis of the relationship between PSD and ketamine dose delivered during the EEG measurement showed a negative correlation between dosage with Δ alpha (R = -0.40; p = 0.028) and Δ low beta (R = -0.40; p = 0.031) in the Pre-EC vs Post-EC contrast only (Figure 4 B). This result was confirmed when using the relative Δ alpha (R = -0.41; p = 0.024) and Δ low beta (R = -0.36; p = 0.049) change.

*Irregular Resampling Auto-Spectral Analysis (IRASA)*

No significant correlations were found between dose and raw changes in oscillatory power in any of the analyzed contrasts (Figure 10). When considering the relative difference, there was a statistically significant negative correlation between oscillatory Δ broadband (R = -0.38 ; p = 0.039) and Δ theta (R = -0.40 ; p = 0.027) in the Pre-EC vs Post-EC contrast.

*Power-law exponent (PLE)*

There was a significant negative correlation between dosage and the raw Δ $PLE_{beta}$ range (R = - 0.37 ; p = 0.047) in the Pre-EC vs Post-EC contrast only (Figure 10 B).

*Lempel–Ziv Complexity (LZc)*

There was a statistically significant positive correlation between dose and raw (R = 0.40 ; p = 0.028; Figure 10 B) and relative (R = 0.39 ; p = 0.034) Δ LZc in the Pre-EC vs Post-EC contrast only.

*Complexity via State-space Entropy Rate (CSER)*

There was a negative correlation between dose and raw Δ CSER in the alpha (R = -0.51, p = 0.004) and low beta band (R = -0.40, p = 0.027) in the Pre-EO vs Post-EO contrast (Figure 4 A). Using the relative change the same correlations were observed: dose and Δ CSER alpha (R = -0.49, p = 0.006), dose and CSER low beta (R = -0.39, p = 0.031). A negative correlation was also present

between dose and raw (R = -0.41, p =0.023; Figure 4 B) and relative (R = -0.41, p =0.024) Δ CSER and in the alpha band and dose in the Pre-EC vs Post-EC contrast.

None of the observed correlations between EEG metrics and ketamine dosage survived correction for multiple comparisons.

***Correlation between EEG metrics and CADDS***

*Power Spectral Density (PSD)*

Analysis of the correlation between PSD and CADSS scores showed a statistically significant positive correlation between Δ broadband PSD and total CADSS (R = 0.39; p = 0.035) and derealization (R = 0.52; p = 0.003) scores in the Pre-EO vs Post-EO contrast. The Pre-EC vs Post-EC contrast showed a positive correlation between Δ delta and CADSS derealization (R = 0.39; p = 0.033). When using the relative difference, the correlations between CADSS derealization and Δ broadband in the Pre-EO vs Post-EO contrast (R = 0.48; p = 0.007) and with Δ delta and in the Pre-EC vs Post-EC contrast (R = 0.36; p = 0.047) held.

With the exclusion of the outlier on the CADSS, there was a positive correlation between total CADSS score and Δ broadband in the Pre-EO vs Post-EO (R = 0.44; p = 0.016; Figure 10 A) and Pre-EC vs Post-EC (R = 0.40; p = 0.032; Figure 10 B) contrasts. In particular, Δ broadband correlated positively with CADSS derealization scores in the Pre-EO vs Post-EO (R = 0.62; p < 0.001; Figure 4 A) and Pre-EC vs Post-EC (R = 0.48; p = 0.009; Figure 10 B) contrasts. Scores on CADSS derealization correlated positively with Δ theta (R = 0.41; p = 0.027), alpha (R = 0.40; p = 0.030), and high beta (R = 0.40; p = 0.031) In the Pre-EO vs Post-EO contrast (Figure 10 A) and with Δ delta (R = 0.49; p = 0.007) and theta (R = 0.41; p = 0.028) in the Pre-EC vs Post-EC contrast (Figure 10 B). Using the relative change, the correlation between CADSS derealization Δ broadband (R = 0.47; p = 0.009) and high beta (R = 0.42; p = 0.022) was maintained in the Pre-EO vs Post-EO contrast and with Δ delta in the Pre-EC vs Post-EC contrast (R = 0.45; p = 0.014).

*Irregular Resampling Auto-Spectral Analysis (IRASA)*

No significant correlations were found between CADSS scores and raw changes in oscillatory power in any of the analyzed contrasts. With the relative change, there was a negative correlation between the oscillatory Δ low beta and CADSS depersonalization scores (R = -0.37; p = 0.044) in the Pre-EO vs Post-EO contrast.

The exclusion of the outlier leads to a significant positive correlation between raw Δ oscillatory broadband and scores in total (R = 0.41; p = 0.030) and derealization (R = 0.39; p = 0.034) CADSS scores in the Pre-EC vs. Post-EC contrast (Figure 10 B).

*Power-law exponent (PLE)*

No significant correlations were found between CADSS scores and changes in $PLE_{beta}$ in any of the analyzed contrasts (Figure 10).

*Lempel–Ziv Complexity (LZc)*

No significant correlations were found between CADSS scores and changes in LZc in any of the analyzed contrasts (Figure 10).

*Complexity via State-space Entropy Rate (CSER)*

No significant correlations were found between CADSS scores and changes in CSER in any of the analyzed contrasts (Figure 10).

None of the observed correlations survived comparison for multiple comparisons.

*Correlation between EEG metrics and MADRS T2 (EEG day)*

No significant correlations were found between MADRS scores before ketamine and changes in EEG metrics in any of the analyzed contrasts (Figure 10).

***Early vs Late responders***

Modulation of EEG metrics induced by ketamine was compared between patients who responded to ketamine treatment at T1 (i.e., ER group) and patients who responded after repeated exposures (i.e., LR group). The groups showed no statistically significant differences in MADRS at T2 and baseline EEG metrics.

*Power Spectral Density (PSD)*

No statistically significant interactions were observed between raw changes in PSD and groups in any of the analyzed contrasts.

*Irregular Resampling Auto-Spectral Analysis (IRASA)*

No statistically significant interactions were observed between raw or relative changes in oscillatory power and groups in any of the analyzed contrasts.

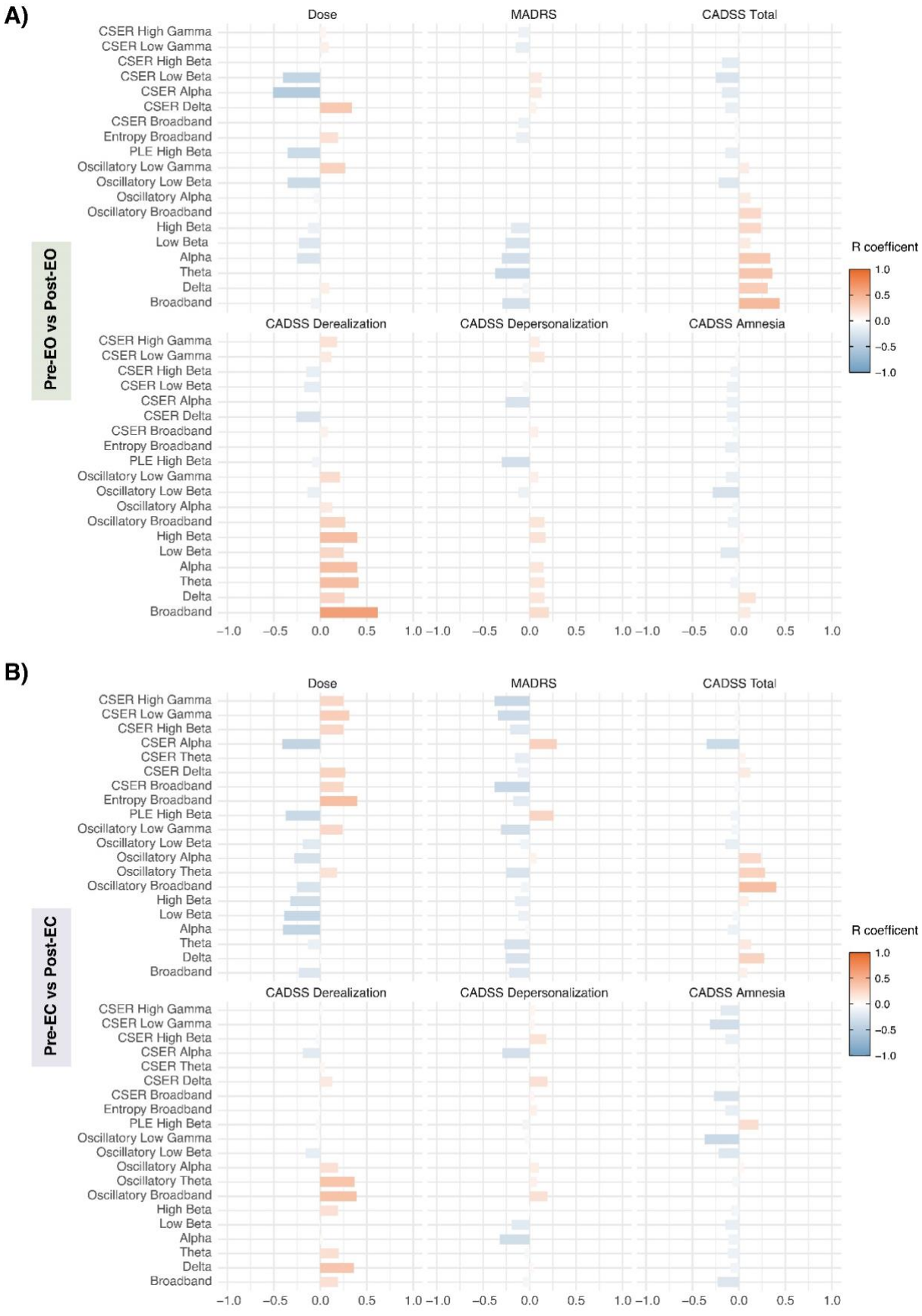


*Figure 10. The correlations between EEG metrics and ketamine dose, CADSS,*

*(Clinician-Administered Dissociative States Scale) and MADRS (Montgomery-Åsberg Depression Rating Scale) scores at T2. A) The Spearman correlation coefficient is plotted for each pairwise correlation between EEG metrics and ketamine dose, CADSS scores, and MADRS scores at T2 for the eyes open condition. B) The Spearman correlation coefficient is plotted for each pairwise correlation between EEG metrics and ketamine dose, CADSS scores, and MADRS scores at T2 for the eyes closed condition. All correlations are shown with the raw change in EEG metrics. All correlations with the CADSS are shown without the inclusion of the outlier. T0 = the time of recruitment*; T1 = *1 week after the beginning of the treatment*; T2 = *before the ketamine infusion with concurrent EEG recording (T2)*. CSER = *Complexity via State-space Entropy Rate; PLE = Power Law Exponent.*

*Power-law exponent (PLE)*

There was a significant difference between the ER and LR groups in $PLE_{beta}$ decrease in the Pre-EC vs Post-EC contrast (Cluster-based stats = 43.40; p = 0.007; CI = 0.005). In particular, the LR group showed a higher decrease in $PLE_{beta}$ as compared to the LR group following ketamine exposure. Given the previously reported correlation between $PLE_{beta}$ decrease and dose in the Pre-EC vs. Post-EC contrast and that LR had higher dosages than ER due to the treatment schedule, we performed an analog analysis correcting for dose. The interaction effect was still significant after using dose as a covariate ($\chi^2$ = 4.50; p= 0.034; Figure 11 C).

*Lempel–Ziv Complexity (LZc)*

There was a significant difference in LZc increase between the ER and LR groups in the Pre-EC vs. Post-EC contrast (Cluster-based stats = -15.85; p = 0.031; CI = 0.011). In particular, the LR group showed a higher increase in LZc as compared to the ER group following ketamine exposure. After correcting for dose, the interaction effect was still significant ($\chi^2$ = 5.62; p= 0.018; Figure 11 D).

*Complexity via State-space Entropy Rate (CSER)*

The comparison of the change in broadband CSER averaged across channels did not show a statistically significant change between the ER and LR groups in either contrast, even though it followed the same trend of LZc but not as robustly. Spectral decomposition of the CSER showed that the LR had a steeper decrease in CSER within the alpha band in both the Pre-EO vs Post-EO ($\chi^2$ = 10.39; p= 0.001) and Pre-EC vs Post-EC ($\chi^2$ = 9.62; p= 0.002) contrasts. Those effects were not altered when correcting for ketamine dose for both contrasts: Pre-EO vs Post-EO ($\chi^2$ = 10.39; p= 0.001; Figure 11 A); Pre-EC vs Post-EC ($\chi^2$ = 9.62; p= 0.002; Figure 11 E). The LR had a steeper decrease in CSER within the low beta ($\chi^2$ = 9.13; p= 0.003; Figure 11 B) band in the Pre-EO vs Post-EO, which was not affected by dose. Also, LR had a higher increase in the low gamma CSER ($\chi^2$ = 4.19; p= 0.041; Figure 11 F) as compared to ER in the Pre-EC vs Post-EC contrast, independent of drug dosage.

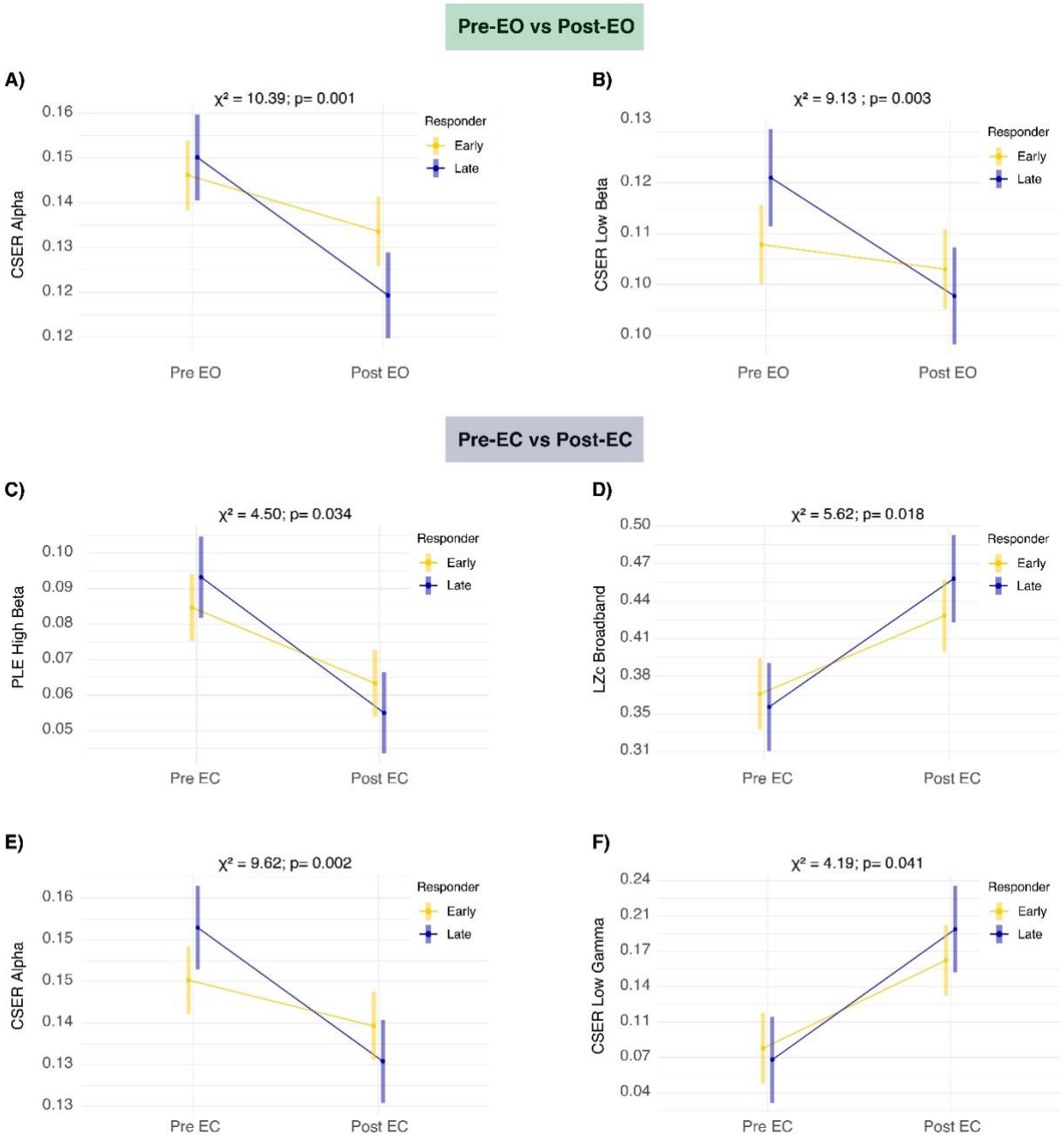


*Figure 11. The difference in EEG metrics of ketamine action between early and late responders. A) The difference in Complexity via State-space Entropy Rate (CSER) decreases within the alpha band in the eyes open condition. B) The difference in CSER decreases within the low beta band in the eyes open condition. C) The difference in high beta power-law exponent (PLE) reduction in the eyes closed condition. D) The difference in normalized Lempel–Ziv complexity (LZc) increases in the eyes closed condition. E) The difference in CSER decreases within the alpha band in the eyes closed condition. F) The difference in CSER increases within the low gamma band in the eyes closed condition. Significance levels for the interaction effects were defined at α < 0.05. All p-values are corrected for the ketamine dose.*

# Discussion

The EEG changes induced by a single administration of a sub-anesthetic dose of ketamine were investigated in a cohort of hospitalized patients with TR-BP undergoing treatment for depression in the frame of a fully ecological setting. At the time of the ketamine infusion with concurrent EEG measurement, all patients had manifested a clinical response to the repeated infusion treatment protocol. The chosen ketamine dose for acute EEG recording fell within the known range associated with clinically meaningful subjective effects, as corroborated by scores on the CADSS. The analysis focused on rhythmic and arrhythmic features of the resting-state EEG signal before and immediately after one of the infusions of ketamine envisaged by the treatment protocol and related those metrics with the subjective experience induced by the drug. Additionally, the neurophysiological changes induced by ketamine were compared between patients who responded within one week of treatment and those who reacted later.

The analysis revealed an intricate pattern of EEG changes induced by ketamine across various rhythmic and arrhythmic signal features. Most of the observed EEG changes in spectral power and its oscillatory and spectral components (Figure 8) and measures of scale-free activity and entropy (Figure 9) were distributed across the scalp. In fact, using cluster-based permutation as test statistics without selecting a-priori regions of interest is not informative about spatially specific effects (Sassenhagen & Draschkow, 2019). Therefore, the presented results and subsequent interpretation will be understood as generalized across EEG channels.

### *Ketamine's Effects on Rhythmic and Arrhythmic EEG Features*

Ketamine elicited a broad reduction in spectral power, particularly evident in the delta, theta, alpha, and beta bands, irrespective of whether patients had their eyes open or closed. This observation aligns with findings from prior studies employing similar dosing administration protocols in both healthy individuals and patients with depression (de la Salle et al., 2016, 2022; A. E. M. Forsyth et al., 2021; V. J. Knott et al., 2011; Lijffijt et al., 2022; McMillan et al., 2019, 2020; Shaw et al., 2015; Vlisides et al., 2018). The EEG spectra oscillatory component analysis revealed that ketamine predominantly diminished low-frequency oscillatory activity in the theta, alpha, and low beta bands while concurrently increasing activity in the low gamma frequency band. This elevated oscillatory power in the high-frequency band is consistent with previously documented observations in both pre-clinical and human studies (for a review, see McMillan & Muthukumaraswamy, 2020). These outcomes reinforce existing evidence regarding the ketamine-induced effects of low-frequency desynchronization and increased high-frequency activity.

The data presented herein align with the "disinhibition hypothesis" concerning ketamine's acute mechanism of action, as discussed in the previous chapter. At sub-anesthetic doses, ketamine is postulated to diminish low-frequency synchronous activity by selectively inhibiting GluN2D-containing NMDA receptors expressed on GABA-inhibitory interneurons. This inhibition interrupts local cortical circuit firing due to the disinhibition of cortical pyramidal neurons. Consequently, there is a desynchronization of slow rhythmic activities, such as delta, theta, alpha, and low beta, coupled with an overall increase in local activity levels due to glutamate release, determining an elevation of gamma frequency (Zanos & Gould, 2018). Ketamine's impact on NMDA receptors expressed in fast-spiking interneurons is proposed to disrupt the regulatory feedback of the PING mechanism to generate the increase in tonic gamma activity. This is substantiated by evidence demonstrating that NMDA receptor antagonists enhance gamma activity across various brain regions (Pinault, 2008). Pharmacological restoration of GABAergic input to pyramidal neurons disrupts the ketamine-induced increase in cortical excitation. The dysfunction of NMDA receptors expressed on inhibitory interneurons enhances baseline cortical gamma rhythms, as shown in-vivo and in-silico (Carlén et al., 2012; Ma & Leung, 2007; Susin & Destexhe, 2023). Consequently, alterations in gamma rhythms are posited to result from a shift in the cortical excitatory/inhibitory balance toward higher excitability, serving as a crucial index of cognitive and emotional functioning within the brain.

Several studies indicate that brain oscillations may serve as a potential biomarker for depression and the antidepressant effects of ketamine (de Aguiar Neto & Rosa, 2019). In a large-scale investigation conducted by Grin-Yatsenko et al. (2010), patients exhibited increased activity in theta, alpha, and beta bands compared to healthy subjects, suggesting a potential role for modulating slow-wave activity in the antidepressant action of ketamine (Grin-Yatsenko et al., 2010). This result was confirmed by later studies, even though some discrepancies exist in the literature (de Aguiar Neto & Rosa, 2019). Nonetheless, the result is intriguing in light of neuroimaging findings showing ketamine-induced decreases in low-frequency activity. It increases high-frequency activity in brain networks associated with depressive symptomatology, such as the default-mode network (Zacharias et al., 2020). Recently, gamma rhythms have received considerable attention as potential biomarkers of depression and antidepressant action, as reviewed by Fitzgerald and Watson (2018) (Fitzgerald & Watson, 2018). The authors also summarize evidence showing that gamma rhythms in individuals with unipolar depression are distinct (generally higher) from those found in bipolar disorder, including bipolar depression. While mixed findings exist due to methodological heterogeneity and standardization challenges in the gamma frequency range, the notion of an "optimal" amount of gamma corresponding to stable mood states has been proposed. In this perspective, one possible ketamine mechanism of action would involve the modulation of gamma rhythms. However, caution is warranted in

interpreting data from non-invasive EEG measures of gamma oscillations in humans due to the inherent difficulty in achieving reliable measurements (Hipp & Siegel, 2013). To summarize, the results regarding the effects of ketamine on rhythmic brain activity align largely with the existing literature, and these findings can be extended to a cohort TR-BP in a real-world hospital setting.

The modulation of oscillatory activity patterns was accompanied by a reduction in fractal (scale-free) arrhythmic activity, particularly in the low frequencies. While the exact significance of the power of scale-free activity remains uncertain, the functional importance of the slope of the 1/f distribution has been proposed (B. J. He et al., 2010). Ketamine produced a "flattening" of the slope of the power spectra, evident in both eyes open and closed conditions. This effect is consistent with what was reported in healthy subjects by the only available study that quantified the PLE with ketamine (Muthukumaraswamy & Liley, 2018). With the present experiment, the findings of Muthukumaraswamy and Liley have been extended to a patient population with TR.BP. In particular, the flattening of the slope was observed in the high-frequency band (20 to 80 Hz) and was predominately localized in the high beta-frequency band. The specificity of the effect above the "knee" frequency of 20 Hz in the data is in striking accordance with the modeling work of Gao et al. (2017) (Gao et al., 2017). They demonstrated that the slope of the 1/f distribution of the fractal component of a spectrum, simulated by an excitatory and an inhibitory neural population, correlates with the excitatory/inhibitory ratio for frequencies above 20 Hz. Decreasing the excitatory/inhibitory ratio steepens the slope of the power spectra, as evidenced by invasive EEG recordings in macaques during propofol sedation. Therefore, there is an intriguing possibility that the observed changes in the slope of the scale-free component of the power spectra are influenced by the stimulation of glutamatergic activity by ketamine, connecting rhythmic and arrhythmic effects (discussed below). While further research is necessary to substantiate this conclusion, the results of the present study suggest a potential role for the scale-free properties of EEG as biomarkers of mood disorders and ketamine antidepressant effect.

***Increases in Brain Entropy***

The analysis of the temporal non-linear properties of the EEG signal revealed that ketamine-induced a widespread increase in the entropy of brain activity. This effect was consistent for both eyes open and closed conditions and aligned with observations in healthy subjects and a cohort of late-life patients with depression (Farnes et al., 2020, 2020; D. Li & Mashour, 2019; Murphy et al., 2023; M. M. Schartner et al., 2017). Additionally, a novel measure of informational complexity was applied to achieve the spectral decomposition of signal entropy (Mediano et al., 2023). The analysis indicated that the increase in broadband entropy induced by ketamine was driven by changes within the high frequencies, such as high beta and low and high gamma, while signal

entropy tended to decrease in the low frequencies, particularly in alpha and low beta (despite an increase in delta). The observed increase in gamma and reduction in alpha is akin to the findings reported by Mediano et al. in the validation of the method on healthy individuals following acute administration of classic psychedelics. The present study represents the first application of the novel estimator CSER to investigate the effects of ketamine on spectrally decomposed neural entropy. While little is known about the neurophysiological significance of complexity measures of circuit neural activity, alterations of such metrics have been reported in several neuropsychiatric conditions (for a review, see Lau 2022 (Lau et al., 2022)). Modulations of brain signal entropy following exposure to ketamine and classic psychedelics have been proposed to underlie the "richness" of the content of conscious experience, indicating a state of higher meta-stability and cognitive flexibility, potentially providing a mechanism for the anti-depressive effects of these compounds (Carhart-Harris, 2018). Previous studies have reported overall lower values of complexity in the EEG signals of individuals with depression compared to healthy controls, suggesting a link with depressive symptoms, such as rumination and a tendency to fixate on negative emotional states, both associated with lower EEG complexity (de Aguiar Neto & Rosa, 2019). However, a causal link between the acute state of complexity induced by ketamine and classic psychedelics and therapeutic response remains uncertain.

Moreover, some studies report an opposite trend, with positive relationships between the severity of depressive symptoms and various EEG complexity indexes. For instance, a study found that depressed patients had higher baseline LZc compared to controls, and antidepressant treatment normalized brain complexity (Méndez et al., 2012). Discrepancies in the literature may arise from the heterogeneity of complexity measures used and the high state-dependency of these metrics. The present results support the proposition of increased neural entropy as a mechanism of ketamine action, and future comparative research should address differences in this mechanism with conventional antidepressants.

The analysis of the interplay between rhythmic and arrhythmic components of the EEG signal revealed that the reduction in broadband oscillatory power (predominantly low-frequency) and the flattening of the slope of the fractal component of the spectra induced by ketamine were both associated with the increase in signal entropy. Those parameters were also modulated by ketamine dosage, providing evidence for a coherent neurophysiological profile of ketamine action. The frequency-specific investigation of the EEG signal revealed an intricate relationship among EEG metrics. The modulation of complexity and oscillatory power demonstrated concordant changes in the alpha, low beta, and gamma frequencies. Precisely, the reduction in oscillatory activity in alpha and low beta corresponded to a decrease in signal entropy within those frequencies, while increases in low gamma oscillatory activity were associated with

heightened entropy. Given that entropy measures the unpredictability of the neural signal, an increase in its value with increases in high-frequency activity is likely expected. Conversely, the reduction of entropy alongside diminished slow-wave synchronous activity is noteworthy. However, in the obtained data, the complexity and oscillatory power reduction were significantly correlated only in the low beta but not in alpha. Further research is necessary to elucidate the neurophysiological significance of this finding. Additionally, no clear relationship between oscillatory activity and signal entropy for frequencies such as delta, theta, high beta, and gamma was discerned.

Regarding the relationship between oscillatory activity and the 1/f distribution of the spectra, interesting associations were identified specifically within alpha and low gamma activity. The correlation between alpha oscillatory power and the 1/f properties of the spectra supports the model proposed by Muthukumaraswamy and Liley, suggesting that the dampening of the alpha oscillator is a fundamental determinant of changes in the slope of the fractal distribution of power spectra (Muthukumaraswamy & Liley, 2018). The association between changes in PLE and low gamma oscillatory power also implies the involvement of high-frequency oscillators in modulating the slope of the fractal component of the spectra. However, the effect in gamma was smaller in magnitude compared to alpha and not consistent across conditions. Nevertheless, this result suggests that alterations in the excitatory/inhibitory balance, influenced by the glutamatergic action of ketamine, may represent a common mechanism underlying high-frequency rhythmic activity and the arrhythmic properties of the spectra. Notably, the reduction in brain entropy within alpha and the increase in gamma frequencies were the only ones associated with changes in the slope of the 1/f distribution, an association also observed at the broadband level. This relationship between signal entropy and PLE reductions introduces a novel possible effect of ketamine manifested in the non-linear dynamics of the signal. Specifically, since the power spectrum is equivalent to the Fourier transform of the autocovariance function (as per the "Wiener-Khinchin theorem"), a reduced PLE indicates shorter/weaker autocorrelation in the time domain. According to He's proposition (2014), the reduction of temporal autocorrelation (i.e., redundancy) underlies higher online information processing. This finding might have important implications for the "entropic brain hypothesis," providing a link with the underlying excitatory/inhibitory balance that warrants further investigation (B. J. He, 2014).

Of note, a differential effect of ketamine was observed within the beta frequency, with low beta and high beta exhibiting markedly different EEG profiles. The intersection between low and high beta was the "knee" frequency of the fractal component of the spectra in the data, and the change in PLE was observed in the high beta frequency, suggesting an essential role for the beta frequency in the overall neurophysiological effects of ketamine. Additionally, the differential

behavior within the beta frequency may help explain some of the inconsistencies in the literature regarding the effects of ketamine within this frequency band.

Taken together, the observed EEG effects of ketamine, including low-frequency desynchronization, increased gamma oscillatory activity, reduction of the slope of scale-free activity, and high-frequency increases in brain entropy, collectively indicate a global shift in brain activity toward a more autonomous and unpredictable state. There is suggestive evidence that these changes may be manifestations of an altered excitatory/inhibitory balance induced by the glutamatergic action of ketamine. Such alterations could contribute to the disintegration and desegregation of higher-order functional networks, potentially underpinning the altered state of consciousness produced by subanaesthetic doses of ketamine.

***Relationship Between EEG Changes and Subjective Experience***

In this regard, analyzing the relationship between EEG modulation and reported dissociation experiences induced by ketamine yielded unexpected results. The overall reduction in spectral power and its oscillatory component were predominantly positively correlated with scores on the CADSS, suggesting that a smaller magnitude of EEG effects of ketamine is associated with a higher intensity of subjective experience. However, these effects were not robust against correction for multiple comparisons. Additionally, no significant associations were found with the arrhythmic components of the EEG. Limitations of the study might help to elucidate these findings. The study utilized the CADSS to measure the subjective effects of ketamine, which was chosen for its widespread use in similar studies, but the scale has several limitations. Inconsistent results have been reported when employing the CADSS to study the subjective effects of ketamine. In particular, comparisons of the CADSS with qualitative reports of the subjective experience induced by ketamine have indicated that the scale fails to capture important themes of the experience. Low scores on the CADSS were often associated with reports of clinically significant drug effects (van Schalkwyk et al., 2018). These limitations may stem from the fact that the CADSS was originally developed to capture symptoms of dissociation in conditions such as dissociative disorders and trauma (Bremner et al., 1998), possibly making it unsuitable for capturing the transitory and psychedelic-like alteration of consciousness induced by ketamine. The unique nature of the ketamine subjective experience warrants a more specific scale, which is currently lacking. Future research into ketamine action should also consider adopting the neurophenomenological approach to altered states of consciousness proposed by Timmerman et al. (2022), aiming to extract fine-graded and specific properties of the drug (Timmermann et al., 2023). However, the application of thorough yet time-consuming methods for investigating

subjective experience might be challenging in real-world, hospitalized settings. Finally, the present study employed a non-validated scale translation, introducing additional bias.

One of the most intriguing findings of the current study pertains to the divergence in neurophysiological responses to ketamine intervention between patients who exhibited a response after one week of treatment and those who responded later. Specifically, patients with a delayed response to repeated ketamine administration displayed a greater magnitude of change in EEG features following ketamine exposure compared to patients with an early response. Importantly, these effects were not attributable to ketamine dosage, nor were they determined by differences in neurophysiological markers or the severity of depression before drug administration. This distinctive response suggests that individual differences in the pathological phenotype of patients may dictate a specific sensitivity to drug effects. This perspective aligns with a recent model proposed by Girn et al. (2023), positing that the spatiotemporal trajectory of neural dynamics in response to mind-altering drugs varies based on an individual's brain structural and functional architecture, as well as their acute psychological state (Girn et al., 2023). Notably, the effect observed in this investigation was specific to the arrhythmic properties of the EEG signal, underscoring the functional relevance of these metrics. In particular, the major effects were detected for the modulation of the PLE and broadband, alpha, and low gamma complexity measures. Based on what was discussed above, this suggests that the differences in response to ketamine between early and late responders might be due to a different response to excitatory/inhibitory balance shifts. Although speculative, these conclusions may stimulate future research with important implications for personalized and precision psychiatry.

***Impact of Traumatic Experiences and Drug Therapy on Dissociative States***

It is important to consider whether major psychological traumatic experiences (TEs) or concurrent drug therapies could influence the susceptibility to dissociative states observed during the study. However, none of the patients enrolled reported experiencing dissociation in their daily lives. Comprehensive anamnesis and diagnostic evaluations were conducted by psychiatrists at the Psychiatric Unit of the University Hospital of Siena, which confirmed that dissociation was not a symptom present in their clinical profiles. Additionally, a significant proportion of the patients were being treated with mood stabilizers, including lithium and antiepileptic drugs. While these medications are known to influence mood and cognition, there is no evidence to suggest that they contribute to the specific dissociative states observed in this study.

Notably, the dissociative states were exclusively reported during the acute phase of ketamine treatment. These states were transient, resolving shortly after administration, and did not recur

between treatment sessions. This pattern strongly supports the hypothesis that the dissociative states were directly linked to ketamine induction rather than pre-existing vulnerabilities related to TEs or the effects of concurrent drug therapy. The findings suggest that the dissociative phenomena observed in this study are specific to the pharmacological effects of ketamine, aligning with prior evidence of its transient dissociative impact.

Future studies could benefit from further examining the potential interactions between traumatic experiences, drug therapy, and ketamine-induced dissociation. However, the current findings provide strong support for the conclusion that the dissociative states in this cohort were primarily ketamine-induced.

***Limitations***

It is crucial to acknowledge the naturalistic nature of the study, which brings both strengths and weaknesses. The study offers novel insights into the neurophysiological effects of ketamine in TR-BP in a real-world clinical setting. On the other hand, differences in the number of previous exposures to ketamine before the EEG recording, along with the concurrent and heterogeneous poly-pharmacological treatment of the patients, limit the generalizability of the results. The relatively limited sample size and the absence of controls also represent further study design limitations. Nevertheless, replicating many previous findings in standardized and controlled settings underscores the robustness of the EEG measures.

***Conclusion***

In conclusion, our study provides comprehensive insights into the acute neurophysiological effects of ketamine in patients with TR-BP. The observed EEG changes across multiple rhythmic and arrhythmic components of the neurophysiological signal highlight the potential utility of EEG as a valuable tool for assessing and monitoring the neurobiological effects of ketamine in real-world, ecologically valid clinical settings. Moreover, the differential responses between early and late responders promote the importance of considering individual differences in treatment outcomes and their neural correlates.

# Chapter 5: Disrupted Neural Dynamics in Addiction: The Role of Gamma Activity in Risky Decision-Making

## Introduction

Addictive behaviors, classified under the Diagnostic and Statistical Manual of Mental Disorders, Fifth Edition (DSM-5), encompass both substance use disorders, such as alcohol and tobacco addiction, and behavioral addictions, like gambling and gaming (American Psychiatric Association, 2022). These conditions are characterized by compulsive engagement despite negative outcomes, reflecting an impaired reward system that drives individuals toward maladaptive behaviors. Compounding this, addiction often coexists with psychiatric comorbidities such as depression and anxiety, complicating treatment efforts and highlighting the need for a deeper understanding of the underlying neurobiological mechanisms (*Common Comorbidities with Substance Use Disorders Research Report*, 2020).

At the core of addictive behaviors lies a profound dysregulation within the brain's reward circuitry, notably within the mesocorticolimbic dopamine system, which is pivotal for reinforcement learning and reward anticipation (Koob & Volkow, 2016). This network, which includes key structures like the ventral striatum and prefrontal cortex, becomes hyper-responsive in individuals with addiction, leading to an overvaluation of immediate rewards and a diminished ability to assess long-term consequences (Bickel et al., 2012). Dysregulated dopamine transmission in these regions shifts the balance toward impulsive behavior, exacerbating risk-taking tendencies—a hallmark of addiction (Bechara, 2005). Consequently, addiction manifests as an impaired capacity to modulate behavior in response to feedback and loss, reflecting broader deficits in cognitive control and decision-making.

Cognitive control, particularly in decision-making processes, is heavily dependent on the prefrontal cortex functions and its associated networks, including subregions as the dorsolateral prefrontal cortex (DLPFC), ventromedial prefrontal cortex (vmPFC), together with the anterior cingulate cortex (ACC). These regions are integral to the executive control network (ECN) and the

salience network (SN), which coordinate higher-order cognitive functions such as planning, impulse control, and adaptive decision-making. The default mode network (DMN), typically active during rest and self-referential thoughts, also plays a role in shifting between internally and externally directed attention, and its proper disengagement is critical during goal-directed tasks. Dysregulation in these networks, particularly the ECN and SN, is often observed in addiction, leading to impaired cognitive control and risky decision-making behaviors.

In addictive behaviors, these networks—especially the DLPFC and ACC—fail to regulate impulses and reward evaluation effectively. At the same time, the DMN often remains overly active, interfering with task-related focus and cognitive flexibility (Goldstein & Volkow, 2002). Neuroimaging and electrophysiological studies have consistently demonstrated impairments in these areas. However, much of this work has focused on resting-state brain activity or event-related potentials (ERPs), providing limited insight into the dynamic neural mechanisms that underpin real-time decision-making in addiction (Cavanagh & Shackman, 2015; Mas-Herrero et al., 2015). Moreover, many of these studies rely on healthy populations, limiting their relevance to the unique neural dysfunctions observed in individuals with addictive behaviors (Mas-Herrero et al., 2015).

While previous research has predominantly focused on clinical populations, many studies investigating the neural underpinnings of addiction have utilized techniques like fMRI or EEG at rest, often aimed at correlating neural activity with substance consumption or craving (Ahmed et al., 2024; Goldstein & Volkow, 2011; Khajehpour et al., 2019; Moreno-López et al., 2012; Sutherland et al., 2012; Verdejo-García et al., 2012; Zilverstand et al., 2018). These studies provide valuable insights into the static neural markers associated with addiction but may fall short of capturing the real-time dynamics of decision-making processes. Event-related EEG studies, by contrast, have primarily been conducted in healthy subjects (Cavanagh & Frank, 2014; Mas-Herrero et al., 2015a; Schutte et al., 2020), offering a more direct examination of cognitive and reward-related processes but without fully addressing the pathological mechanisms in clinical populations.

The focus of many patient studies has been on the clinical aspects, such as the relationship between neuroimaging findings and levels of substance use or cravings. However, this approach overlooks the real-time cognitive deficits during decision-making that are central to addiction. By integrating event-related EEG measures into the study of individuals with addictive behaviors, this research uniquely captures the dynamic neural processes that underlie risky decision-making. Specifically, this study moves beyond traditional clinical neuroimaging approaches by utilizing event-related spectral perturbation (ERSP) analysis during tasks that simulate real-world decision-making under risk, offering a novel perspective on the neural dysfunctions that

characterize addiction. This approach allows for a more nuanced understanding of how specific neural oscillations, such as theta, beta, and gamma, reflect the interaction between reward sensitivity and cognitive control, bridging a crucial gap in the literature.

The present study aims to address this gap by investigating risky decision-making in individuals with addictive behaviors, focusing specifically on the interaction between EEG spectral activity and behavioral performance during the Iowa Gambling Task (IGT) (Bechara, 2000). Using event-related spectral perturbation (ERSP) analysis, this study provides a more nuanced examination of brain dynamics, moving beyond traditional ERP or resting-state paradigms to capture real-time neural oscillations as participants engage in risky decision-making. Importantly, the study seeks to clarify how key frequency bands—particularly theta, beta, and gamma—reflect the interplay between reward sensitivity and cognitive control. This approach allows for a more comprehensive understanding of how addictive behaviors disrupt the neural circuits involved in decision-making.

Further complicating the neurobiology of addiction is the theory of disrupted excitatory-inhibitory (E/I) balance, particularly as it relates to neural plasticity and energy regulation (Voytek & Knight, 2015). According to this theory, addiction involves a dysregulation of the balance between excitatory glutamatergic and inhibitory GABAergic activity, leading to heightened cortical excitability and impaired cognitive control. This imbalance manifests as a predominance of high-frequency oscillatory activity, such as beta and gamma, which can overwhelm the lower-frequency oscillations responsible for integrating cognitive control and feedback processing (B. J. He, 2011). The resulting neural dysregulation is thought to underlie the deficits in feedback sensitivity and learning observed in individuals with addiction, particularly during decision-making tasks like the IGT.

The necessity of defining precise neurophysiological markers for addiction is underscored by the potential for developing advanced therapeutic interventions. A better understanding of the disrupted neural oscillations in addiction, particularly in relation to the E/I balance, could pave the way for novel treatments, such as noninvasive neuromodulation techniques that target specific brain rhythms to restore cognitive control and improve decision-making. Identifying these markers is critical, as they could inform the development of personalized interventions aimed at mitigating the cognitive deficits associated with addiction.

This study hypothesizes that gamma oscillations, closely linked to dopamine regulation, play a central role in both risky decision-making and baseline neural activity in individuals with addiction. Although gamma activity has been associated with reward processing and cognitive integration, its specific involvement in addiction, particularly in real-time decision-making scenarios, remains underexplored. By investigating gamma oscillations both during the IGT and

at rest, this study aims to elucidate their role in the dysregulated dopamine release characteristic of addiction. The study posits that gamma activity is not only a marker of risky decision-making but also a reflection of the broader neurophysiological dysfunctions that underlie addictive behaviors. Through this approach, the research seeks to provide novel insights into the neural mechanisms of addiction and offer potential pathways for therapeutic interventions targeting gamma oscillatory activity.

## Methods

### *Participants*

*Inclusion criteria.* The study included two groups of participants: individuals with addictive behaviors (ADD group) and a control group (CTL group). Participants in the ADD group were selected based on meeting the criteria for at least one form of addiction, as outlined in the Diagnostic and Statistical Manual of Mental Disorders, 5th edition (DSM-5) (American Psychiatric Association, 2013), which covers both substance-related and behavioral addictions. The Italian version of standardized assessments was administered, including the Fagerstrom Test for Nicotine Dependence (FTND) (Heatherton et al., 1991), the Alcohol Use Disorders Identification Test (AUDIT) (Saunders et al., 1993), the Cannabis Use Disorders Identification Test (CUDIT) (Adamson et al., 2010), the South Oaks Gambling Screen (SOGS) ("The South Oaks Gambling Screen (SOGS)," 1987), the Drug Use Disorders Identification Test (DUDIT) (A. H. Berman et al., 2005), and the Internet Gaming Disorder Scale-Short Form (Pontes & Griffiths, 2016). The control group consisted of participants who did not meet the criteria for substance use or addictive behaviors, with scores that did not indicate problematic behavior on these clinical scales.

*ADD Group.* The ADD group consisted of 11 participants (1 female, all right-handed, mean age: 31 ± 9 years), with an average education level of 14 ± 3 years. All participants in this group exhibited at least one form of addictive behavior. Five participants were diagnosed based on DSM-5 criteria and were receiving treatment for substance use disorders or gambling addiction (*ADD-T*). All five participants from the ADD-T subgroup were smokers. Cocaine use was present in all five participants, and two participants had evident alcohol dependence, as reported by their AUDIT scores. Problematic gambling behavior was observed in two out of five participants. These participants were also undergoing psychiatric treatment, including medications (Escitalopram, Valproate, Delorazepam, Paroxetine, Carbamazepine, and Quetiapine) and psychotherapy.

The remaining six participants in the ADD group demonstrated addictive behaviors but were not currently receiving treatment (*ADD-NT*). Among them, three were regular smokers, one

frequently consumed alcohol, and another reported regular cannabis use. Notably, three participants demonstrated problematic gambling behavior, and three others scored high on the IGDS9-SF, indicating potential gaming addiction.

*CTL group.* The CTL group comprised 17 participants (9 female, two left-handed, mean age: 25 ± 3 years), with an average education level of 14 ± 2.5 years. None of the participants in the control group demonstrated behaviors indicative of addiction, as their scores on the aforementioned scales did not reach levels suggestive of problematic behavior.

*Psychological Assessment*

Mood, anxiety, and impulsivity were assessed across both groups to investigate psychological dimensions associated with addictive behaviors.

Mood assessment was measured using the *Beck Depression Inventory-II (BDI)* (Beck et al., 2011). The BDI consists of 21 items, each scored on a 4-point scale, with higher scores indicating more severe depressive symptoms. For analysis, the total BDI score was divided into three subscales to differentiate between the cognitive, somatic, and affective components of depression. The *cognitive* subscale assesses negative thoughts, pessimism, and self-worth; the *somatic* subscale measures physical symptoms, such as fatigue and sleep disturbances; and the *affective* subscale evaluates emotional symptoms, including sadness and irritability. The ADD group's mean total score was 9.4 ± 5, suggesting mild to moderate depressive symptoms (cut-off for clinical depression: ≥10). In contrast, the CTL group presented a lower mean BDI score of 6.9 ± 7, indicating minimal depressive symptoms.

Anxiety was evaluated using the *State-Trait Anxiety Inventory (STAI)* (Spielberger et al., 1983). The ADD group demonstrated a mean state anxiety score (STAI-I) of 39.1 ± 7.1 and a mean trait anxiety score (STAI-II) of 41.1 ± 8, reflecting moderate levels of anxiety. The CTL group had a higher mean state anxiety score (STAI-I = 49.53 ± 2.48), while their trait anxiety (STAI-II = 40.2 ± 9.1) was comparable to the ADD group.

Impulsivity was assessed using the *Barratt Impulsiveness Scale (BIS-11)* (Patton et al., 1995), a self-report questionnaire with 30 items rated on a 4-point Likert scale. The ADD group exhibited a higher level of impulsivity, with a mean BIS-11 total score of 67.3 ± 12.1, close to the cut-off for high impulsivity (typically ≥72). In contrast, the CTL group had a lower mean BIS-11 score of 55.8 ± 8.8, indicative of normative impulsivity levels. BIS-11 assesses impulsiveness across three main subscales: motor impulsiveness (reflecting rashness and perseverance), attention impulsiveness (relating to cognitive complexity and maintaining focus), and non-planning impulsiveness (reflecting deficits in cognitive instability and self-control). The total score and scores for each subscale were analyzed separately.

Further details on the participants, including individual scores and treatment specifics, can be found in Table 6-8.

| | ADD | CTL | p-value |
|---|---|---|---|
| **Demographic Data** | | | |
| N° of participants (female) | 11 (1) | 17 (9) | 0.225 (**0.022***) |
| Age (years) | 31 ± 9 | 25 ± 3 | 0.085 |
| Education (years) | 14 ± 3 | 14 ± 2.5 | 0.703 |
| **Clinical Assessment** | | | |
| *Mood* | | | |
| BDI | 9.4 ± 5 | 4.9 ± 4 | **0.027*** |
| BDI – COG | 2.9 ± 2.5 | 2.1 ± 2.5 | 0.09 |
| BDI – SOM | 3.6 ± 3.1 | 3.1 ± 3.3 | 0.29 |
| BDI – AFF | 2.8 ± 1.5 | 1.8 ± 2.2 | **0.013*** |
| *Anxiety* | | | |
| STAI – I | 38.5 ± 7.6 | 50 ± 2.3 | **<0.001***** |
| STAI – II | 41.1 ± 8 | 40.2 ± 9.1 | 0.741 |
| *Impulsiveness* | | | |
| BIS 11 | 67.3 ± 12.1 | 55.8 ± 8.8 | **0.012*** |
| BIS 11 – Mot_Imp | 14 ± 4.8 | 12.1 ± 2.8 | 0.32 |
| BIS 11 – Att_Imp | 9.4 ± 5 | 10.9 ± 2.4 | 0.11 |
| BIS 11 – No_Plan_Imp | 9.4 ± 5 | 9.4 ± 5 | **<0.001***** |
| BIS 11 – Focus | 10.7 ± 2.2 | 8.5 ± 2.7 | **0.015*** |
| BIS 11 – Rashness | 14 ± 4.8 | 12.1 ± 2.8 | 0.5 |
| BIS 11 – CoCo | 14.2 ± 2.7 | 10.9 ± 2.4 | **0.005**** |
| BIS 11 – Self Control | 15.7 ± 2.5 | 12.2 ± 3 | **0.01**** |
| BIS 11 – CoIn | 5 ± 1.4 | 5.5 ± 1.4 | 0.40 |
| BIS 11 – Perseverance | 8.6 ± 1.4 | 8.2 ± 1.5 | 0.35 |
| **Neurocognitive Evaluation** | | | |
| *Risk Taking Behavior* | | | |
| BART – Risk-taking score | 31 ± 9.5 | 19 ± 8.8 | **0.003**** |
| BART – EB (%) | 31.8 ± 18.9 | 17.6 ± 13.8 | **0.034*** |
| BART – PE | 620.5 ± 321.7 | 455 ± 249.2 | 0.13 |
| BART – Increment | 196.8 ± 57.5 | 123.4 ± 44.2 | **0.002**** |
| *Response Inhibition* | | | |
| Go/NoGo – Hits Rate (%) | 70.45 ± 9.1 | 71.2 ± 15.15 | 0.88 |
| Go/NoGo – False Alarms (%) | 0.03 ± 0.06 | 0.02 ± 0.07 | 0.62 |
| Go/NoGo – Ratio | 1.14 ± 0.05 | 1.13 ± 0.13 | 0.64 |
| Go/NoGo – RT (ms) | 982.6 ± 379 | 921.6 ± 268.8 | 0.62 |
| *Selective Attention* | | | |
| STROOP – congruent Accuracy (%) | 0.95 ± 0.09 | 0.98 ± 0.06 | 0.3 |
| STROOP – congruent RT | 1358.6 ± 424 | 1145 ± 172 | 0.73 |
| STROOP – incongruent Accuracy (%) | 0.97 ± 0.03 | 0.99 ± 0.01 | 0.055 |
| STROOP – incongruent RT | 973.1 ± 363.1 | 855.8 ± 192 | 0.27 |
| STROOP – Accuracy Interference | 0.017 ± 0.01 | 0.008 ± 0.05 | 0.75 |
| STROOP – RT Interference (ms) | -385.5 ± 216.8 | -289.2 ± 173 | 0.2 |

| | | | |
|---|---|---|---|
| *Cognitive Flexibility* | | | |
| WCST – Categories Completed (%) | 3.03 ± 10.05 | 1.96 ± 8.1 | 0.76 |
| WCST – NPE | 8.2 ± 6.5 | 9.6 ± 5.9 | 0.56 |
| WCST – PE | 2.4 ± 2.15 | 3.5 ± 3.4 | 0.32 |
| WCST – CLR (%) | 54.84 ± 34.5 | 44.5 ± 33.3 | 0.43 |

*Table 6. Demographic Data of people with addictive behavior (ADD) and controls (CTL), and clinical assessment. The mean ± standard deviation for each group is reported. BDI = Beck Depression Inventory (COG = Cognitive symptoms, SOM = Somatic symptoms, AFF =Affective symptoms); STAI-I = State Anxiety Inventory - State subscale; STAI-II = State Anxiety Inventory - Trait subscale; BIS 11 = Barratt Impulsiveness Scale (Mot_Imp = Motor Impulsivity, Att_Imp = Attentional Impulsivity, No_Plan_Imp = Non-Planning, CoCo = Cognitive Complexity, CoIn = Cognitive Instability); BART = Balloon Analogue Risk Task; BART – EB = number of balloons that exploded; BART – PE = total points; BART – Increment = total number of pumps across both banked (non-exploded) and exploded balloons. BART – Risk-Taking Score = the average number of pumps on banked balloons (unexploded) divided by the total number of unexploded balloons; RT =reaction time calculated in milliseconds (ms); WCST = Wisconsin Card Sorting Test; WCST – NPE = non-perseverative errors; WCST – PE = perseverative errors; WCST – CLR =Conceptual Level Responses; p-value according to Mann-Whitney U test.*

| | **SUDIT (cut off =8)** | **FTND (cut off =3)** | **AUDIT (cut off =8)** | **CUDIT (cut off =8)** | **SOGS (cut off =5)** | **GRCS** | **IGDS9_SF (cut off =20)** |
|---|---|---|---|---|---|---|---|
| **ADD-T** | | | | | | | |
| SBJ01 | **16*** | **3*** | 3 | 1 | 0 | 23 | - |
| SBJ02 | **13*** | **4*** | 2 | 0 | **17*** | 23 | - |
| SBJ03 | **27*** | **4*** | **16*** | 6 | **10*** | 26 | - |
| SBJ04 | **25*** | **6*** | **17*** | 2 | 0 | 23 | - |
| SBJ05 | **27*** | **5*** | 3 | **15*** | 0 | 23 | - |
| **ADD-NT** | | | | | | | |
| SBJ06 | 0 | 0 | 5 | 1 | 1 | **41*** | 16 |
| SBJ07 | 0 | 0 | 2 | 0 | 0 | 23 | **25*** |
| SBJ08 | 0 | **5*** | 1 | 0 | 0 | 24 | 11 |
| SBJ09 | 0 | 2 | 4 | **9*** | **6*** | **66*** | **20*** |
| SBJ10 | 0 | **3*** | 4 | 2 | 1 | **37*** | 13 |
| SBJ11 | 0 | **3*** | **8*** | 0 | 0 | 23 | **21*** |

*Table 7 Clinical scales related to substance use disorder. Subjects are divided according to whether they are under treatment (ADD-T) or not (ADD-NT). SUDIT = Substance Use Disorder Identification Test; FTND = Fagerstrom Test for Nicotine Dependence; AUDIT = Alcohol Use Disorders Identification Test; CUDIT = Cannabis Use Disorders Identification Test; SOGS = South Oaks Gambling Screen; GRCS = Gaming-related Cognition Scale; IGDS9-SF = Internet Gaming Disorder Scale Short Form. Asterisks (*) indicate scores that exceed clinical cut-off thresholds.*

| | **Cocaine Use Disorder** | | | **Tobacco Use Disorder** | | **Cannabis Use Disorder** | | **Alcohol Use Disorder** | |
|---|---|---|---|---|---|---|---|---|---|
| | **Years Since Starting** | **Use Per Week** | **Months Since Last Relapse** | **Years Since Starting** | **Cigarettes per day** | **Years Since Starting** | **Gr per day** | **Years Since Starting** | **Units Per Week** |
| **ADD-T** | | | | | | | | | |
| SBJ01 | 10 | < 1 | 5 | 12 | 15 | - | - | - | - |
| SBJ02 | 29 | 1 | 12 | 29 | 20 | - | - | - | - |
| SBJ03 | 25 | 2 | 3 | 25 | 15 | - | - | - | - |
| SBJ04 | 5 | 1 | 11 | 11 | 20 | - | - | 11 | 30 |
| SBJ05 | 24 | 1 | 3 | 24 | 15 | 24 | 1 | - | - |

| | Pathological gambling | | | Treatment History | |
|---|---|---|---|---|---|
| | Years Since Starting | Use Per Week | Type | Psychotherapy (Frequency) | Medications |
| **ADD-T** | | | | | |
| SBJ01 | - | - | - | Once per month | Escitalopram, Valproate, |
| SBJ02 | 14 | 4 | Slot machine | Once every two weeks | Paroxetine, Carbamazepine |
| SBJ03 | 25 | 2 | Poker online | Once per week | Quetiapine |
| SBJ04 | - | - | - | Once per month | - |
| SBJ05 | - | - | - | Once every two weeks | Paroxetine |

*Table 8 Pathological History and Treatment Overview*

### *Neurocognitive Evaluation*

Higher-order cognitive functions, including *risk-taking behavior*, *selective attention*, *inhibitory control*, and *cognitive flexibility*, were assessed using a battery of computerized tasks administered via E-Prime 3.0 (Psychology Software Tools, Pittsburgh, PA), ensuring precise stimulus presentation and accurate timing. *Tasks have been selected from the E-Prime Experiment Library.*

*Risk-taking behavior* was evaluated with the *Balloon Analogue Risk Task (BART)* (Lejuez et al., 2002). In this task, participants inflated a virtual balloon to maximize potential rewards, but each pump increased the risk of the balloon exploding. This paradigm simulates real-life risk-reward decision-making by balancing potential gains against the risk of loss. After a practice session consisting of 5 trials (5 balloons), participants were presented with 30 balloons to pump and earn points.

*Inhibitory control* was assessed using the *Go/No-Go Task* (Gomez et al., 2007). Participants were required to respond to auditory stimuli: a single beep served as the Go stimulus, while two beeps indicated a No-Go stimulus, measuring their capacity to suppress inappropriate responses in a dynamic testing environment. The task was structured as follows: participants first completed 2 training trials for each session (Go and No-Go) to ensure they understood the rules, followed by 10 test trials for the Go session and 10 for the No-Go session.

*Selective attention* was measured by the *Stroop Test* (Stroop, 1935), in which participants were presented with color words displayed in incongruent ink colors. They were instructed to identify the ink color while ignoring the word's semantic content, thus evaluating their ability to manage cognitive interference. The task consisted of an initial training phase with 15 congruent stimuli, followed by a test phase with 60 incongruent stimuli.

*Cognitive flexibility and perseveration* were examined through the *Wisconsin Card Sorting Test (WCST) (Grant & Berg, 2014).* Participants were required to sort 30 cards according to rules that periodically changed without notice, assessing their ability to adapt to new rules and inhibit previously reinforced responses.

***Decision-Making and Risky Choices***

Decision-making under risk was evaluated using the *Modified Iowa Gambling Task (mIGT)*, described by *Cauffman et al. (Cauffman et al., 2010)*. The original *Iowa Gambling Task (IGT)*, developed by *Bechara et al. (Bechara, 2000)* is a widely employed paradigm for assessing decision-making under conditions of uncertainty. In this task, participants must select cards from four decks associated with distinct reward and punishment schedules. Two decks provide high immediate rewards but result in substantial long-term losses, thus making them disadvantageous. In contrast, the other two decks offer smaller, consistent rewards that ultimately yield long-term gains, making them advantageous. The task effectively simulates real-world decision-making scenarios where individuals must weigh short-term rewards against long-term consequences.

In this study, the *Cauffman et al. (Cauffman et al., 2010)* modified version of the IGT was employed to make the risk-reward contingencies more explicit. Unlike the original task, the modified IGT delivers more transparent feedback regarding the probabilities of rewards and punishments, enabling participants to evaluate their decisions better. Although the fundamental structure of balancing risky versus safe choices remains intact, the mIGT enhances participants' understanding of the long-term consequences of their choices through more transparent feedback. To minimize potential triggers for individuals with pathological gambling tendencies, points were used instead of monetary rewards.

The task was implemented using a custom *MATLAB script* (*MATLAB R2023a*, MathWorks Inc., Natick, MA) provided by *Cauffman and colleagues (Cauffman et al., 2010)*. The script is set to select decks randomly. Real-time feedback on participants' total points was provided after each decision. The starting total was 2000 points, with the objective being to accumulate as many points as possible. The task consisted of 120 trials, with feedback appearing 100 ms after participants' responses and the subsequent trial starting 2 seconds after feedback. Participant decisions (play/pass), reaction times, and outcomes were all logged for further analysis.

Furthermore, the task was synchronized with an EEG recording system via a UDP interface. An ad-hoc code sent task-related markers to synchronize EEG data acquisition, ensuring precise alignment between behavioral responses and neural activity.

### *EEG Data Recording*

EEG data were recorded both during a resting state and throughout the modified Iowa Gambling Task (mIGT). Resting-state EEG was collected over a 3-minute period with eyes open**,** followed by 3 minutes with eyes closed**.** Data acquisition utilized a 64-channel EEG system integrated with the *g.HIamp* amplifier and g.tec Suite 2020 (*g.tec medical engineering GmbH, Austria*), configured according to the international 10-20 electrode placement system, with a sampling rate of 512 Hz**.** Impedance levels were maintained below 10 kΩ to ensure optimal signal quality throughout the recording sessions.

For the mIGT, EEG data were recorded using the same configuration as the resting-state setup, employing a 64-channel system integrated with the g.HIamp amplifier and g.HIsys Highspeed Online Processing for Simulink (MATLAB R2023a, MathWorks Inc., Natick, MA). This setup enabled real-time synchronization of task events with EEG recordings by adding task-related markers, reflecting both stimulus presentations (Deck A, B, C, D) and participant responses (PLAY/PASS), ensuring precise temporal alignment between behavioral and neural data.

### *Behavioral data scoring*

*Neurocognitive data*

*Risk-Taking Propensity.* The Balloon Analogue Risk Task (BART) provides several metrics related to risk-taking behavior. The number of balloons that exploded (BART_EB) was recorded to indicate a participant's risk-taking propensity, while the total points earned (BART_PE) reflect their ability to balance risk and reward effectively. The BART increment represents the total number of pumps across both banked (non-exploded) and exploded balloons. The composite BART Risk-Taking Score was calculated as the average number of pumps on banked balloons (unexploded) divided by the total number of unexploded balloons, providing an overall measure of the participant’s willingness to engage in risky behavior.

*Response Inhibition.* The Go-NoGo Hits Rate represents the percentage of correct responses on Go trials, indicating the participant's ability to correctly respond when required. The Go-NoGo False Alarms measured the frequency of incorrect responses during No-Go trials (when participants were supposed to withhold their response), assessing impulse control. Finally, the Go-NoGo ratio was considered: a ratio greater than 1 indicates a higher proportion of correct responses compared to false alarms, suggesting better inhibitory control. Conversely, a ratio less than 1 indicates more false alarms than correct responses, reflecting poorer inhibition. Reaction times were also recorded to provide further insight into the participant's processing speed and cognitive control during the task.

*Selective Attention.* The Stroop Task was used to evaluate selective attention and cognitive control. Accuracy was measured in both congruent and incongruent trials to assess participants' ability to handle interference. Higher Stroop Incongruent Accuracy scores indicated stronger selective attention and resistance to interference. Reaction times were measured for both congruent and incongruent conditions, with the Stroop Reaction Time Interference calculated to quantify the additional time required to respond during incongruent trials. This measure provided insight into the participant's cognitive flexibility and executive control.

*Cognitive Flexibility.* The Wisconsin Card Sorting Test (WCST) was used to assess cognitive flexibility and executive functioning. The number of Categories Completed represented the number of correct sorting categories completed by the participant, reflecting their cognitive flexibility. Perseverative Errors were recorded to evaluate the participant's tendency to repeat previously incorrect sorting strategies, with a higher number indicating cognitive rigidity. Additionally, the percentage of WCST Conceptual Level Responses was computed to reflect the participant's understanding of the task rules and their overall problem-solving ability.

*Decision making (mIGT)*

The Modified Iowa Gambling Task (mIGT) (Cauffman et al., 2010)) was employed to assess decision-making under risk. mIGT, as developed by Cauffann, involved metrics such as the Percentage of Bad Plays (reflecting the selection of disadvantageous decks with high immediate rewards but more considerable long-term losses) and the Percentage of Good Plays (reflecting the selection of advantageous decks) were calculated. The 120 trials were divided into six blocks of 20 trials each, enabling the examination of potential learning effects over time. The mIGT Net Score was derived as the difference between good and bad plays, offering a summary of the participant's decision-making abilities under risk. Additionally, the mean values for reward (points won), loss (points lost), and score balance (current total points for each trial) were computed for each block to examine the role of these factors in shaping risk-taking behavior. To clarify, "bad plays" will now be referred to as "risky choices" (representing the selection of disadvantageous decks), while "good plays" will be referred to as "not risky choices" (representing the selection of advantageous decks). The term "Net Score" will now refer to the difference between not risky choices and risky choices, representing overall decision-making performance.

***EEG data: preprocessing and analysis***

*Resting State EEG Analysis*

The EEG data were preprocessed using EEGLAB (version 2022) (Delorme & Makeig, 2004) in MATLAB. Signals were bandpass filtered between 1 Hz (high-pass) and 80 Hz (low-pass), and a notch filter was applied between 48 and 52 Hz to remove power line noise. Channels with poor signal quality were manually rejected using the VisEd plugin for EEGLAB, and independent component analysis (ICA) using the "runica" algorithm was applied to remove artifactual signals, including muscle activity, blinks, ocular movements, and cardiac activity. On average, 30 ± 10 components were retained for the ADD group and 28 ± 11 for the CTL group. Spherical spline interpolation was used to reconstruct bad channels (3 ± 1 channels for the ADD group and 2 ± 1 for the CTL group), resulting in 61 electrodes. The data were then re-referenced to the average of all channels and converted to FieldTrip format for subsequent analyses.

*Power Spectral Density Analysis.* The grand average of the power spectra was computed using the open-source toolbox FieldTrip (Oostenveld et al., 2011) across all participants in the two groups (ADD and CTL). A Laplacian spatial filter was applied to enhance spatial resolution by subtracting the average signal from neighboring electrodes at each electrode site. Frequency analysis was then conducted using a multitaper Fast Fourier Transform (FFT), with the power spectrum computed using a Hanning taper across a frequency range of 1 to 80 Hz in 0.5 Hz increments. Power was averaged across trials, and data were zero-padded to the next power of 2 for faster computation. The analysis included all channels, and group-level grand averages were calculated for both the ADD and control groups.

*The Irregular-Resampling Auto-Spectral Analysis (IRASA).* IRASA algorithm was used to separate the oscillatory and fractal components of the EEG power spectrum, as described by Wen and Liu (Wen & Liu, 2016). The IRASA method was applied to the Laplacian filtered data to compute both components (frequency range: 1-80 Hz, frequency resolution: 0.5 Hz). First, the fractal component of the power spectrum was estimated by configuring the analysis to output the fractal signal. The original power spectrum was then computed separately. The oscillatory component was derived by subtracting the fractal signal from the original power spectrum, isolating the pure oscillatory activity. The grand averages of both the fractal and oscillatory components were then computed. The oscillatory and fractal spectra were calculated for each subject, and the group grand averages were derived using the ft_freqgrandaverage function.

*Power Law Exponent (PLE).* To estimate the PLE of the EEG power spectra, the fractal component of the power spectrum (1/f β) was log-transformed, and linear regression was

performed in log-log space to extract the β coefficient, representing the slope of the power spectrum. To prevent bias toward higher frequencies, frequency estimates were resampled to ensure an even distribution in logarithmic space before applying the regression. The data were split into two frequency bands based on visual inspection: low-frequency (1-19 Hz) and high-frequency (20-80 Hz). Separate linear regressions were performed for each band, and the PLE values for each subject and channel were extracted.

*Event-related Spectral Perturbation (ERSP)*

The task-related EEG data were preprocessed using the same pipeline described for the resting EEG data. After the ICA decomposition, on average, 30 ± 10 components were retained for the ADD group and 28 ± 11 for the CTL group. Spherical spline interpolation was used to reconstruct bad channels (3 ± 1 channels for the ADD group and 2 ± 1 for the CTL group), resulting in 61 usable electrodes. The data were then average referenced and segmented into epochs centered around specific event markers. The markers of interest were renamed according to the type of response (PLAY or PASS) and the associated deck type (risky: A and B, or not risky: C and D). This means that markers for playing after selecting a risky deck (A or B) were renamed "risky_play," while those for passing after a risky deck were labeled "risky_pass." Similarly, markers for playing after selecting a not risky deck (C or D) were renamed "not_risky_play," and passing after a not risky deck was labeled "not_risky_pass". These renamed markers were used to define epochs ranging from -1.2 to 1.5 seconds around each event of interest.

Four distinct epoch sets were created for each subject based on the different response and deck combinations. Each epoch set was baseline-corrected using the pre-stimulus period (before deck appearance) from -1200 ms to -900 ms. Baseline correction was conducted following Gratton's considerations for ERSP analysis in continuous cognitive tasks, such as decision-making. He advises against using a pre-choice window, as it is influenced by ongoing cognitive processes (preparation to action) and thus unreliable. Instead, the most accurate approach is to use a baseline from -300 to 0 ms before stimulus appearance (in this case, the deck), as it better reflects a neutral "waiting period" before the onset of decision-related cognitive activity (Gratton, 2018).

Successively, data was converted to the FieldTrip format for further analysis. Laplacian filtering was applied to enhance spatial resolution, followed by wavelet-based time-frequency analysis to extract spectral power across trials. The analysis was conducted with frequencies of interest ranging from 2 to 80 Hz, with an interval of 0.5 Hz. The number of wavelet cycles varied from 3 to 10, and the time of interest spanned from -800 ms to 1300 ms, with an interval of 0.01 seconds.

Subsequently, grand averages were computed for each group (ADD and control) and each risk condition (risky and not risky) to enable direct comparisons between groups and conditions.

### *Statistical analysis*

*Behavioral data*

Between-group comparisons of behavioral data were conducted using non-parametric Mann-Whitney U tests via JASP software (version 0.18.3) (Jasp Team, 2024). Behavioral task performance was evaluated across several tasks, including the Stroop Test, Balloon Analogue Risk Task (BART), Go-NoGo Task, and Wisconsin Card Sorting Test (WCST). Task scores were calculated according to standardized scoring procedures for each task. Statistical significance was set at $p < 0.05$ for all analyses.

*Modified Iowa Gambling Task (mIGT).* The data were transformed using a linear, logarithmic scale to reduce variability and address potential skewness in the distribution, thereby enhancing the stability of the analyses. To examine the interaction between group differences (CTL vs. ADD) and learning effects across blocks (1 through 6), a generalized linear mixed model (GLMM) was employed. This approach was chosen for its ability to account for the nested structure of the data, handling repeated measures across time while modeling individual variability. Additionally, the GLMM allowed for a detailed assessment of the influence of reward, loss, and score balance on both group differences and learning effects. To control for the potential inflation of type I errors due to multiple comparisons, a false discovery rate (FDR) correction was applied, ensuring the robustness and reliability of the findings. The results of the FDR correction are reported as "p adj." in the main text. Corrections for multiple comparisons were applied where necessary, and statistical significance was considered at $p < 0.05$.

*EEG data – Resting state*

Monte Carlo cluster-based permutation testing was employed using *FieldTrip* to identify significant group differences in original, oscillatory, and fractal spectral power across several frequency bands. The analysis targeted the following frequency ranges: delta (1–4 Hz), theta (4–8 Hz), alpha (8.5–13 Hz), beta1 (13.5–20 Hz), beta2 (20.5–29 Hz), gamma (30–80 Hz), low gamma (30–48 Hz), and high gamma (52–80 Hz). A Monte Carlo method with 10,000 random permutations was applied, and a cluster-level alpha of 0.05 was used to control for multiple comparisons.

A triangulation method based on the electrode layout was employed to define neighboring channels, with a minimum of two neighboring electrodes required for the formation of a cluster. A paired-sample t-test was conducted to compare each participant's spectral power in the pre- and post-treatment conditions. The resulting clusters were evaluated for statistical significance, with correction for multiple comparisons based on the maximum sum of cluster-level test statistics.

For each frequency band, topographical plots were generated to compare the power spectra between the ADD and control groups. Cluster-based significant electrodes were highlighted in the statistical maps, with significant clusters (both positive and negative) identified based on the cluster probabilities (stat. prob) indicated on the statistical maps.

*EEG data – ERSP*

A cluster-based permutation analysis was conducted between the ADD and control groups during the pre-response window (-800 to 0 ms) to examine pre-choice neural activity. The analysis involved 10,000 permutations, with at least two neighboring channels required for cluster formation and a cluster-level alpha threshold of 0.05. Frequency bands of interest (theta, alpha, beta, and gamma) were averaged to assess group-level spectral differences in anticipatory activity. Additionally, the same cluster-based analysis was applied to the post-choice window (0 to 1200 ms) to investigate post-decision EEG activity between the groups.

*Correlations*

Correlations between clinical scales, behavioral performance, and EEG metrics were conducted using JASP software (version 0.18.3). Spearman's rank-order correlation coefficient was calculated to assess relationships between scores on the BDI, STAI, and BIS-11, behavioral task performance (Stroop, Go-NoGo, WCST, BART, and mIGT), and EEG measures, including resting-state original, oscillatory, and fractal power spectra, PLE, and ERSP. The EEG metrics were examined across standard frequency bands (delta, theta, alpha, beta, gamma). Electrodes belonging to statistically significant clusters, identified through permutation tests, were extracted for each comparison and EEG metric. The non-parametric Spearman correlation coefficient was calculated, with statistical significance set at $p < 0.05$.

*Predictive Analysis*

Given the limited sample size of 28 participants, the use of more complex, high-performance models was not feasible due to concerns about overfitting and model reliability. As such, logistic regression was selected as the most appropriate predictive model. The aim was to assess whether EEG correlates could significantly predict group membership (ADD vs. CTL). Logistic regression provided sufficient predictive power within these constraints, with model performance evaluated using McFadden's $R^2$ and Nagelkerke's $R^2$.

# Results

## *Clinical and Psychometric Assessment*

### *Mood Assessment*

*After o*utliers have been identified by using Tukey's rule and removed, the Beck Depression Inventory (BDI) revealed significantly higher total depressive symptom scores in the ADD group compared to the CTL group (U = 39.5, p = 0.027). Further analysis of the BDI subscales—cognitive, somatic, and affective symptoms—indicated that the significant difference was specific to the affective symptoms' subscale, with ADD participants exhibiting higher affective symptom scores than controls (U = 35, p = 0.013). These results suggest that individuals in the ADD group experience more pronounced affective depressive symptoms (Figure 12, Table 6).

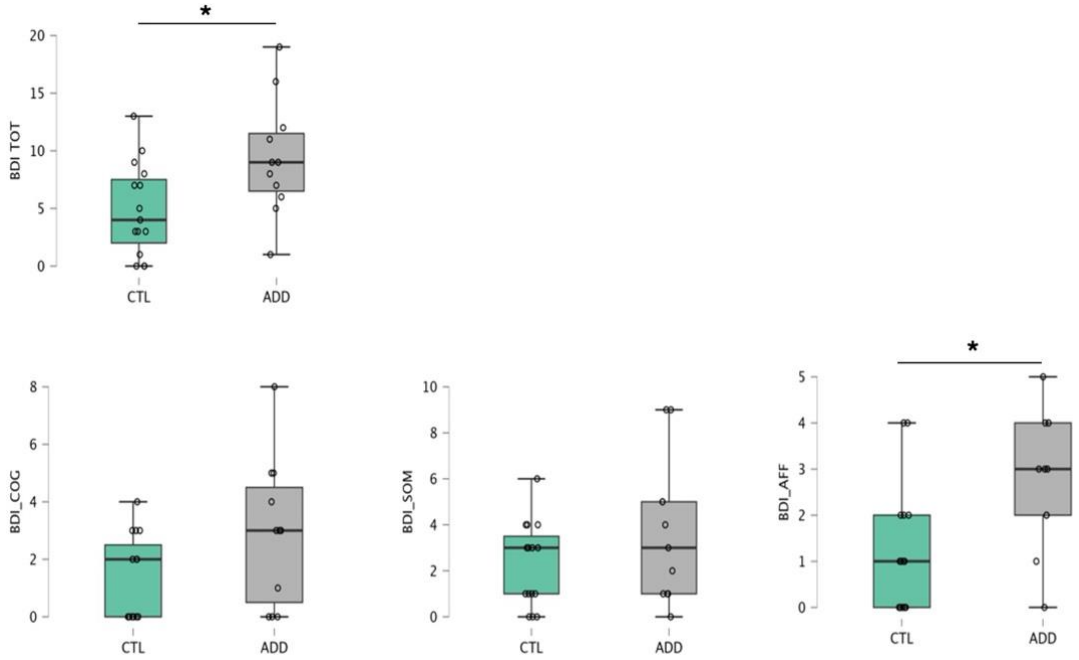


*Figure 12. Boxplots of Mood Assessment of People with addictive behavior (ADD) and controls (CTL). BDI = Beck Depression Inventory (COG = Cognitive symptoms, SOM = Somatic symptoms, AFF =Affective symptoms). p-value according to the Mann-Whitney U test. * p<0.05, ** p<0.01, *** p<0.001.*

### *Anxiety Assessment*

STAI revealed significantly higher scores for state anxiety (STAI-I) in the CTL group compared to the ADD group (U = 168, p < 0.001). In contrast, the trait anxiety subscale (STAI-II) showed a nearly identical distribution between the two groups (Figure 13, Table 6).

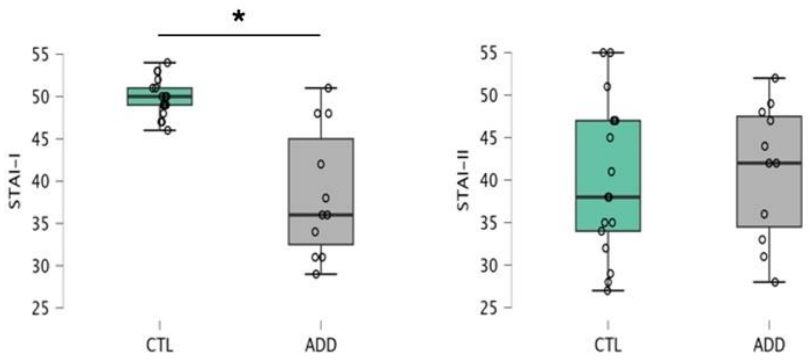


*Figure 13. Boxplots of Anxiety Assessment of People with addictive behavior (ADD) and controls (CTL). STAI-I = State Anxiety Inventory - State subscale; STAI-II = State Anxiety Inventory - Trait subscale. p-value according to the Mann-Whitney U test. * p<0.05, ** p<0.01, *** p<0.001.*

*Impulsiveness Assessment*

The BIS-11 total impulsiveness score was significantly higher in the ADD group compared to controls (U = 39.5, p = 0.012). A significant difference was found within the subscales in the non-planning impulsiveness subscale (U = 19.5, p < 0.001), with ADD participants scoring higher than controls. Additionally, significant group differences were observed in the focus subscale (U = 41.5, p = 0.015), self-control (U = 38.5, p = 0.01), and cognitive complexity (U = 33.5, p = 0.005) components (Figure 14, Table 6).

***Behavioral Performance in Risk-Taking and Cognitive Control Task***

Group comparisons in neurocognitive task performance revealed a significant difference only in risk-taking tendencies, with the ADD group demonstrating higher scores on the Balloon Analog Risk Task (BART). Specifically, the ADD group exhibited a greater number of exploded balloons (U = 49, p = 0.034), a higher number of pumps, as indicated by increased pump levels (U = 26, p = 0.002), and an overall elevated risk-taking score (U = 33, p = 0.03; Figure 15, Table 6).

Performance on the remaining neurocognitive tasks did not reveal significant differences between the groups. As no significant differences emerged from the statistical analyses, we have presented only the key performance metrics to provide a general overview of the data trends. Specifically, we have selected the *Go-NoGo Hits Rate*, *Stroop Reaction Time Interference*, and *Perseverative Errors* from the Wisconsin Card Sorting Test (WCST) for visualization (Figure 16, Table 6).

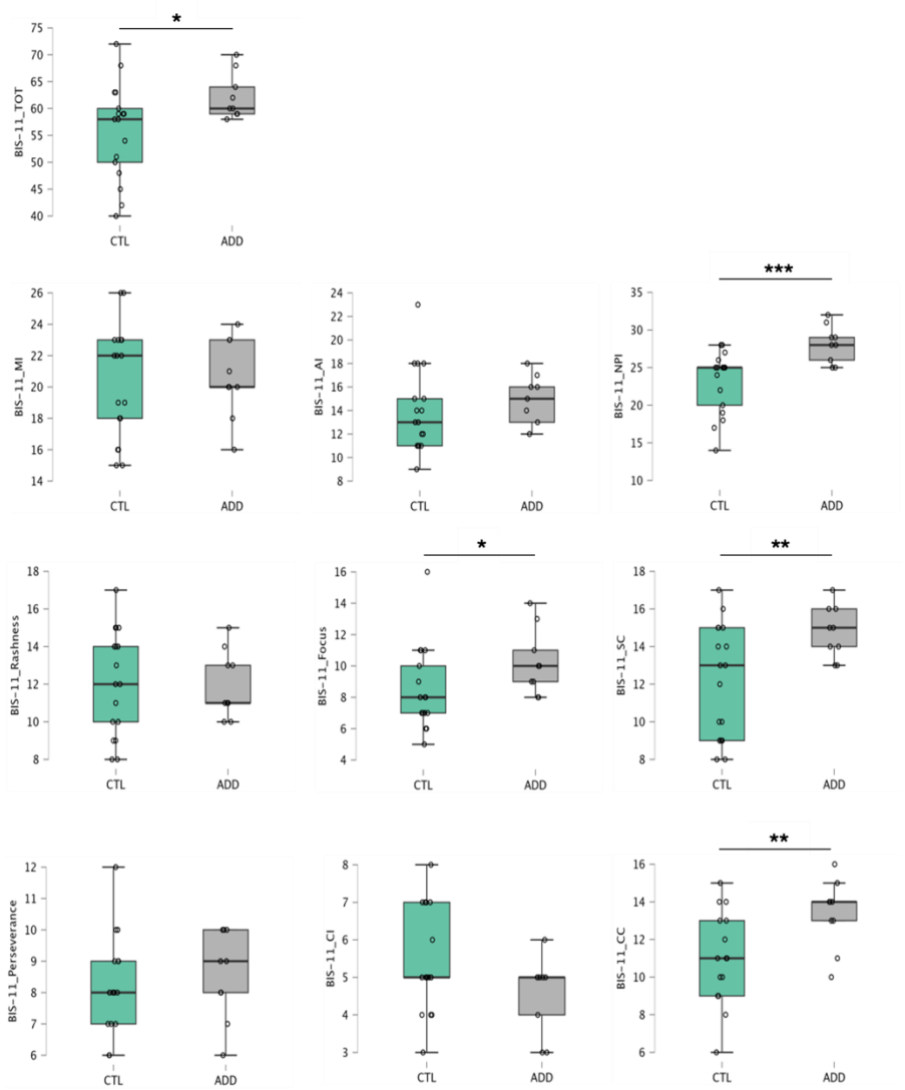


*Figure 14. Boxplots of Impulsiveness Assessment of People with addictive behavior (ADD) and controls (CTL). BIS 11 = Barratt Impulsiveness Scale (MI = Motor Impulsivity, AI = Attentional Impulsivity, NPI = Non-Planning, SC = Self Control, CC = Cognitive Complexity, CI = Cognitive Instability). p-value according to the Mann-Whitney U test. * p<0.05, ** p<0.01, *** p<0.001.*

### *Risky Decision-Making and Feedback Sensitivity*

*Net Score*

GLMM analysis found no significant effect of group ($\chi^2_{(1)=}$ 0.134, p= 0.71), block ($\chi^2_{(5)}$= 6.726, p= 0.24), or their interaction ($\chi^2_{(5)}$= 7.784, p= 0.17) on net score. However, significant interactions emerged: group*block*reward ($\chi^2_{(5)=}$ 16.789, adj. p= 0.009), block*reward ($\chi^2_{(5)=}$ 40.328, adj. p= 0.003) (Figure 17A), group*block*loss ($\chi^2_{(5)}$= 29.417, adj. p= 0.002), group*loss ($\chi^2_{(1)=}$ 9.170, adj. p= 0.002), and block*loss ($\chi^2_{(5)=}$ 52.023, adj. p= 0.002) (Figure 17B), group*block*score balance ($\chi^2_{(5)}$= 18.641, adj. p= 0.014), and block*score balance ($\chi^2_{(5)=}$ 18.154, adj. p= 0.01) (Figure 17C).

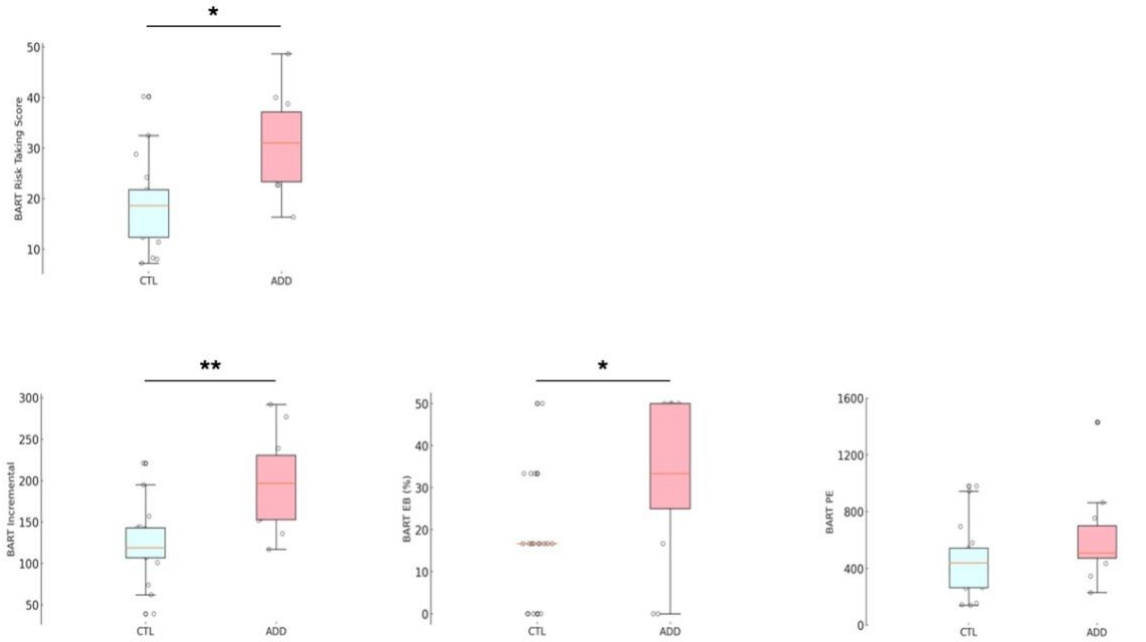


*Figure 15. Boxplots of Balloon Analog Risk Task (BART). Bart_EB(%)= percentage of balloon exploded; Bart_PE= point earned. p-value according to the Mann-Whitney U test. * p<0.05, ** p<0.01, *** p<0.001.*

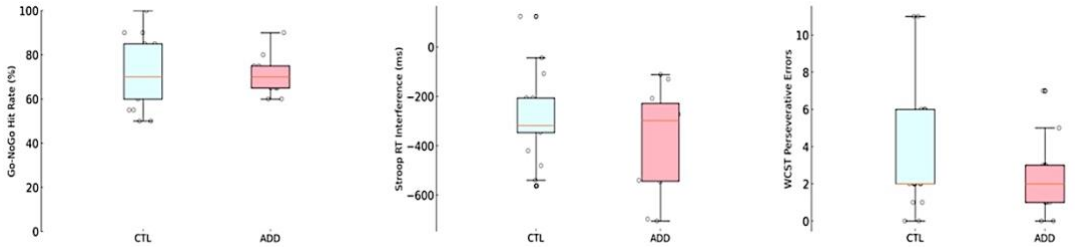


*Figure 16. Boxplots of GO-NOGO HIT RATE (reported in percentage), STROOP reaction times Interference (ms = milliseconds), and Perseverative Errors from the Wisconsin Card Sorting Test (WCST) of People with addictive behavior (ADD) and controls (CTL).*

*Risky choice*

No significant group ($\chi^2_{(1)=}$ 0.176, p= 0.67), block ($\chi^2_{(5)=}$ 3.322, p= 0.65), or group*block effects ($\chi^2_{(5)}$= 1.365, p= 0.92) were observed. However, group*block*loss was significant ($\chi^2_{(5)}$= 37.110, adj. p= 0.002), as were block*loss ($\chi^2_{(5)=}$ 47.372, adj. p= 0.002) and group*loss ($\chi^2_{(1)}$= 6.292, adj. p= 0.017) (Figure 17B). Group*block*score balance was significant ($\chi^2_{(5)=}$ 12.403, adj. p= 0.04), as were group*score balance ($\chi^2_{(1)=}$ 6.986, adj. p= 0.008) and block*score balance ($\chi^2_{(5)=}$ 12.646, adj. p= 0.0315) (Figure 17C).

*Not risky Choices*

No main effects were observed for group ($\chi^2_{(1)}$= 0.176, p= 0.67), block ($\chi^2_{(5)}$= 3.322, p= 0.65), or interaction between group and block ($\chi^2_{(5)}$= 1.365, p= 0.92). However, significant interactions for group*block*loss ($\chi^2_{(5)}$= 37.110, adj. p= 0.002), block*loss ($\chi^2_{(5)}$= 47.372, adj. p= 0.002), and group*loss ($\chi^2_{(1)}$= 6.292, adj. p= 0.017) were observed (Figure 17B). Additionally, significant interactions were found for group*block*score balance ($\chi^2_{(5)}$= 12.403, adj. p= 0.04), group*score balance ($\chi^2_{(1)}$= 6.986, adj. p= 0.008), and block*score balance ($\chi^2_{(5)}$= 12.646, p= 0.027, adj. p= 0.0315) (Figure 17C).

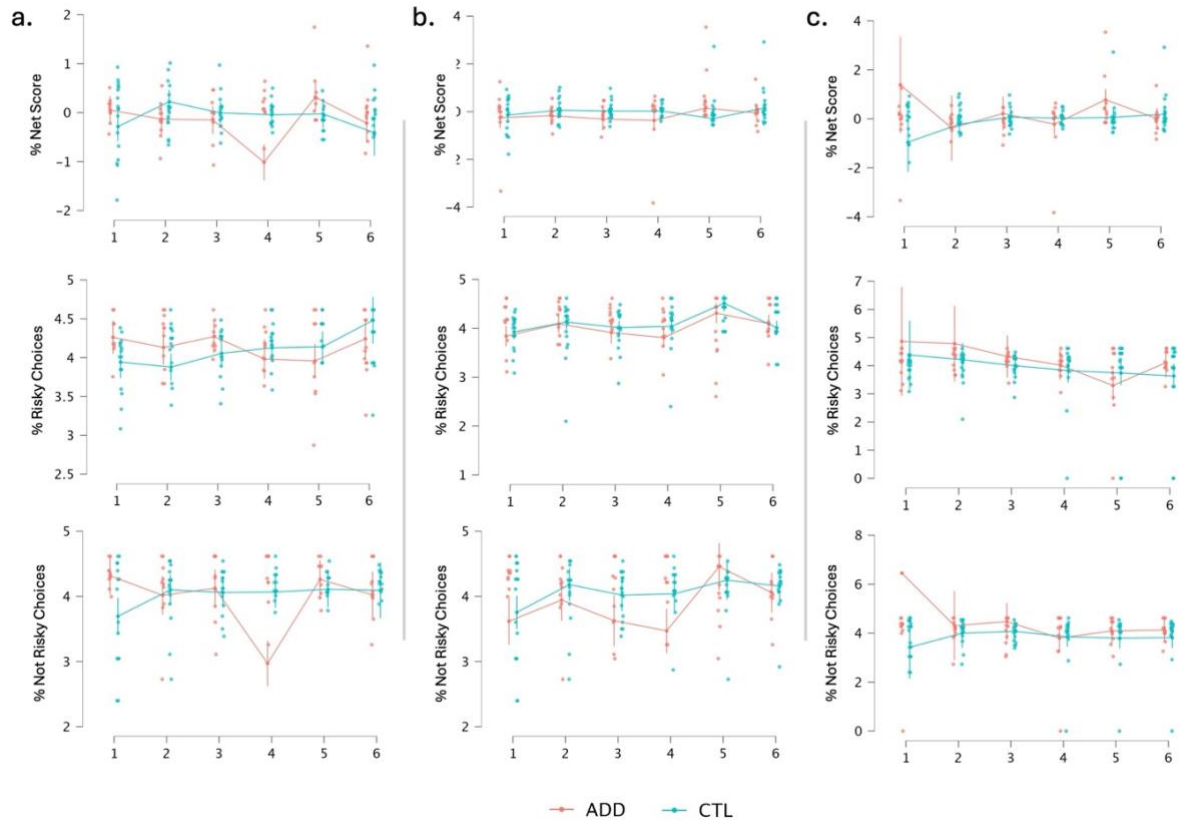


*Figure 17. Line graphs of modified Iowa Gambling Task results. The performance of individuals with addictive behaviors (ADD, in red) and controls (CTL, in light blue) is shown. For each category (% of Risky Choices, % of Not Risky Choices, and Net Score), trends across blocks (x-axis: 1–6) are displayed. Panel a. shows the results influenced by reward rate, panel b. by loss, and panel c. by score balance (current total point updates).*

*Post-Hoc Analysis*

*ADD Group.* Net score showed significant effects for block*reward interaction ($\chi^2_{(5)}$= 22.192, adj. p= 0.001), block*loss interaction ($\chi^2_{(5)}$= 64.547, adj. p= 0.001) ), and block*score balance interaction ($\chi^2_{(5)=}$ 13.958, adj. p= 0.048). For risky choices, significant effects were found for block*reward interaction ($\chi^2$(5)= 35.377, adj. p< 0.001), and reward ($\chi^2_{(1)}$= 20.214, adj. p<

0.001). For not risky choices, significant effects were found for block*loss interaction ($\chi^2_{(5)}$= 73.033, adj. p< 0.001), and loss ($\chi^2_{(1)}$= 5.091, adj. p= 0.036).

*CTL Group.* Net score showed significant effects for block*reward interaction ($\chi^2_{(5)}$= 23.960, adj. p= 0.001), and reward ($\chi^2_{(1)}$= 5.928, adj. p= 0.015). For risky choices, significant effects were found for block*reward interaction ($\chi^2_{(5)}$= 47.972, adj. p< 0.001), reward ($\chi^2_{(1)}$= 25.655, adj. p< 0.001), block*loss interaction ($\chi^2_{(5)}$= 13.344, adj. p= 0.02), and loss ($\chi^2_{(1)}$= 11.148, adj. p= 0.003). No significant effects were found for not risky choices.

*Learning effect.* A Mann-Whitney U test comparing CTL and ADD groups across individual blocks and blocks grouped (first three and last three) revealed a significant difference in risky choices during the first three blocks, with the CTL group playing less risky decks (U = 1091, p = 0.022). No other significant differences were found in net score or not risky choices across the remaining blocks.

To sum up, the CTL group showed a quicker reduction in risky choices and more adaptive behavior, adjusting to feedback effectively. In contrast, the ADD group exhibited prolonged engagement in risky plays, likely driven by heightened reward reactivity, reflecting more chaotic and less strategic decision-making.

***Task-Related EEG (ERSP) Results***

The cluster-based permutation test (CBS) identified significant differences between the *ADD* and control groups exclusively in the risky play condition. Notably, in the pre-choice time window (-0.8 to 0 seconds), the *ADD* group exhibited significantly lower power in both the theta and gamma frequency bands. In the theta band, two significant clusters were detected: the first cluster demonstrated a cluster-based stat of -17.31 (p = 0.003, CI = 0.003), while the second showed a cluster-based stat of -9.54 (p = 0.002, CI = 0.004). Furthermore, during the same pre-choice window, the *ADD* group displayed reduced power in the gamma band (cluster-based stat = -143.1, p < 0.001, CI = 0.0006), with a more pronounced effect in the high gamma range (cluster-based stat = -154.53, p = 0.002, CI = 0.0008) (Figure 18 B).

In the post-choice time window (0 to 1.3 seconds), CBS also revealed significant differences between the ADD and control groups. During this period, the ADD group exhibited higher power in the theta band (cluster-based stat = 9.1, p = 0.05, CI = 0.004) and the beta band (cluster-based stat = 30.46, p = 0.014, CI = 0.004). Additionally, the ADD group showed increased power in the gamma band (cluster-based stat = 87.44, p = 0.004, CI = 0.001), with significant effects in both the low gamma (cluster-based stat = 9.62, p = 0.044, CI = 0.004) and high gamma bands (cluster-based stat = 74.01, p = 0.007, CI = 0.001) relative to the control group (Figure 18 B).

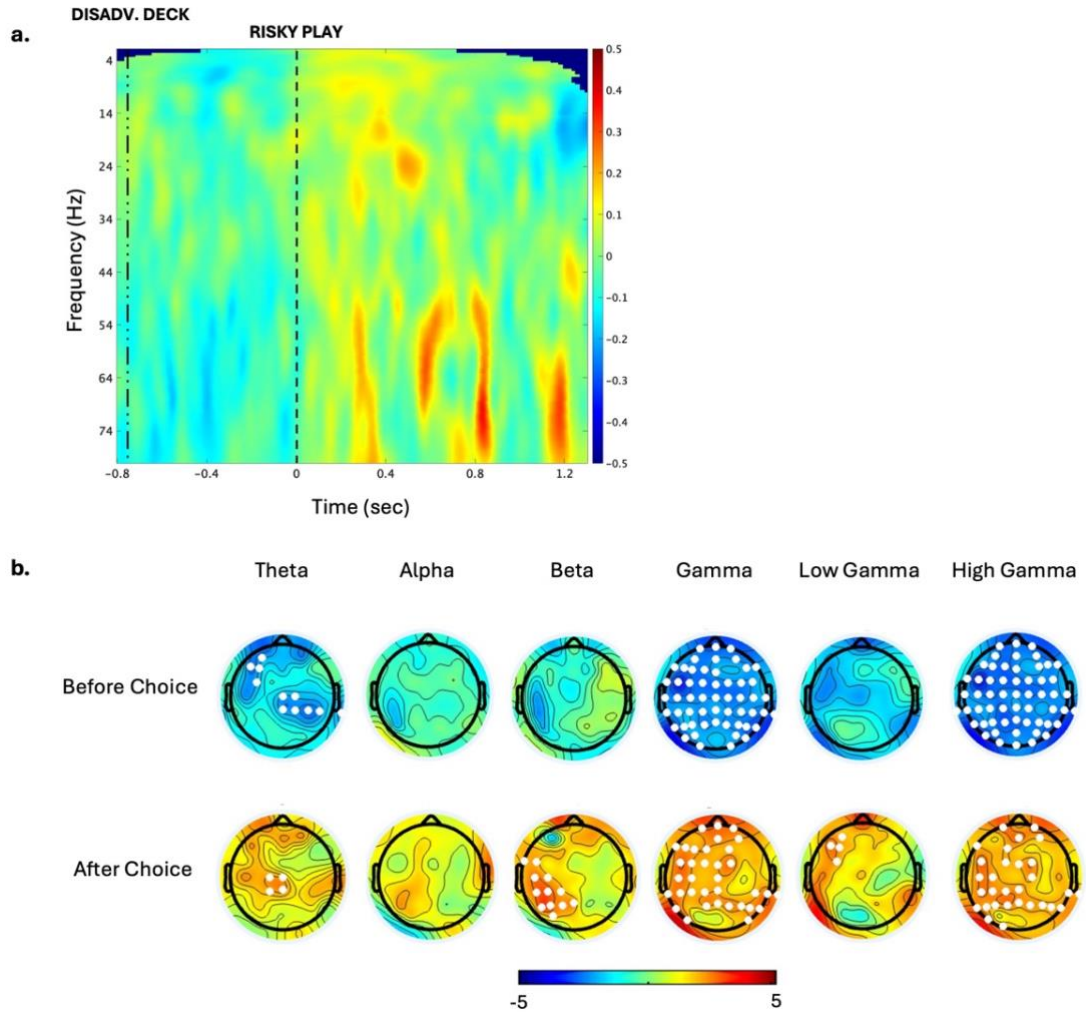


*Figure 18. Panel a. Time-frequency representation of neural activity during risky decision-making in the modified Iowa Gambling Task. The color scale represents power changes (in dB) relative to baseline, with warm colors (red) indicating increased power and cool colors (blue) indicating decreased power. The plot illustrates the comparison between individuals with addictive behaviors (ADD) and controls (CTL). Panel b. T-maps of group comparisons (ADD vs. CLT) before the risky choice (above) for the theta, alpha, beta, and gamma (low and high) bands. The exact comparisons after the risky choice are reported below. White dots indicate electrodes with significant group differences after cluster correction for multiple comparisons.*

### *Resting State EEG Analysis*

#### *Power Spectral Density*

Cluster-based permutation statistics (CBS) of the resting-state power spectrum revealed two significant positive clusters in the beta frequency band, indicating that the ADD group exhibited greater beta power at rest relative to the control group. The first cluster was localized to the left frontocentral region (cluster statistic = 9.225, p = 0.045, CI = 0.004), while the second cluster was observed in the right frontotemporal region (cluster statistic = 8.58, p = 0.047, CI = 0.004) (Figure 19 A-C).

*Oscillatory vs Fractal components*

Following decomposition using irregular resampling auto-spectral analysis (IRASA), separate analyses of the oscillatory and fractal components were performed. CBS of the oscillatory component replicated the finding of increased beta power in the ADD group, though restricted to a single positive cluster in the left frontocentral region (cluster statistic = 11.9, p = 0.045, CI = 0.004). In contrast, analysis of the fractal component revealed elevated power in the ADD group compared to controls in both the alpha band (cluster statistic = 8.12, p = 0.048, CI = 0.004) and the beta band (cluster statistic = 7.9, p = 0.049, CI = 0.004), with these effects localized to the right frontotemporal region (Figure 19 A-D-E).

*Power-Law Exponent (PLE)*

Cluster-based permutation analysis of the power-law exponent (PLE), which reflects the balance between low- and high-frequency activity in the brain, revealed a significant group difference in the high-frequency range (20–80 Hz). The ADD group exhibited a steeper PLE compared to the control group (cluster statistic = 23.25, p = 0.016, CI = 0.003), indicating a shift in power distribution towards higher frequencies (Figure 19 B-F).

***Correlations Between EEG Metrics and Behavioral Performance***

*Risk-Taking Behavior and Pre-Choice ERSP*

No significant correlations were identified in the CTL group. However, within the ADD group, a significant negative correlation was found between the number of exploded balloons in the Balloon Analog Risk Task (BART) and theta power preceding risky decisions (risky choices) ($\rho$ = -0.827, p = 0.002). Similar negative correlations were observed with gamma power ($\rho$ = -0.836, p = 0.001) and high gamma power ($\rho$ = -0.836, p = 0.001) before risky decisions (Figure 20).

Moreover, a significant positive correlation was identified between the points earned during the BART and theta power before risky plays ($\rho$ = 0.679, p = 0.017). Similar correlations were observed with gamma power ($\rho$ = 0.936, p < 0.001) and high gamma power ($\rho$ = 0.936, p < 0.001).

Additionally, theta power preceding risky decisions exhibited a significant negative correlation with the BIS-11 cognitive complexity subscale ($\rho$ = -0.641, p = 0.034), with similar negative correlations for gamma power ($\rho$ = -0.636, p = 0.035) and high gamma power ($\rho$ = -0.636, p = 0.035) (Figure 20).

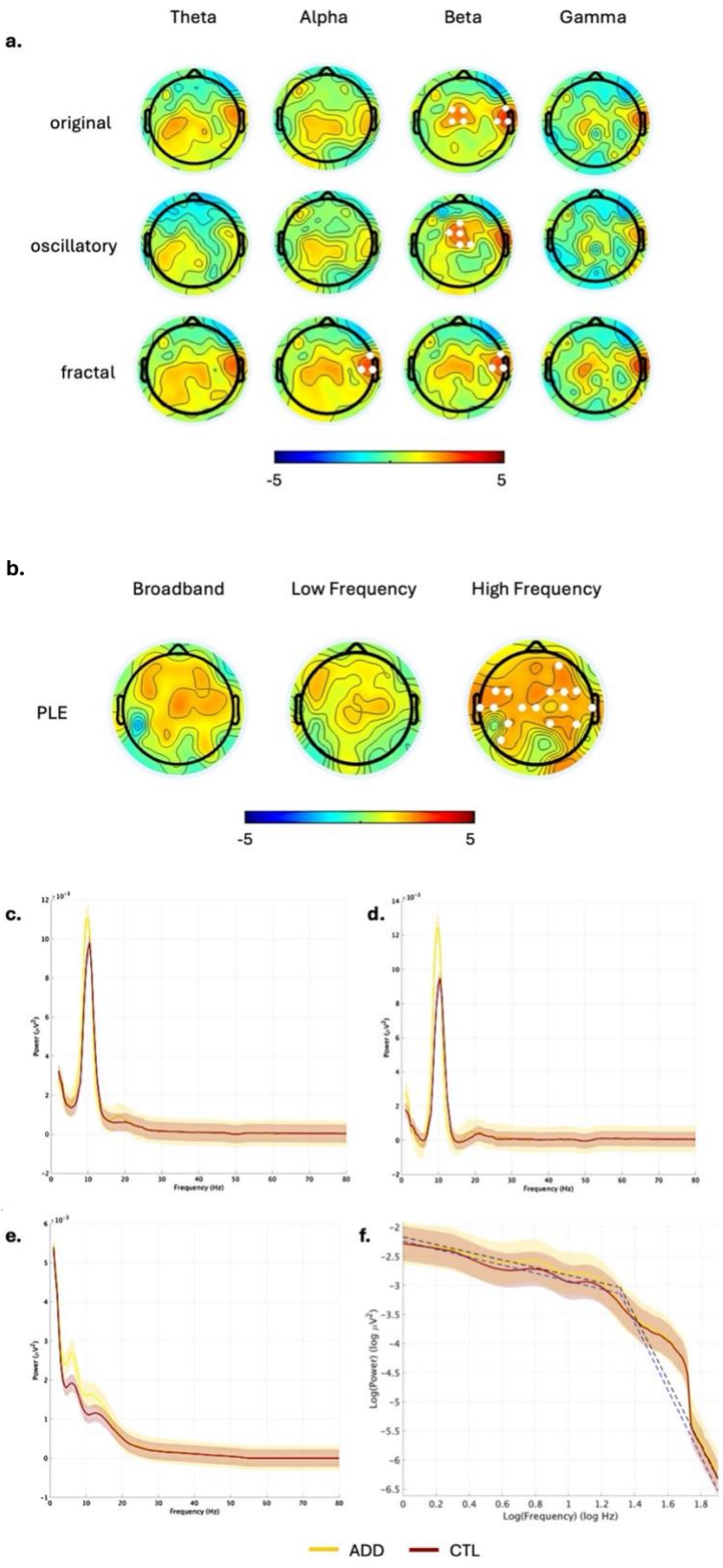


*Figure 19. T-maps and spectral plots comparing individuals with addictive behaviors (ADD) and controls (CTL) at resting state for different frequency bands. Panel a. T-maps of group comparisons for the original, oscillatory, and fractal components across theta (4-8 Hz), alpha (8-13 Hz), beta (13-30 Hz), and gamma (30-80 Hz) frequency bands. Panel b. T-maps showing group differences in Power Law Exponent (PLE) for broadband (2-80 Hz), low frequency (2-19 Hz), and high frequency (20-80 Hz) ranges. White dots indicate electrodes with significant group differences after cluster correction*

*for multiple comparisons. Panels c.-e. Power Spectral Density line plots comparing ADD (yellow) and CTL (red) groups across different frequency bands: theta, alpha, beta, and gamma. Panel f. shows the log-log representation of power spectral density for low and high frequencies. Shaded areas indicate each group's standard error of the mean (SEM). Dashed lines (blue for CTL and black for ADD) show the interpolated regression lines used to estimate the power-law exponent (PLE) for the low (1- 20 Hz) and high frequencies (20-80 Hz).*

*Impulsiveness and Post-Choice ERSP*

A significant negative correlation was also found between theta power following risky decisions and the BIS-11 cognitive complexity subscale ($\rho = -0.719$, $p = 0.013$). Similar findings were observed for beta power ($\rho = -0.641$, $p = 0.034$) and low gamma power ($\rho = -0.631$, $p = 0.037$). Furthermore, theta power after risky decisions negatively correlated with the BIS-11 cognitive instability subscale ($\rho = -0.647$, $p = 0.031$) (Figure 20).

*Resting-State EEG and Iowa Gambling Task (IGT) Performance.* In the control group (CTL), no significant correlations were found. However, in the addiction group (ADD), a significant positive correlation was observed between resting-state fractal alpha power in the right frontotemporal region and the percentage of not risky choices ($\rho = 0.655$, $p = 0.034$) (Figure 21).

*Attention/Arousal and Resting-State EEG Metrics*

No significant correlations were detected in the CTL group. However, in the ADD group, a significant negative correlation was identified between Stroop accuracy (interference effect) and resting-state fractal beta power ($\rho = -0.741$, $p = 0.009$) as well as fractal alpha power ($\rho = -0.838$, $p = 0.001$) (Figure 21).

*Clinical scales and Resting-State Metrics.*

In the ADD group, a significant negative correlation was found between the higher frequency PLE and the State-Trait Anxiety Inventory (STAI-I) ($\rho = -0.613$, $p = 0.045$). Oscillatory beta was found to correlate positively with the loss rate slope (rho = 0.682, $p = 0.025$) and negatively with the risky choice slope (rho = -0.764, $p = 0.009$) (Figure 21).

In the CTL group, a significant positive correlation emerged between high-frequency PLE at the resting state and the BIS-11 non-planning subscale ($\rho = 0.529$, $p = 0.03$), and a positive correlation between PLE and loss rate ($\rho = 642$, $p = 0.007$) (Figure 21).

## Predicting Addiction Status Using Logistic Regression

A logistic regression model predicting group membership (CTL vs. ADD) was fitted using high-frequency PLE (20-80 Hz), impulsivity (BIS-11), and gender as predictors. The model explained between 55.9% (McFadden $R^2$) and 71.4% (Nagelkerke $R^2$) of the variance in group classification ($\chi^2 = 20.963$, $p < 0.001$).


*Figure 20. Correlations between EEG metrics during the modified Iowa Gambling Task (mIGT) and impulsiveness and risk-taking behavior in ADD group. The Spearman correlation coefficient is plotted for each pairwise comparison. All correlations are presented with z-transformed EEG metrics and raw behavioral data. Behavioral measures include the Balloon Analog Risk Task (BART: EB = Exploded Balloons, PE = Points Earned, RTS = Risk-Taking Score) and the Barratt Impulsiveness Scale (BIS-11: CC = Cognitive Complexity subscale). Framed bars indicate significant correlations.*

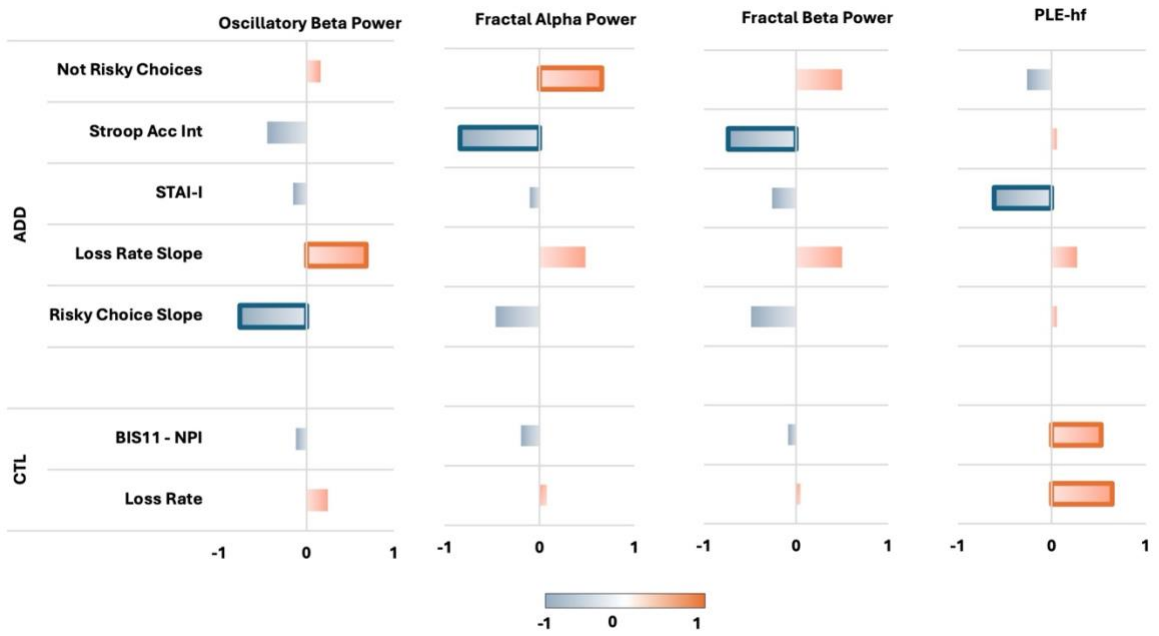


*Figure 21. Correlations between resting-state EEG metrics and decision-making and psychological assessments. The Spearman correlation coefficient is plotted for each pairwise comparison. All correlations are presented with z-transformed EEG metrics and raw behavioral data. Behavioral and psychological measures include STROOP Accuracy Interference (STROOP Acc Int), State-Trait Anxiety Inventory – State Subscale (STAI-I), and Barratt Impulsiveness Scale (BIS-11: NPI = Non-Planning Impulsiveness subscale). Framed bars indicate significant correlations.*

*PLE High Frequency:* A lower PLE slope was significantly associated with higher odds of being in the ADD group (Estimate = -2.358, $p = 0.007$).

*Impulsivity (BIS-11):* Higher impulsivity scores also significantly predicted ADD membership (Estimate = 0.357, $p = 0.012$).

*Gender:* While not significant, the male gender approached significance as a predictor (Estimate = 5.729, $p = 0.066$).

*Classification Accuracy:* The model correctly classified 88.2% of CTL and 81.8% of ADD subjects, with an overall accuracy of 85.7%.

The ADD group showed a flatter power slope in the high-frequency range (lower PLE), highlighting neurophysiological differences in the beta-to-gamma frequency dynamics. These findings, combined with impulsivity, provide predictors of addiction status and offer meaningful insights into EEG biomarkers in addictive behaviors. While the results were significant, caution is warranted in interpreting these findings due to the sample size limitations.

# Discussion

### *Affective Dysregulation and Impulsivity in Addiction*

The clinical assessment revealed that individuals in the ADD group exhibited significantly higher levels of depressive symptoms, specifically in the affective domain, alongside increased impulsiveness across several cognitive domains. These findings are consistent with extensive literature showing that affective dysregulation, particularly emotional instability, is a core feature of addictive behaviors and substance use disorders. Studies have shown that depressive symptoms, especially those related to mood regulation, often co-occur with substance use as individuals turn to substances to cope with emotional distress(Koob & Volkow, 2016). The higher affective symptom scores in the ADD group suggest that emotional dysregulation may be driving their maladaptive coping mechanisms, such as substance use, in line with research indicating that heightened emotional reactivity is a predictor of addiction vulnerability (Koob & Volkow, 2016).

Increased impulsiveness, particularly in non-planning and cognitive complexity subdomains, is also consistent with previous findings that individuals with substance use disorders often exhibit deficits in executive function and self-control (Chamberlain & Sahakian, 2007). Impulsivity has been linked to poor decision-making, where individuals prioritize immediate rewards over long-term consequences (Bechara, 2005). Our findings support this hypothesis, suggesting that impaired cognitive complexity and planning may contribute to the inability of individuals with addiction to control their impulses, reinforcing the cycle of substance abuse. This is further corroborated by neuroimaging studies showing that structural and functional deficits in the prefrontal cortex, a region critical for cognitive control, are commonly observed in addiction (Goldstein & Volkow, 2002).

Interestingly, the lower state of anxiety observed in the ADD group contrasts with much of the literature, which often reports higher anxiety levels in individuals with addiction (Kushner, 2000). One possible explanation is that chronic substance use may result in emotional blunting, leading to a dampened response to stress or acute anxiety (Zakiniaeiz et al., 2019). This emotional numbing might explain why trait anxiety remains comparable between groups, as chronic substance users may not experience the acute fluctuations in emotional states that characterize high-state anxiety. This finding aligns with research suggesting that prolonged substance use can alter emotional processing, reducing the typical stress responses seen in non-addicted individuals (Sinha, 2008).

### *Risk-Taking Behavior and Feedback Sensitivity*

The pronounced risk-taking behavior observed in the ADD group during the Balloon Analog Risk Task (BART) is a hallmark of addictive behavior. Risk-taking in addiction has been widely linked to deficits in reward evaluation and delayed gratification (Cavanagh et al., 2011; L. Clark et al., 2009). The ADD group's greater number of exploded balloons and higher pump levels suggest an overvaluation of immediate rewards and a diminished ability to accurately gauge future adverse consequences, a phenomenon supported by the somatic marker hypothesis(Bechara, 2000). This hypothesis posits that emotional signals guide decision-making, and in individuals with addiction, these signals may be attenuated or distorted, leading to risky and impulsive choices.

The lack of significant differences in other neurocognitive tasks, such as the Go-NoGo task, Stroop, and Wisconsin Card Sorting Test (WCST), suggests that the cognitive deficits in the ADD group are domain-specific, particularly affecting reward-related decision-making rather than global executive function. This specificity aligns with previous studies showing that while individuals with addiction may not exhibit broad cognitive deficits, they tend to perform poorly on tasks involving risk, reward, and feedback sensitivity (Verdejo-García et al., 2012). Our findings are in agreement with the reward deficiency syndrome (Blum et al., 2022) , which suggests that addiction results from an underactive reward system, making individuals more likely to engage in risky behaviors to achieve the desired level of reward.

The Iowa Gambling Task (IGT) results further support the notion that individuals with addiction are particularly sensitive to feedback, especially when it comes to reward. Significant group × block × feedback interactions indicate that individuals in the ADD group were more influenced by immediate rewards than penalties, which aligns with research showing that addiction involves impaired feedback processing (Hester & Garavan, 2004). This heightened sensitivity to rewards suggests an underlying neurobiological dysfunction in reward processing pathways, likely involving the ventral striatum and dopaminergic circuits (Bickel et al., 2012), which are known to be altered in substance users.

### *Neural Correlates of Impaired Decision-Making*

The EEG findings offer critical insights into the neural mechanisms underlying impaired decision-making in the ADD group. The pre-choice suppression of theta power, particularly before risky decisions, suggests deficits in the neural circuits that govern cognitive control and reward anticipation, confirming results found by Cavanagh and colleagues in healthy subjects, who described Theta oscillations as often associated with cognitive control and conflict

monitoring (Cavanagh & Frank, 2014), which is pivotal in decision-making and reward processing. The reduced activity found in this frequency band within the ADD group implies difficulties integrating relevant information before making decisions, potentially resulting in more impulsive and riskier choices.

Our data's post-choice results show that the ADD group exhibited higher power in the theta, beta, and gamma bands after making risky choices. These findings align with studies conducted on healthy subjects by Mas-Herrero (2015), HajiHosseini (2012), and Yaple (2012) (HajiHosseini et al., 2012a; Mas-Herrero et al., 2015; Yaple et al., 2018) but also suggest a possible hyperactivation or hypersensitivity in the ADD group during feedback processing.

The increased theta power post-choice reflects a more robust engagement in feedback evaluation. HajiHosseini and Yaple's work shows that theta oscillations in healthy individuals are closely linked to feedback processing, particularly when there is a need to adjust future behavior based on the outcome of a risky choice. This increased theta power indicates that the ADD group may be more hyper-focused on feedback, likely in response to positive or negative outcomes (typically high during risky choices). However, while theta power in healthy individuals helps guide adaptive behavior, the exaggerated theta response in the ADD group may not result in effective learning but rather indicates an overactive response to feedback without proper behavioral adjustments.

The elevated beta power observed in the ADD group post-choice aligns with findings from (HajiHosseini et al., 2012a; Mas-Herrero et al., 2015; Yaple et al., 2018), where beta oscillations increase during reward-related feedback processing. In healthy individuals, beta power increases during positive feedback (rewards) and plays a role in reinforcing behavior. However, in the ADD group, this increase in beta activity likely reflects an over-sensitivity to feedback, especially in the context of risk, where feedback (both positive and negative) is heightened. The heightened beta response could suggest that individuals with addiction over-process reward feedback, which might contribute to their maladaptive reinforcement patterns and risky behavior repetition instead of learning to avoid risks.

Finally, the increased gamma power, particularly in both low and high gamma bands, is another sign of heightened reward processing in the ADD group. Gamma oscillations are typically linked to integrating feedback information and updating behavior (HajiHosseini et al., 2012a). While healthy individuals also show gamma activity after receiving feedback, the exaggerated gamma response in the ADD group suggests that their reward system is hyperactive, possibly making them overly reactive to both gains and losses during risky decisions. This hyperactivity might prevent them from learning efficiently from negative feedback and avoiding future risky decisions, a hallmark of compulsive decision-making in addiction.

Furthermore, the gamma oscillations result from the EEG study in the ADD group align closely with the findings discussed by Furth et al. (2013) and FitzGerald et al. (2015) (FitzGerald et al., 2015; Furth et al., 2013), particularly concerning the role of D4 receptors and dopamine's influence on cognitive function, reward learning, and neural synchronization. The pre-choice suppression of gamma power in the ADD group can be interpreted in the context of D4 receptor dysregulation, as outlined by Furth et al. (Furth et al., 2013). D4 receptors, highly expressed in the prefrontal cortex, are pivotal for regulating gamma oscillations, which play a crucial role in cognitive flexibility and the integration of reward signals during decision-making. When D4 receptor activity is disrupted, as may be the case in individuals with addictive behaviors, gamma oscillatory activity is reduced, leading to deficits in reward anticipation and executive function. This reduction in gamma power before risky decisions suggests that the ADD group struggles with adequately processing and integrating relevant information, likely contributing to more impulsive and risk-prone decision-making. The findings from Furth et al. highlight that D4 receptor modulation of gamma oscillations is critical for cognitive processes, and its impairment can result in poor decision-making outcomes, as observed in the ADD group.

The post-choice increase in gamma power, particularly following rewards, aligns with the reward learning model discussed by FitzGerald et al. (FitzGerald et al., 2015). According to this model, dopamine influences how reward feedback is processed and incorporated into future decision-making. The exaggerated gamma response post-reward in the ADD group suggests hyper-reactivity towards reward feedback, which may be linked to the dopaminergic overactivity seen in addiction. They propose that dopamine-driven reward learning involves the precision of prediction errors, and the exaggerated gamma power post-reward could reflect heightened sensitivity to outcomes. This response may align with the "active inference" model, where the brain becomes overly focused on reward feedback, prioritizing immediate outcomes over longer-term goals. In individuals with addiction, this manifests as an increased tendency toward maladaptive reward-seeking behaviors, reinforcing the feedback sensitivity and disrupted decision-making observed in the ADD group.

The strong correlations between pre-choice theta and gamma power and risk-taking behavior in the ADD group suggest that these neural oscillations are critical markers of decision-making ability. Individuals with lower pre-choice power in these bands were more likely to engage in risky decisions, while those with higher power earned more points, indicating better decision-making outcomes. These findings are consistent with previous research demonstrating that theta oscillations predict successful cognitive control and risk evaluation (Cavanagh & Frank, 2014).

The negative correlations between impulsiveness traits and both pre-choice theta and gamma power highlight the importance of cognitive control in decision-making for individuals with addiction. As impulsiveness increased, theta and gamma power (considered markers of cognitive control) decreased, suggesting that impulsive individuals present a reduced neural activity during decision-making tasks. This finding aligns with literature showing that impulsivity is strongly associated with reduced neural engagement in regions responsible for planning and self-regulation, such as the prefrontal cortex (Goldstein & Volkow, 2011).

***Resting-State Neural Dynamics in Addiction***

Resting-state EEG analysis revealed increased beta power in the frontocentral and frontotemporal regions in the ADD group, which is consistent with findings from previous studies showing heightened cortical arousal and dysregulated neural activity in individuals with addiction (Zilverstand et al., 2018). Increased beta activity has been associated with hyperactivity in executive networks. It may reflect an overactive state of the brain's reward and control systems, contributing to impulsive behavior and poor decision-making.

Intriguing findings emerged when evaluating oscillatory and fractal components separately after IRASA analysis. Notably, these results emphasize the pivotal role of beta oscillatory activity in shaping punishment sensitivity and behavioral adaptation. The positive correlation between beta power and the loss rate slope suggests that heightened beta activity correlates with greater responsiveness to penalties yet paradoxically reflects maladaptive responses, as evidenced by continued losses. By isolating the beta oscillatory component through IRASA, we demonstrate that this component, rather than the fractal part, is crucial in driving punishment sensitivity. This extends the framework of Massar et al. (Massar et al., 2012), deepening our understanding of beta oscillations' contribution to maladaptive decision-making. These findings not only clarify beta's involvement in feedback processing but also offer insights into its role in impaired behavioral regulation, particularly in individuals with addiction, who exhibit reduced sensitivity to feedback.

Shifting the focus to the fractal component, elevated fractal power in both alpha and beta bands in the right frontotemporal region further indicates a disruption in the balance of neural oscillations, which may underpin the behavioral and cognitive deficits seen in addiction (B. J. He, 2011). The positive correlation between resting-state fractal alpha power and not risky choices further emphasizes the role of stable baseline neural activity in guiding adaptive decision-making. These results suggest that individuals with more stable neural oscillations can better integrate feedback and make informed decisions, supporting models that link baseline neural dynamics to behavioral control (Voytek & Knight, 2015).

The power-law exponent analysis adds another layer of understanding to these findings. The shallower PLE slope observed in the ADD group suggests a shift towards higher frequency activity, indicative of altered cortical excitability and dysregulation of brain homeostasis (Voytek & Knight, 2015). Such alterations have been associated with cognitive impairments, particularly in decision-making tasks, as high-frequency oscillations tend to dominate over the low-frequency, integrative activity necessary for cognitive control (B. J. He, 2011).

According to PLE fundings, flatter PLE (indicative of increased high-frequency activity) was prominently observed in the ADD group. This finding aligns with the notion of neural dysregulation, where an overrepresentation of high-frequency activity is associated with cognitive control and decision-making impairments. High-frequency oscillations, such as beta and gamma, are typically linked to cognitive engagement and task processing, but when disproportionately elevated, they may reflect inefficiency or cognitive overload. This could impair the ability of individuals with addiction to integrate feedback from their environment effectively, particularly when it comes to learning from rewards and penalties. This neural dysregulation, as reflected in the flatter PLE, suggests that individuals with addiction may struggle to adapt their decision-making strategies over time in tasks that involve risk and reward, such as the Iowa Gambling Task (IGT).

Interestingly, the hypothesis that a flatter PLE is indicative of dysregulated behavior is further substantiated by the correlations observed within the CTL group as well. The positive correlation between PLE and penalty rate suggests that individuals with a flatter PLE (i.e., more high-frequency activity) are less sensitive to punishment as they continue to accrue penalties without effectively adjusting their behavior. Moreover, the positive correlation between PLE and the BIS-11 non-planning subscale supports this interpretation. Higher PLE values in the CTL group were associated with greater impulsivity, specifically non-planning impulsiveness, where individuals struggle with planning and cognitive control. This indicates that the elevated high-frequency activity in these individuals may reflect a reduced capacity for executive function.

Additionally, it is worth highlighting the fact that the negative correlation between PLE and state anxiety (STAI-I) in the ADD group presents a different dynamic. This result suggests that higher anxiety levels (though still moderate, as indicated by the scores on anxiety scales) may act as a protective factor for individuals with addiction. In contrast to the typical interpretation of a flatter PLE as a marker of dysregulation, higher anxiety (associated with a lower PLE) appears to support greater engagement with the task at hand. State anxiety reflects an individual's response to immediate situational stress and the need for vigilance and control. In this context, anxiety might be driving a heightened focus on goal-directed behavior and the necessity to regulate immediate actions. This finding aligns with research suggesting that moderate levels of anxiety

can enhance cognitive control and attentional focus, particularly in tasks requiring sustained attention and goal-directed behavior (Peschard & Philippot, 2016). For individuals with addiction, who often struggle with impulsivity and poor decision-making, heightened state anxiety may serve as a protective mechanism and, in the short term, enhance their ability to stay engaged with the task and exert greater cognitive control. Unfortunately, this correlation is not significant in the control group, where subjects showed less impulsiveness and higher state anxiety.

***Novel findings***

This study reveals novel findings regarding abnormal gamma activity in individuals with addictive behaviors during both pre- and post-risky choices linked to probable dopamine dysregulation. Unlike earlier research, which focused on ERSP in healthy individuals (Cavanagh et al., 2011; HajiHosseini et al., 2012b; Mas-Herrero et al., 2015b; Yaple et al., 2018), this is the first to apply Event-Related Spectral Perturbation (ERSP) analysis to examine decision-making in individuals with addiction during the Iowa Gambling Task (IGT)**,** offering fresh insights into their neural dynamics.

The suppression of gamma power before risky choices suggests deficits in anticipatory control, likely tied to disruptions in dopaminergic regulation, which plays a central role in reward processing and decision-making. This impaired anticipatory activity likely reflects the dysfunction in D4 receptor modulation of gamma oscillations, affecting cognitive flexibility and the integration of reward signals (Furth et al., 2013). The reduced gamma activity before risky decisions in the ADD group contrasts with patterns observed in healthy subjects, where normal gamma oscillations support proactive control and risk evaluation.

Regarding post-risky choices, the increase in gamma power, particularly after receiving rewards, indicates hyper-reactivity to feedback. This overactive response reflects dopamine-driven reward hypersensitivity, which aligns with addiction models where individuals prioritize immediate rewards over long-term outcomes (FitzGerald et al., 2015; Koob & Volkow, 2016). These findings suggest that gamma oscillations play a critical role in feedback processing for those with addiction, where the brain's reward system is hyper-activated, impairing learning from negative feedback and contributing to persistent risky behavior.

Moreover, the study links gamma dysregulation with the higher PLE (Power Law Exponent), suggesting disruptions in cortical networks' E/I (excitatory-inhibitory) balance. This dysregulation impacts neural network communication, particularly in regions related to cognitive control and emotion regulation, and aligns with addiction models that emphasize an

inability to shift from resting-state processes to task-related mental states. The flattened PLE slope in the frontocentral-parietal regions reflects an inability to disengage from the Default Mode Network (DMN), further exacerbating decision-making deficits (Voytek & Knight, 2015).

Another noteworthy point is the result from the logistic regression, which confirms the significant role of PLE with impulsiveness in predicting addiction. This finding aligns with Chambers et al.'s Scale-Free Systems Theory of Motivation and Addiction, which suggests that addiction arises from dysregulation in hierarchical, scale-free neural systems that govern motivation and decision-making (Chambers et al., 2007). Similarly, Jones et al.'s work on scale-free behavioral and cortical dynamics supports the idea that a flatter PLE reflects a breakdown in the brain's flexible, fractal-like organization, leading to impaired cognitive control and compulsive behaviors. These models highlight how disruptions in scale-free dynamics contribute to impulsivity, where the brain becomes less adaptive in processing rewards and managing behavioral regulation. The fact that PLE is a predictor of addiction underscores its potential as a neural marker, reflecting the brain's impaired ability to regulate behavior across multiple scales of functioning, particularly in relation to decision-making and reward sensitivity—key components of addictive behaviors.

By focusing on pre- and post-risky choice gamma dysregulation and its relationship with dopaminergic imbalances, this study adds a new perspective on the neurophysiological underpinnings of addiction and how these disrupted neural markers contribute to compulsive, maladaptive decision-making.

***Limitations***

The present study provides findings that align with existing literature and contribute valuable insights to the field of addiction and decision-making research. However, several limitations must be acknowledged. The primary limitation is the relatively small sample size, which reduces the generalizability of the findings. The results warrant replication and further data collection to confirm the observed patterns. Nevertheless, the robustness of the results was supported by post hoc analyses, including cluster-based statistics and false discovery rate (FDR) corrections, which validated the findings.

Another significant limitation concerns the variability in addictive behaviors and substance use within the ADD group. While the study aimed to evaluate the EEG correlates of decision-making in individuals with addictive behaviors, it is well established that the neural circuits and brain regions involved in addiction are broadly consistent across different substances and behaviors (Koob & Volkow, 2016). Consequently, the inclusion of individuals with varied

addictions—whether to substances such as alcohol or tobacco or pathological behaviors like gambling—does not undermine the validity of the results. This heterogeneity, instead, could be viewed as a strength, as it reflects the broad spectrum of addiction-related disorders recognized in the DSM-5, even though many individuals avoid seeking help for legal substances or behaviors until their condition becomes severe (Hasin et al., 2013). The study's inclusion criteria, therefore, reflect real-world challenges in diagnosing addiction and provide a meaningful contribution to neuroscience research, where the type of addiction may be considered a secondary factor as long as it meets the criteria for pathological use. Nonetheless, future studies would benefit from a more homogenous sample with individuals exhibiting similar addictive behaviors to enhance the precision of the findings.

Additionally, the gender imbalance within the ADD group presents another limitation. The ADD group is predominantly male, while the control group is more balanced in terms of gender. This is consistent with epidemiological reports, which suggest that men are more likely to develop addictive behaviors than women (Geneva: World Health Organization, 2024). However, gender has been found to influence addictive behavior and decision-making processes, and this factor emerged as a marginally significant predictor in logistic regression analyses within this study. Future research should aim to ensure a more balanced representation of genders in both groups further to examine potential gender-related differences in addiction and decision-making.

Regarding methodology and EEG analysis, a potential limitation of this study is the use of a notch filter and handling of saccadic movements, which may affect gamma oscillatory findings. A standard 50 Hz notch filter and ICA were applied to remove line noise and detect saccades, following established practices (Widmann et al., 2015). While this conservative approach minimizes distortions to gamma frequencies, alternative methods like adaptive notch filtering (Olguın et al., n.d.) or advanced artifact correction techniques (Plöchl et al., 2012) could further refine gamma band analyses. Future studies might consider these methods to enhance reliability.

In summary, while this study's findings are robust and supported by rigorous statistical validation, they should be interpreted cautiously due to the limitations above. Future research should aim to replicate these findings with larger, more homogenous samples and consider the impact of gender differences to strengthen the conclusions drawn.

***Future directions***

This study can serve as a valuable foundation for future research in several ways, particularly by offering new insights and paving the way for more refined studies on addiction-related neural mechanisms, decision-making, and therapeutic interventions based on targeted neuromodulation of dysfunctional networks.

The findings on altered theta, beta, and gamma oscillations in the addiction group provide essential markers of how addiction affects neural dynamics during decision-making. Future research can build on this by investigating whether these oscillatory changes are causal or consequential concerning addiction, exploring whether targeting these specific oscillations through neuromodulation could directly improve decision-making or reduce addictive behaviors.

The detailed pre- and post-choice neural activity analysis offers precise targets for neuromodulation interventions, such as TMS or tACS, as well as neurofeedback protocols. Future research can use the oscillatory markers identified in this study (e.g., pre-choice suppression of theta and gamma power) to develop personalized neuromodulation protocols that address reward anticipation and cognitive control deficits. This study's findings can inform parameter choices (e.g., frequency bands, brain regions) for neuromodulation treatments aimed at improving decision-making in addiction.

By using ERSP analysis to assess dynamic neural responses to risk and reward in real-time, this study sets a precedent for employing frequency-based, temporally sensitive techniques in future research. ERSP offers a more nuanced understanding of how the brain processes feedback during decision-making tasks, which can be applied to explore other psychiatric conditions (e.g., impulsivity in ADHD, risk-taking in bipolar disorder) where decision-making deficits are present. This could lead to comparative studies across disorders.

The resting-state EEG findings, characterized by elevated beta power and disrupted PLE dynamics in the addiction group, offer critical baseline neural signatures that could prove valuable in identifying individuals at heightened risk for developing addictive behaviors. Future longitudinal research could leverage these neural markers to predict addiction susceptibility or relapse risk, thereby informing early interventions before such behaviors become deeply ingrained.

The novel discovery of flatter PLE slopes in individuals with addiction introduces a significant new dimension to existing models of addiction-related neural dysregulation. Further investigations could explore the potential of PLE as a biomarker for monitoring addiction severity or assessing treatment efficacy over time. This insight may also pave the way for developing neurofeedback or other interventions designed to normalize PLE slopes, enhancing cognitive control and mitigating risk-taking behaviors. For future studies, it would be valuable to replicate these findings with larger and more diverse samples to validate the predictive power of PLE and impulsivity using more advanced machine learning models, such as Random Forest or Support

Vector Machines. This would help determine whether PLE consistently serves as a robust predictive factor across varied populations.

Furthermore, there is a compelling case for integrating PLE/EEG research with neurochemical studies, particularly those examining the role of dopamine in reward processing and cognitive regulation. Dopamine is central to addiction-related behaviors, influencing neural circuits involved in both inhibitory control and reward sensitivity. The flatter PLE slopes observed in addiction could reflect dysregulated dopaminergic function, particularly in critical areas such as the prefrontal cortex and striatum. Future research could explore whether these PLE changes correlate with dopamine activity using advanced neuroimaging techniques such as Positron emission tomography (PET) or magnetic resonance spectroscopy (MRS). This approach could provide critical insights into how neural oscillations and dopamine-driven behaviors interact, offering a more comprehensive understanding of addiction. Linking PLE dynamics to neurochemical pathways may also help identify individuals who are more susceptible to addiction and provide tailored interventions that target both neural oscillatory disruptions and dopamine imbalances.

***Conclusion***

In conclusion, this study underscores the importance of altered neural oscillations, particularly gamma activity and Power Law Exponent (PLE) dynamics, as key markers of decision-making impairments in individuals with addictive behaviors. The findings reveal that dysregulation in pre- and post-choice gamma power, coupled with flatter PLE slopes, is predictive of risky decision-making, highlighting these neural metrics as potential biomarkers for addiction-related cognitive dysfunction. These insights suggest that gamma oscillations and PLE could serve as promising targets for novel therapeutic interventions, such as neuromodulation, aimed at restoring cognitive control and reducing maladaptive risk-taking behaviors in addiction.

# Conclusion

In this comprehensive analysis of EEG markers across different psychiatric conditions, including mood disorders, substance use disorders (SUDs), and addictive behaviors, a consistent theme emerges: the disruption of neural oscillations and connectivity plays a critical role in the neurobiological underpinnings of these disorders. This conclusion integrates the findings from three discussions, each focusing on different facets of psychiatric disorders—depression, ketamine treatment, and addiction—unifying these insights into a broader understanding of how altered neural dynamics can serve as biomarkers for diagnosis, treatment response, and therapeutic interventions.

**Oscillatory Activity and ERSP Across Studies**

Oscillatory activity and event-related spectral perturbation (ERSP) offer a crucial window into understanding the neurophysiological underpinnings of psychiatric disorders, spanning depression, bipolar disorder, and addiction.

In *Chapter 3*, elevated beta and gamma power in fronto-parietal regions during resting-state EEG was observed in individuals with high BDI scores compared to controls. The increase in high-frequency oscillations (beta and gamma) is linked to cognitive inflexibility and emotional dysregulation. Beta oscillations are crucial for attentional processes and working memory, while gamma oscillations are associated with cognitive functions like emotion regulation. The lack of beta power increases after task performance in the high-BDI group suggests impaired neuroplasticity and an inability to adapt cognitive resources in response to task demands. This rigidity reflects energy dysregulation in key regions involved in emotion and executive function, aligning with theories that position depression as a disorder of network inflexibility.

In *Chapter 4*, ketamine's effects on bipolar depression demonstrated an intriguing shift in oscillatory activity. After ketamine treatment, there was a reduction in theta, alpha, and low beta

activity, paired with increased gamma power. This oscillatory shift mirrors some of the observations in *Chapter 3*, with gamma increases reflecting improved network connectivity and flexibility. In contrast to the rigidity observed in depression, ketamine has been thought to enhance the brain's adaptability by modulating high-frequency activity, which is associated with neuroplasticity. This increase in gamma after ketamine indicates restored network flexibility and a more balanced excitatory/inhibitory activity, a promising effect for treating mood disorders.

*Chapter 5* delves into the oscillatory dynamics in addiction, where pre-choice suppression of theta and gamma power during risky decision-making tasks points to deficits in anticipatory control. This lack of theta and gamma activity suggests an inability to prepare for and evaluate potential risks, paralleling the cognitive control deficits observed in depression. Post-choice, individuals with addiction displayed heightened theta, beta, and gamma power, especially after receiving feedback, indicating a hyperactive reward system. Unlike the emotional overcompensation seen in depression, the oscillatory hyperactivity in addiction is linked to an overprocessing of reward signals driven by a dysregulated dopamine system. The findings show that addiction, like depression, involves disrupted high-frequency oscillations, but here, it manifests as a maladaptive sensitivity to reward feedback.

ERSP analysis in *Chapter 5* provided further insights into how oscillations change in response to tasks. The suppression of theta and gamma power before risky decisions and the post-decision increases in these bands, particularly after rewards, highlight the dysfunctions in anticipatory control and feedback processing in individuals with addiction. The increased post-choice gamma power reflects the hyperactivation of reward systems, making individuals more reactive to rewards and less capable of learning from negative outcomes. The dynamic changes captured by ERSP in addiction are comparable to the resting-state findings in depression, with both conditions showing oscillatory disruptions that point to impaired network communication and energy regulation. However, while depression is characterized by cognitive rigidity, addiction involves heightened reactivity to rewards, creating different yet related neural deficits.

Across these studies, beta and gamma oscillations emerge as critical markers of dysfunction in both mood disorders and addiction. In depression, beta and gamma power reflect compensatory mechanisms for cognitive deficits, while in addiction, they signal an exaggerated sensitivity to reward. Ketamine's effect of increasing gamma power further supports the notion that modulating these high-frequency oscillations can restore neuroplasticity and flexibility, potentially offering therapeutic benefits for both mood and addictive disorders.

**Scale-Free Dynamics, Power-Law Exponent (PLE), Entropy, and Complexity**

Fractal dynamics and the power-law exponent (PLE) provide essential insights into neural networks' energy regulation and stability across psychiatric disorders.

In *Chapter 3*, the flatter PLE observed in individuals with high BDI scores indicates increased neural noise and reduced efficiency in brain communication. The flatter PLE suggests that the brain's energy is poorly regulated, leading to cognitive rigidity and emotional dysregulation. This finding reflects a broader disruption in the brain's ability to balance excitatory and inhibitory activity, consistent with the idea that depression is characterized by network inefficiency and energy dysregulation.

In *Chapter 4*, ketamine treatment also resulted in a flattening of the PLE, particularly in higher frequency bands. However, unlike the flatter PLE in depression, ketamine-induced changes reflect an enhancement in neural flexibility and complexity. The increase in signal entropy after ketamine administration indicates greater variability and adaptability in brain activity, which is essential for cognitive and emotional flexibility. By modulating fractal dynamics, ketamine helps to restore network balance and energy regulation, which could explain its rapid antidepressant effects. The increase in entropy and neural complexity further supports the idea that ketamine fosters a more dynamic and adaptable brain state, which is crucial for effective mood regulation and cognitive functioning.

In *Chapter 5*, individuals with addiction exhibited a flatter PLE in the frontocentral and frontotemporal regions, reflecting heightened cortical excitability and impaired decision-making processes. Similar to the findings in depression, the flatter PLE in addiction indicates a breakdown in network efficiency, particularly in regions involved in cognitive control and reward processing. The altered fractal dynamics in addiction suggest that the brain's energy resources are mismanaged, leading to poor integration of feedback and an inability to learn from negative outcomes. Like in depression, the dysregulated balance between high- and low-frequency activity reflects broader issues of energy regulation, though, in addictive behaviors, this manifests as maladaptive reward sensitivity rather than emotional dysregulation.

The correlation between resting-state fractal alpha power and adaptive decision-making in *Chapter 5* emphasizes the role of stable baseline neural activity in guiding behavior. Individuals with more stable neural oscillations were better able to integrate feedback and make informed decisions, supporting models of brain function that link stable fractal dynamics to behavioral control. This highlights how both oscillatory and fractal dynamics are crucial for maintaining cognitive flexibility and controlling impulsivity.

**Functional Connectivity**

Phase-amplitude coupling, which reflects the interaction between slow and fast brain rhythms, was a focus of *Chapter 3*. The individuals with high BDI scores showed increased theta–beta and theta–gamma PAC during resting-state EEG, particularly in the parietal and occipital regions. PAC is critical for coordinating cognitive processes like attention and working memory by linking slower oscillations (theta) to faster ones (beta and gamma). The elevated PAC in depression suggests that the brain is attempting to synchronize its activity more tightly to maintain cognitive function in the face of deficits. This overcompensation may reflect a compensatory mechanism for reduced neural efficiency, as seen in the flatter PLE findings. However, after task performance, the control group showed increased PAC, while the high-BDI group did not, further supporting the idea that depression involves impaired neuroplasticity and network adaptability.

PAC provides essential insights into functional connectivity, revealing how different brain regions synchronize to support cognitive processes. The lack of PAC modulation in individuals with depression indicates a broader failure of network flexibility, highlighting the role of energy regulation in maintaining healthy brain communication.

**Neuroplasticity and Energy Regulation**

Voytek & Knight (2015) emphasized that dynamic network communication is essential for healthy cognitive and emotional functioning. Across the three research works, the disruptions in oscillatory activity, fractal dynamics, and PAC point to a failure of neuroplasticity and energy regulation in depression, bipolar disorder, and addiction.

The oscillatory rigidity seen in depression, combined with the flatter PLE, reflects a breakdown in the brain's ability to manage energy effectively, leading to cognitive and emotional inflexibility. In addictive behaviors, the dysregulated reward system, reflected in exaggerated beta and gamma responses, shows how maladaptive neural dynamics can lead to poor decision-making. Ketamine's ability to restore network flexibility by modulating both oscillatory and fractal dynamics offers a potential therapeutic pathway for addressing these disruptions. By enhancing gamma power and increasing neural entropy, ketamine helps to re-establish the brain's capacity for dynamic, adaptive communication, providing a promising target for treating psychiatric disorders.

In conclusion, the findings across these papers highlight the central role of oscillatory dynamics, fractal properties, and functional connectivity in understanding the neurophysiological underpinnings of psychiatric disorders. Targeting these disruptions through interventions that promote neuroplasticity and improve energy regulation, such as ketamine or neuromodulation

techniques, holds promise for developing personalized treatments for mood disorders and addiction.

**Clinical Implications and Future Directions**

The findings from these three studies underscore the potential of EEG as a tool for identifying biomarkers of psychiatric disorders. The consistent disruptions in oscillatory activity, PAC, and fractal dynamics across depression, bipolar disorder, and addiction suggest that these neural markers could be used to guide personalized treatment strategies. For example, pre-task suppression of theta and gamma power, combined with post-task increases in beta and gamma, could serve as indicators of impaired cognitive control and reward processing in individuals with addiction. Similarly, reductions in low-frequency oscillatory power and flattening of the PLE could predict treatment response in individuals receiving ketamine for depression.

Future research should focus on integrating EEG with other neuroimaging techniques, such as magnetic resonance spectroscopy (MRS), to further elucidate the relationship between neural oscillations and energy metabolism. Additionally, the application of neuromodulation techniques, such as transcranial magnetic stimulation (TMS) or transcranial alternating current stimulation (tACS), as well as deep brain stimulation (DBS), could target specific frequency bands to improve cognitive control and emotional regulation in individuals with psychiatric disorders.

In conclusion, the consistent findings of altered neural dynamics across depression, bipolar disorder, and addiction highlight the importance of EEG in advancing our understanding of psychiatric conditions. By identifying biomarkers that reflect disruptions in oscillatory activity, PAC, and fractal dynamics, this body of research offers promising avenues for developing personalized treatment strategies aimed at restoring neural plasticity and improving patient outcomes.

# References


Acevedo-Diaz, E. E., Cavanaugh, G. W., Greenstein, D., Kraus, C., Kadriu, B., Zarate, C. A., & Park, L. T. (2020). Comprehensive assessment of side effects associated with a single dose of ketamine in treatment-resistant depression. *Journal of Affective Disorders*, *263*, 568–575. https://doi.org/10.1016/j.jad.2019.11.028

Adamson, S. J., Kay-Lambkin, F. J., Baker, A. L., Lewin, T. J., Thornton, L., Kelly, B. J., & Sellman, J. D. (2010). An improved brief measure of cannabis misuse: The Cannabis Use Disorders Identification Test-Revised (CUDIT-R)☆. *Drug and Alcohol Dependence*, *110*(1–2), 137–143. https://doi.org/10.1016/j.drugalcdep.2010.02.017

Agnorelli, C., Cinti, A., Barillà, G., Lomi, F., Scoccia, A., Benelli, A., Neri, F., Smeralda, C. L., Cuomo, A., Santarnecchi, E., Tatti, E., Godfrey, K., Tarantino, F., Fagiolini, A., & Rossi, S. (2025). Neurophysiological correlates of ketamine-induced dissociative state in bipolar disorder: Insights from real-world clinical settings. *Molecular Psychiatry*. https://doi.org/10.1038/s41380-025-02889-2

Agyapong-Opoku, G., Agyapong, B., Obuobi-Donkor, G., & Eboreime, E. (2023). Depression and Anxiety among Undergraduate Health Science Students: A Scoping Review of the Literature. *Behavioral Sciences*, *13*(12), 1002. https://doi.org/10.3390/bs13121002

Ahmed, Z., Wali, A., Shahid, S., Zikria, S., Rasheed, J., & Asuroglu, T. (2024). Psychiatric disorders from EEG signals through deep learning models. *IBRO Neuroscience Reports*, *17*, 300–310. https://doi.org/10.1016/j.ibneur.2024.09.003

Allen, J. J. B., & Cohen, M. X. (2010). Deconstructing the "Resting" State: Exploring the Temporal Dynamics of Frontal Alpha Asymmetry as an Endophenotype for Depression. *Frontiers in Human Neuroscience*, *4*. https://doi.org/10.3389/fnhum.2010.00232

American Psychiatric Association. (2022). *Diagnostic and Statistical Manual of Mental Disorders* (DSM-5-TR). American Psychiatric Association Publishing. https://doi.org/10.1176/appi.books.9780890425787

American Psychiatric Association, & American Psychiatric Association (Eds.). (2013). *Diagnostic and statistical manual of mental disorders: DSM-5* (5th ed). American Psychiatric Association.

Arns, M., Etkin, A., Hegerl, U., Williams, L. M., DeBattista, C., Palmer, D. M., Fitzgerald, P. B., Harris, A., deBeuss, R., & Gordon, E. (2015). Frontal and rostral anterior cingulate (rACC) theta EEG in

depression: Implications for treatment outcome? *European Neuropsychopharmacology*, *25*(8), 1190–1200. https://doi.org/10.1016/j.euroneuro.2015.03.007

Aust, S., Gärtner, M., Basso, L., Otte, C., Wingenfeld, K., Chae, W. R., Heuser-Collier, I., Regen, F., Cosma, N. C., van Hall, F., Grimm, S., & Bajbouj, M. (2019). Anxiety during ketamine infusions is associated with negative treatment responses in major depressive disorder. *European Neuropsychopharmacology*, *29*(4), 529–538. https://doi.org/10.1016/j.euroneuro.2019.02.005

Ballard, E. D., & Zarate, C. A. (2020). The role of dissociation in ketamine's antidepressant effects. *Nature Communications*, *11*(1), Article 1. https://doi.org/10.1038/s41467-020-20190-4

Barth, B., Rohe, T., Deppermann, S., Fallgatter, A. J., & Ehlis, A. (2021). Neural oscillatory responses to performance monitoring differ between high- and low-impulsive individuals, but are unaffected by TMS. *Human Brain Mapping*, *42*(8), 2416–2433. https://doi.org/10.1002/hbm.25376

Bas-Orth, C., Schneider, J., Lewen, A., McQueen, J., Hasenpusch-Theil, K., Theil, T., Hardingham, G. E., Bading, H., & Kann, O. (2020). The mitochondrial calcium uniporter is crucial for the generation of fast cortical network rhythms. *Journal of Cerebral Blood Flow & Metabolism*, *40*(11), 2225–2239. https://doi.org/10.1177/0271678X19887777

Bechara, A. (2000). Emotion, Decision Making and the Orbitofrontal Cortex. *Cerebral Cortex*, *10*(3), 295–307. https://doi.org/10.1093/cercor/10.3.295

Bechara, A. (2005). Decision making, impulse control and loss of willpower to resist drugs: A neurocognitive perspective. *Nature Neuroscience*, *8*(11), 1458–1463. https://doi.org/10.1038/nn1584

Beck, A. T., Steer, R. A., & Brown, G. (2011). *Beck Depression Inventory–II* [Dataset]. https://doi.org/10.1037/t00742-000

Beck, A. T., Ward, C. H., Mendelson, M., Mock, J., & Erbaugh, J. (1961). An inventory for measuring depression. *Archives of General Psychiatry*, *4*, 561–571. https://doi.org/10.1001/archpsyc.1961.01710120031004

Beggs, J. M., & Plenz, D. (2003). Neuronal Avalanches in Neocortical Circuits. *The Journal of Neuroscience*, *23*(35), 11167–11177. https://doi.org/10.1523/JNEUROSCI.23-35-11167.2003

Benjamini, Y., & Hochberg, Y. (1995). Controlling the False Discovery Rate: A Practical and Powerful Approach to Multiple Testing. *Journal of the Royal Statistical Society: Series B (Methodological)*, *57*(1), 289–300. https://doi.org/10.1111/j.2517-6161.1995.tb02031.x

Berman, A. H., Bergman, H., Palmstierna, T., & Schlyter, F. (2005). Evaluation of the Drug Use Disorders Identification Test (DUDIT) in Criminal Justice and Detoxification Settings and in a Swedish Population Sample. *European Addiction Research*, *11*(1), 22–31. https://doi.org/10.1159/000081413

Berman, R. M., Cappiello, A., Anand, A., Oren, D. A., Heninger, G. R., Charney, D. S., & Krystal, J. H. (2000). Antidepressant effects of ketamine in depressed patients. *Biological Psychiatry*, *47*(4), 351–354. https://doi.org/10.1016/S0006-3223(99)00230-9

Bhagwagar, Z., Wylezinska, M., Jezzard, P., Evans, J., Ashworth, F., Sule, A., Matthews, P. M., & Cowen, P. J. (2007). Reduction in occipital cortex gamma-aminobutyric acid concentrations in medication-free recovered unipolar depressed and bipolar subjects. *Biological Psychiatry*, *61*(6), 806–812.

https://doi.org/10.1016/j.biopsych.2006.08.048

Bickel, W. K., Jarmolowicz, D. P., Mueller, E. T., Koffarnus, M. N., & Gatchalian, K. M. (2012). Excessive discounting of delayed reinforcers as a trans-disease process contributing to addiction and other disease-related vulnerabilities: Emerging evidence. *Pharmacology & Therapeutics*, *134*(3), 287–297. https://doi.org/10.1016/j.pharmthera.2012.02.004

Blum, K., McLaughlin, T., Bowirrat, A., Modestino, E. J., Baron, D., Gomez, L. L., Ceccanti, M., Braverman, E. R., Thanos, P. K., Cadet, J. L., Elman, I., Badgaiyan, R. D., Jalali, R., Green, R., Simpatico, T. A., Gupta, A., & Gold, M. S. (2022). Reward Deficiency Syndrome (RDS) Surprisingly Is Evolutionary and Found Everywhere: Is It "Blowin' in the Wind"? *Journal of Personalized Medicine*, *12*(2), 321. https://doi.org/10.3390/jpm12020321

Bradley, K. A. L., Mao, X., Case, J. A. C., Kang, G., Shungu, D. C., & Gabbay, V. (2016). Increased ventricular cerebrospinal fluid lactate in depressed adolescents. *European Psychiatry*, *32*, 1–8. https://doi.org/10.1016/j.eurpsy.2015.08.009

Bremner, J. D., Krystal, J. H., Putnam, F. W., Southwick, S. M., Marmar, C., Charney, D. S., & Mazure, C. M. (1998). Measurement of dissociative states with the Clinician-Administered Dissociative States Scale (CADSS). *Journal of Traumatic Stress*, *11*(1), 125–136. https://doi.org/10.1023/A:1024465317902

Buzsáki, G., Anastassiou, C. A., & Koch, C. (2012a). The origin of extracellular fields and currents—EEG, ECoG, LFP and spikes. *Nature Reviews Neuroscience*, *13*(6), 407–420. https://doi.org/10.1038/nrn3241

Buzsáki, G., Anastassiou, C. A., & Koch, C. (2012b). The origin of extracellular fields and currents—EEG, ECoG, LFP and spikes. *Nature Reviews Neuroscience*, *13*(6), Article 6. https://doi.org/10.1038/nrn3241

Buzsáki, G., & Draguhn, A. (2004). Neuronal oscillations in cortical networks. *Science (New York, N.Y.)*, *304*(5679), 1926–1929. https://doi.org/10.1126/science.1099745

Cai, Y., Guo, H., Han, T., & Wang, H. (2024). Lactate: A prospective target for therapeutic intervention in psychiatric disease. *Neural Regeneration Research*, *19*(7), 1473–1479. https://doi.org/10.4103/1673-5374.387969

Cape, E. G., & Jones, B. E. (1998). Differential modulation of high-frequency gamma-electroencephalogram activity and sleep-wake state by noradrenaline and serotonin microinjections into the region of cholinergic basalis neurons. *The Journal of Neuroscience: The Official Journal of the Society for Neuroscience*, *18*(7), 2653–2666. https://doi.org/10.1523/JNEUROSCI.18-07-02653.1998

Carhart-Harris, R. L. (2018a). The entropic brain—Revisited. *Neuropharmacology*, *142*, 167–178. https://doi.org/10.1016/j.neuropharm.2018.03.010

Carhart-Harris, R. L. (2018b). The entropic brain—Revisited. *Neuropharmacology*, *142*, 167–178. https://doi.org/10.1016/j.neuropharm.2018.03.010

Carlén, M., Meletis, K., Siegle, J. H., Cardin, J. A., Futai, K., Vierling-Claassen, D., Rühlmann, C., Jones, S. R., Deisseroth, K., Sheng, M., Moore, C. I., & Tsai, L.-H. (2012). A critical role for NMDA receptors in parvalbumin interneurons for gamma rhythm induction and behavior. *Molecular Psychiatry*, *17*(5), 537–548. https://doi.org/10.1038/mp.2011.31

Carver, C. S., & White, T. L. (1994). Behavioral inhibition, behavioral activation, and affective responses to impending reward and punishment: The BIS/BAS Scales. *Journal of Personality and Social Psychology*, *67*(2), 319–333. https://doi.org/10.1037/0022-3514.67.2.319

Casali, A. G., Gosseries, O., Rosanova, M., Boly, M., Sarasso, S., Casali, K. R., Casarotto, S., Bruno, M.-A., Laureys, S., Tononi, G., & Massimini, M. (2013). A Theoretically Based Index of Consciousness Independent of Sensory Processing and Behavior. *Science Translational Medicine*, *5*(198), 198ra105-198ra105. https://doi.org/10.1126/scitranslmed.3006294

Cauffman, E., Shulman, E. P., Steinberg, L., Claus, E., Banich, M. T., Graham, S., & Woolard, J. (2010). Age differences in affective decision making as indexed by performance on the Iowa Gambling Task. *Developmental Psychology*, *46*(1), 193–207. https://doi.org/10.1037/a0016128

Cavanagh, J. F., Bismark, A., Frank, M. J., & Allen, J. J. (2011). Larger Error Signals in Major Depression are Associated with Better Avoidance Learning. *Frontiers in Psychology*, *2*. https://doi.org/10.3389/fpsyg.2011.00331

Cavanagh, J. F., Bismark, A. W., Frank, M. J., & Allen, J. J. B. (2019). *Multiple Dissociations Between Comorbid Depression and Anxiety on Reward and Punishment Processing: Evidence From Computationally Informed EEG* (0). *3*(0), Article 0. https://doi.org/10.1162/CPSY_a_00024

Cavanagh, J. F., & Frank, M. J. (2014). Frontal theta as a mechanism for cognitive control. *Trends in Cognitive Sciences*, *18*(8), 414–421. https://doi.org/10.1016/j.tics.2014.04.012

Cavanagh, J. F., Frank, M. J., Klein, T. J., & Allen, J. J. B. (2010). Frontal Theta Links Prediction Errors to Behavioral Adaptation in Reinforcement Learning. *NeuroImage*, *49*(4), 3198. https://doi.org/10.1016/j.neuroimage.2009.11.080

Cavanagh, J. F., & Shackman, A. J. (2015). Frontal midline theta reflects anxiety and cognitive control: Meta-analytic evidence. *Journal of Physiology-Paris*, *109*(1–3), 3–15. https://doi.org/10.1016/j.jphysparis.2014.04.003

Chahine, L. M., Zhu, X., Ehrenkranz, R., Chen, H., Glynn, N. W., & Rosano, C. (2021). Changes in Self-Reported Energy Levels in Prodromal Parkinson's Disease. *Movement Disorders : Official Journal of the Movement Disorder Society*, *36*(5), 1276–1277. https://doi.org/10.1002/mds.28535

Chamberlain, S. R., & Sahakian, B. J. (2007). The neuropsychiatry of impulsivity: *Current Opinion in Psychiatry*, *20*(3), 255–261. https://doi.org/10.1097/YCO.0b013e3280ba4989

Chambers, R. A., Bickel, W. K., & Potenza, M. N. (2007a). A scale-free systems theory of motivation and addiction. *Neuroscience & Biobehavioral Reviews*, *31*(7), 1017–1045. https://doi.org/10.1016/j.neubiorev.2007.04.005

Chambers, R. A., Bickel, W. K., & Potenza, M. N. (2007b). A scale-free systems theory of motivation and addiction. *Neuroscience & Biobehavioral Reviews*, *31*(7), 1017–1045. https://doi.org/10.1016/j.neubiorev.2007.04.005

Choi, K. W., Kim, Y.-K., & Jeon, H. J. (2020). Comorbid Anxiety and Depression: Clinical and Conceptual Consideration and Transdiagnostic Treatment. In Y.-K. Kim (Ed.), *Anxiety Disorders: Rethinking and Understanding Recent Discoveries* (pp. 219–235). Springer. https://doi.org/10.1007/978-981-32-9705-0_14

Ciuciu, P., Varoquaux, G., Abry, P., Sadaghiani, S., & Kleinschmidt, A. (2012). Scale-Free and Multifractal Time

Dynamics of fMRI Signals during Rest and Task. *Frontiers in Physiology*, *3*, 186. https://doi.org/10.3389/fphys.2012.00186

Clark, D. L., Brown, E. C., Ramasubbu, R., & Kiss, Z. H. T. (2016). Intrinsic Local Beta Oscillations in the Subgenual Cingulate Relate to Depressive Symptoms in Treatment-Resistant Depression. *Biological Psychiatry*, *80*(11), e93–e94. https://doi.org/10.1016/j.biopsych.2016.02.032

Clark, L., Lawrence, A. J., Astley-Jones, F., & Gray, N. (2009). Gambling Near-Misses Enhance Motivation to Gamble and Recruit Win-Related Brain Circuitry. *Neuron*, *61*(3), 481–490. https://doi.org/10.1016/j.neuron.2008.12.031

*Common Comorbidities with Substance Use Disorders Research Report*. (2020). National Institutes on Drug Abuse (US). http://www.ncbi.nlm.nih.gov/books/NBK571451/

Cooper, P. S., Karayanidis, F., McKewen, M., McLellan-Hall, S., Wong, A. S. W., Skippen, P., & Cavanagh, J. F. (2019). Frontal theta predicts specific cognitive control-induced behavioural changes beyond general reaction time slowing. *NeuroImage*, *189*, 130–140. https://doi.org/10.1016/j.neuroimage.2019.01.022

Cortes-Briones, J. A., Cahill, J. D., Skosnik, P. D., Mathalon, D. H., Williams, A., Sewell, R. A., Roach, B. J., Ford, J. M., Ranganathan, M., & D'Souza, D. C. (2015). The Psychosis-like Effects of Δ9-Tetrahydrocannabinol Are Associated With Increased Cortical Noise in Healthy Humans. *Biological Psychiatry*, *78*(11), 805–813. https://doi.org/10.1016/j.biopsych.2015.03.023

Cotrena, C., Branco, L. D., Shansis, F. M., & Fonseca, R. P. (2016). Executive function impairments in depression and bipolar disorder: Association with functional impairment and quality of life. *Journal of Affective Disorders*, *190*, 744–753. https://doi.org/10.1016/j.jad.2015.11.007

Cui, L., Li, S., Wang, S., Wu, X., Liu, Y., Yu, W., Wang, Y., Tang, Y., Xia, M., & Li, B. (2024). Major depressive disorder: Hypothesis, mechanism, prevention and treatment. *Signal Transduction and Targeted Therapy*, *9*(1), 30. https://doi.org/10.1038/s41392-024-01738-y

d'Andrea, G., Pettorruso, M., Di Lorenzo, G., Rhee, T. G., Chiappini, S., Carullo, R., Barlati, S., Zanardi, R., Rosso, G., Di Nicola, M., Andriola, I., Marcatili, M., Clerici, M., Dell'Osso, B. M., Sensi, S. L., Mansur, R. B., Rosenblat, J. D., Martinotti, G., & McIntyre, R. S. (2024). The rapid antidepressant effectiveness of repeated dose of intravenous ketamine and intranasal esketamine: A post-hoc analysis of pooled real-world data. *Journal of Affective Disorders*, *348*, 314–322. https://doi.org/10.1016/j.jad.2023.12.038

Dakwar, E., Nunes, E. V., Hart, C. L., Hu, M. C., Foltin, R. W., & Levin, F. R. (2018). A sub-set of psychoactive effects may be critical to the behavioral impact of ketamine on cocaine use disorder: Results from a randomized, controlled laboratory study. *Neuropharmacology*, *142*, 270–276. https://doi.org/10.1016/j.neuropharm.2018.01.005

Davidson, R. J. (1992). Anterior cerebral asymmetry and the nature of emotion. *Brain and Cognition*, *20*(1), 125–151. https://doi.org/10.1016/0278-2626(92)90065-T

Davidson, R. J., Ekman, P., Saron, C. D., Senulis, J. A., & Friesen, W. V. (1990). Approach-withdrawal and cerebral asymmetry: Emotional expression and brain physiology: I. *Journal of Personality and Social Psychology*, *58*(2), 330–341. https://doi.org/10.1037/0022-3514.58.2.330

Davidson, R. J., Pizzagalli, D., Nitschke, J. B., & Putnam, K. (2002). Depression: Perspectives from affective

neuroscience. *Annual Review of Psychology*, *53*, 545–574. https://doi.org/10.1146/annurev.psych.53.100901.135148

de Aguiar Neto, F. S., & Rosa, J. L. G. (2019). Depression biomarkers using non-invasive EEG: A review. *Neuroscience & Biobehavioral Reviews*, *105*, 83–93. https://doi.org/10.1016/j.neubiorev.2019.07.021

de la Salle, S., Choueiry, J., Shah, D., Bowers, H., McIntosh, J., Ilivitsky, V., & Knott, V. (2016). Effects of Ketamine on Resting-State EEG Activity and Their Relationship to Perceptual/Dissociative Symptoms in Healthy Humans. *Frontiers in Pharmacology*, *7*, 348. https://doi.org/10.3389/fphar.2016.00348

de la Salle, S., Phillips, J. L., Blier, P., & Knott, V. (2022). Electrophysiological correlates and predictors of the antidepressant response to repeated ketamine infusions in treatment-resistant depression. *Progress in Neuro-Psychopharmacology & Biological Psychiatry*, *115*, 110507. https://doi.org/10.1016/j.pnpbp.2021.110507

Delorme, A., & Makeig, S. (2004a). EEGLAB: An open source toolbox for analysis of single-trial EEG dynamics including independent component analysis. *Journal of Neuroscience Methods*, *134*(1), 9–21. https://doi.org/10.1016/j.jneumeth.2003.10.009

Delorme, A., & Makeig, S. (2004b). EEGLAB: An open source toolbox for analysis of single-trial EEG dynamics including independent component analysis. *Journal of Neuroscience Methods*, *134*(1), 9–21. https://doi.org/10.1016/j.jneumeth.2003.10.009

Drevets, W. (2002). Functional anatomical correlates of antidepressant drug treatment assessed using PET measures of regional glucose metabolism. *European Neuropsychopharmacology*, *12*(6), 527–544. https://doi.org/10.1016/S0924-977X(02)00102-5

Ehrhardt, N. M., Fietz, J., Kopf-Beck, J., Kappelmann, N., & Brem, A.-K. (2022). Separating EEG correlates of stress: Cognitive effort, time pressure, and social-evaluative threat. *European Journal of Neuroscience*, *55*(9–10), 2464–2473. https://doi.org/10.1111/ejn.15211

Ernst, J., Hock, A., Henning, A., Seifritz, E., Boeker, H., & Grimm, S. (2017). Increased pregenual anterior cingulate glucose and lactate concentrations in major depressive disorder. *Molecular Psychiatry*, *22*(1), 113–119. https://doi.org/10.1038/mp.2016.73

Farnes, N., Juel, B. E., Nilsen, A. S., Romundstad, L. G., & Storm, J. F. (2020). Increased signal diversity/complexity of spontaneous EEG, but not evoked EEG responses, in ketamine-induced psychedelic state in humans. *PloS One*, *15*(11), e0242056. https://doi.org/10.1371/journal.pone.0242056

Feder, A., Parides, M. K., Murrough, J. W., Perez, A. M., Morgan, J. E., Saxena, S., Kirkwood, K., Aan Het Rot, M., Lapidus, K. A. B., Wan, L.-B., Iosifescu, D., & Charney, D. S. (2014). Efficacy of intravenous ketamine for treatment of chronic posttraumatic stress disorder: A randomized clinical trial. *JAMA Psychiatry*, *71*(6), 681–688. https://doi.org/10.1001/jamapsychiatry.2014.62

Fingelkurts, A. A., & Fingelkurts, A. A. (2015). Altered Structure of Dynamic Electroencephalogram Oscillatory Pattern in Major Depression. *Biological Psychiatry*, *77*(12), 1050–1060. https://doi.org/10.1016/j.biopsych.2014.12.011

Fitzgerald, P. J., & Watson, B. O. (2018a). Gamma oscillations as a biomarker for major depression: An

emerging topic. *Translational Psychiatry*, *8*, 177. https://doi.org/10.1038/s41398-018-0239-y

Fitzgerald, P. J., & Watson, B. O. (2018b). Gamma oscillations as a biomarker for major depression: An emerging topic. *Translational Psychiatry*, *8*(1), 177. https://doi.org/10.1038/s41398-018-0239-y

FitzGerald, T. H. B., Dolan, R. J., & Friston, K. (2015). Dopamine, reward learning, and active inference. *Frontiers in Computational Neuroscience*, *9*. https://doi.org/10.3389/fncom.2015.00136

Forsyth, A. E. M., McMillan, R., Dukart, J., Hipp, J. F., & Muthukumaraswamy, S. D. (2021). Effects of Ketamine and Midazolam on Simultaneous EEG/fMRI Data During Working Memory Processes. *Brain Topography*, *34*(6), 863–880. https://doi.org/10.1007/s10548-021-00876-8

Forsyth, A., McMillan, R., Campbell, D., Malpas, G., Maxwell, E., Sleigh, J., Dukart, J., Hipp, J. F., & Muthukumaraswamy, S. D. (2018). Comparison of local spectral modulation, and temporal correlation, of simultaneously recorded EEG/fMRI signals during ketamine and midazolam sedation. *Psychopharmacology*, *235*(12), 3479–3493. https://doi.org/10.1007/s00213-018-5064-8

Frank, M. J., Seeberger, L. C., & O'reilly, R. C. (2004). By carrot or by stick: Cognitive reinforcement learning in parkinsonism. *Science (New York, N.Y.)*, *306*(5703), 1940–1943. https://doi.org/10.1126/science.1102941

Fries, P., Nikolić, D., & Singer, W. (2007). The gamma cycle. *Trends in Neurosciences*, *30*(7), 309–316. https://doi.org/10.1016/j.tins.2007.05.005

Fuchs, E., Czéh, B., Kole, M. H. P., Michaelis, T., & Lucassen, P. J. (2004). Alterations of neuroplasticity in depression: The hippocampus and beyond. *European Neuropsychopharmacology*, *14*, S481–S490. https://doi.org/10.1016/j.euroneuro.2004.09.002

Furth, K. E., Mastwal, S., Wang, K. H., Buonanno, A., & Vullhorst, D. (2013). Dopamine, cognitive function, and gamma oscillations: Role of D4 receptors. *Frontiers in Cellular Neuroscience*, *7*. https://doi.org/10.3389/fncel.2013.00102

Gandal, M. J., Edgar, J. C., Klook, K., & Siegel, S. J. (2012). Gamma synchrony: Towards a translational biomarker for the treatment-resistant symptoms of schizophrenia. *Neuropharmacology*, *62*(3), 1504–1518. https://doi.org/10.1016/j.neuropharm.2011.02.007

Gao, R., Peterson, E. J., & Voytek, B. (2017). Inferring synaptic excitation/inhibition balance from field potentials. *NeuroImage*, *158*, 70–78. https://doi.org/10.1016/j.neuroimage.2017.06.078

Geneva: World Health Organization. (2024). *Global status report on alcohol and health and treatment of substance use disorders.* https://iris.who.int/bitstream/handle/10665/377960/9789240096745-eng.pdf?sequence=1

Ghilardi, M. F., Tatti, E., & Quartarone, A. (2021). Beta power and movement-related beta modulation as hallmarks of energy for plasticity induction: Implications for Parkinson's disease. *Parkinsonism & Related Disorders*, *88*, 136–139. https://doi.org/10.1016/j.parkreldis.2021.05.018

Girn, M., Rosas, F. E., Daws, R. E., Gallen, C. L., Gazzaley, A., & Carhart-Harris, R. L. (2023). A complex systems perspective on psychedelic brain action. *Trends in Cognitive Sciences*, *27*(5), 433–445. https://doi.org/10.1016/j.tics.2023.01.003

Głombik, K., Detka, J., Kurek, A., & Budziszewska, B. (2020). Impaired Brain Energy Metabolism: Involvement in Depression and Hypothyroidism. *Frontiers in Neuroscience*, *14*.

https://doi.org/10.3389/fnins.2020.586939

Gohier, B., Ferracci, L., Surguladze, S. A., Lawrence, E., El Hage, W., Kefi, M. Z., Allain, P., Garre, J.-B., & Le Gall, D. (2009). Cognitive inhibition and working memory in unipolar depression. *Journal of Affective Disorders*, *116*(1–2), 100–105. https://doi.org/10.1016/j.jad.2008.10.028

Goldstein, R. Z., & Volkow, N. D. (2002). Drug Addiction and Its Underlying Neurobiological Basis: Neuroimaging Evidence for the Involvement of the Frontal Cortex. *American Journal of Psychiatry*, *159*(10), 1642–1652. https://doi.org/10.1176/appi.ajp.159.10.1642

Goldstein, R. Z., & Volkow, N. D. (2011). Dysfunction of the prefrontal cortex in addiction: Neuroimaging findings and clinical implications. *Nature Reviews Neuroscience*, *12*(11), 652–669. https://doi.org/10.1038/nrn3119

Gomez, P., Ratcliff, R., & Perea, M. (2007). A model of the go/no-go task. *Journal of Experimental Psychology: General*, *136*(3), 389–413. https://doi.org/10.1037/0096-3445.136.3.389

Grabski, M., McAndrew, A., Lawn, W., Marsh, B., Raymen, L., Stevens, T., Hardy, L., Warren, F., Bloomfield, M., Borissova, A., Maschauer, E., Broomby, R., Price, R., Coathup, R., Gilhooly, D., Palmer, E., Gordon-Williams, R., Hill, R., Harris, J., … Morgan, C. J. A. (2022). Adjunctive Ketamine With Relapse Prevention–Based Psychological Therapy in the Treatment of Alcohol Use Disorder. *American Journal of Psychiatry*, *179*(2), 152–162. https://doi.org/10.1176/appi.ajp.2021.21030277

Grant, D. A., & Berg, E. A. (2014). *Wisconsin Card Sorting Test* [Dataset]. https://doi.org/10.1037/t31298-000

Grineski, S. E., Morales, D. X., Collins, T. W., Nadybal, S., & Trego, S. (2024). Anxiety and depression among US college students engaging in undergraduate research during the COVID-19 pandemic. *Journal of American College Health*, *72*(1), 20–30. https://doi.org/10.1080/07448481.2021.2013237

Grin-Yatsenko, V. A., Baas, I., Ponomarev, V. A., & Kropotov, J. D. (2010). Independent component approach to the analysis of EEG recordings at early stages of depressive disorders. *Clinical Neurophysiology: Official Journal of the International Federation of Clinical Neurophysiology*, *121*(3), 281–289. https://doi.org/10.1016/j.clinph.2009.11.015

Grønli, J., Rempe, M. J., Clegern, W. C., Schmidt, M., & Wisor, J. P. (2016). Beta EEG reflects sensory processing in active wakefulness and homeostatic sleep drive in quiet wakefulness. *Journal of Sleep Research*, *25*(3), 257–268. https://doi.org/10.1111/jsr.12380

Gu, X., Ke, S., Wang, Q., Zhuang, T., Xia, C., Xu, Y., Yang, L., & Zhou, M. (2021). Energy metabolism in major depressive disorder: Recent advances from omics technologies and imaging. *Biomedicine & Pharmacotherapy = Biomedecine & Pharmacotherapie*, *141*, 111869. https://doi.org/10.1016/j.biopha.2021.111869

Hajcak, G., MacNamara, A., & Olvet, D. M. (2010). Event-Related Potentials, Emotion, and Emotion Regulation: An Integrative Review. *Developmental Neuropsychology*, *35*(2), 129–155. https://doi.org/10.1080/87565640903526504

HajiHosseini, A., Rodríguez-Fornells, A., & Marco-Pallarés, J. (2012a). The role of beta-gamma oscillations in unexpected rewards processing. *NeuroImage*, *60*(3), 1678–1685. https://doi.org/10.1016/j.neuroimage.2012.01.125

HajiHosseini, A., Rodríguez-Fornells, A., & Marco-Pallarés, J. (2012b). The role of beta-gamma oscillations

in unexpected rewards processing. *NeuroImage*, *60*(3), 1678–1685. https://doi.org/10.1016/j.neuroimage.2012.01.125

Hajós, M., Hoffmann, W. E., Robinson, D. D., Yu, J. H., & Hajós-Korcsok, É. (2003). Norepinephrine but not Serotonin Reuptake Inhibitors Enhance Theta and Gamma Activity of the Septo-Hippocampal System. *Neuropsychopharmacology*, *28*(5), 857–864. https://doi.org/10.1038/sj.npp.1300116

Hang, L., & Lim, K.-L. (2020). Chapter 13—Energy regulation and Parkinson's disease. In C. R. Martin & V. R. Preedy (Eds.), *Genetics, Neurology, Behavior, and Diet in Parkinson's Disease* (pp. 205–220). Academic Press. https://doi.org/10.1016/B978-0-12-815950-7.00013-8

Harvey, P.-O., Fossati, P., Pochon, J.-B., Levy, R., Lebastard, G., Lehéricy, S., Allilaire, J.-F., & Dubois, B. (2005). Cognitive control and brain resources in major depression: An fMRI study using the n-back task. *NeuroImage*, *26*(3), 860–869. https://doi.org/10.1016/j.neuroimage.2005.02.048

Hashimoto, K., Sawa, A., & Iyo, M. (2007). Increased levels of glutamate in brains from patients with mood disorders. *Biological Psychiatry*, *62*(11), 1310–1316. https://doi.org/10.1016/j.biopsych.2007.03.017

Hasin, D. S., O'Brien, C. P., Auriacombe, M., Borges, G., Bucholz, K., Budney, A., Compton, W. M., Crowley, T., Ling, W., Petry, N. M., Schuckit, M., & Grant, B. F. (2013). DSM-5 Criteria for Substance Use Disorders: Recommendations and Rationale. *American Journal of Psychiatry*, *170*(8), 834–851. https://doi.org/10.1176/appi.ajp.2013.12060782

He, B. J. (2011a). Scale-free properties of the functional magnetic resonance imaging signal during rest and task. *The Journal of Neuroscience: The Official Journal of the Society for Neuroscience*, *31*(39), 13786–13795. https://doi.org/10.1523/JNEUROSCI.2111-11.2011

He, B. J. (2011b). Scale-free properties of the functional magnetic resonance imaging signal during rest and task. *The Journal of Neuroscience: The Official Journal of the Society for Neuroscience*, *31*(39), 13786–13795. https://doi.org/10.1523/JNEUROSCI.2111-11.2011

He, B. J. (2014a). Scale-free brain activity: Past, present, and future. *Trends in Cognitive Sciences*, *18*(9), 480–487. https://doi.org/10.1016/j.tics.2014.04.003

He, B. J. (2014b). Scale-free brain activity: Past, present, and future. *Trends in Cognitive Sciences*, *18*(9), 480–487. https://doi.org/10.1016/j.tics.2014.04.003

He, B. J., Zempel, J. M., Snyder, A. Z., & Raichle, M. E. (2010). The Temporal Structures and Functional Significance of Scale-free Brain Activity. *Neuron*, *66*(3), 353–369. https://doi.org/10.1016/j.neuron.2010.04.020

He, E. J., Yuan, H., Yang, L., Sheikholeslami, C., & He, B. (2008). EEG spatio-spectral mapping during video game play. *2008 International Conference on Technology and Applications in Biomedicine*, 346–348. https://doi.org/10.1109/ITAB.2008.4570658

Heatherton, T. F., Kozlowski, L. T., Frecker, R. C., & Fagerstrom, K. (1991). The Fagerström Test for Nicotine Dependence: A revision of the Fagerstrom Tolerance Questionnaire. *British Journal of Addiction*, *86*(9), 1119–1127. https://doi.org/10.1111/j.1360-0443.1991.tb01879.x

Hein, T. P., & Herrojo Ruiz, M. (2022). State anxiety alters the neural oscillatory correlates of predictions and prediction errors during reward-based learning. *NeuroImage*, *249*, 118895. https://doi.org/10.1016/j.neuroimage.2022.118895

Hester, R., & Garavan, H. (2004). Executive Dysfunction in Cocaine Addiction: Evidence for Discordant Frontal, Cingulate, and Cerebellar Activity. *The Journal of Neuroscience*, *24*(49), 11017–11022. https://doi.org/10.1523/JNEUROSCI.3321-04.2004

Hipp, J. F., & Siegel, M. (2013). Dissociating neuronal gamma-band activity from cranial and ocular muscle activity in EEG. *Frontiers in Human Neuroscience*, *7*, 338. https://doi.org/10.3389/fnhum.2013.00338

Hopwood, M. (2023). Anxiety Symptoms in Patients with Major Depressive Disorder: Commentary on Prevalence and Clinical Implications. *Neurology and Therapy*, *12*(1), 5–12. https://doi.org/10.1007/s40120-023-00469-6

Hu, B., Rao, J., Li, X., Cao, T., Li, J., Majoe, D., & Gutknecht, J. (2017). Emotion Regulating Attentional Control Abnormalities In Major Depressive Disorder: An Event-Related Potential Study. *Scientific Reports*, *7*(1), 13530. https://doi.org/10.1038/s41598-017-13626-3

Hu, Y.-T., Tan, Z.-L., Hirjak, D., & Northoff, G. (2023). Brain-wide changes in excitation-inhibition balance of major depressive disorder: A systematic review of topographic patterns of GABA- and glutamatergic alterations. *Molecular Psychiatry*, *28*(8), 3257–3266. https://doi.org/10.1038/s41380-023-02193-x

Huerta, P. T., & Lisman, J. E. (1995). Bidirectional synaptic plasticity induced by a single burst during cholinergic theta oscillation in CA1 in vitro. *Neuron*, *15*(5), 1053–1063. https://doi.org/10.1016/0896-6273(95)90094-2

Jasp Team. (2024). *JASP* (Version 0.19.0) [Computer software].

Jones, S. A., Barfield, J. H., Norman, V. K., & Shew, W. L. (2023). Scale-free behavioral dynamics directly linked with scale-free cortical dynamics. *eLife*, *12*, e79950. https://doi.org/10.7554/eLife.79950

Kamarajan, C., Pandey, A. K., Chorlian, D. B., Manz, N., Stimus, A. T., Bauer, L. O., Hesselbrock, V. M., Schuckit, M. A., Kuperman, S., Kramer, J., & Porjesz, B. (2015). Reward processing deficits and impulsivity in high-risk offspring of alcoholics: A study of event-related potentials during a monetary gambling task. *International Journal of Psychophysiology*, *98*(2), 182–200. https://doi.org/10.1016/j.ijpsycho.2015.09.005

Kasch, K. L., Rottenberg, J., Arnow, B. A., & Gotlib, I. H. (2002). Behavioral activation and inhibition systems and the severity and course of depression. *Journal of Abnormal Psychology*, *111*(4), 589–597. https://doi.org/10.1037/0021-843X.111.4.589

Kaspar, F., & Schuster, H. G. (1987). Easily calculable measure for the complexity of spatiotemporal patterns. *Physical Review A*, *36*(2), 842–848. https://doi.org/10.1103/PhysRevA.36.842

Kauer, J. A., & Malenka, R. C. (2007). Synaptic plasticity and addiction. *Nature Reviews Neuroscience*, *8*(11), 844–858. https://doi.org/10.1038/nrn2234

Kavanaugh, B. C., Fukuda, A. M., Gemelli, Z. T., Thorpe, R., Tirrell, E., Vigne, M., Jones, S. R., & Carpenter, L. L. (2023). Pre-treatment frontal beta events are associated with executive dysfunction improvement after repetitive transcranial magnetic stimulation for depression: A preliminary report. *Journal of Psychiatric Research*, *168*, 71–81. https://doi.org/10.1016/j.jpsychires.2023.10.024

Kempster, P. A., & Perju-Dumbrava, L. (2021). The Thermodynamic Consequences of Parkinson's Disease. *Frontiers in Neurology*, *12*. https://doi.org/10.3389/fneur.2021.685314

Kessler, R. C., Sampson, N. A., Berglund, P., Gruber, M. J., Al-Hamzawi, A., Andrade, L., Bunting, B., Demyttenaere, K., Florescu, S., de Girolamo, G., Gureje, O., He, Y., Hu, C., Huang, Y., Karam, E., Kovess-Masfety, V., Lee, S., Levinson, D., Medina Mora, M. E., … Wilcox, M. A. (2015). Anxious and non-anxious major depressive disorder in the World Health Organization World Mental Health Surveys. *Epidemiology and Psychiatric Sciences*, *24*(3), 210–226. https://doi.org/10.1017/S2045796015000189

Khajehpour, H., Mohagheghian, F., Ekhtiari, H., Makkiabadi, B., Jafari, A. H., Eqlimi, E., & Harirchian, M. H. (2019). Computer-aided classifying and characterizing of methamphetamine use disorder using resting-state EEG. *Cognitive Neurodynamics*, *13*(6), 519–530. https://doi.org/10.1007/s11571-019-09550-z

Knott, V. J., Millar, A. M., McIntosh, J. F., Shah, D. K., Fisher, D. J., Blais, C. M., Ilivitsky, V., & Horn, E. (2011). Separate and combined effects of low dose ketamine and nicotine on behavioural and neural correlates of sustained attention. *Biological Psychology*, *88*(1), 83–93. https://doi.org/10.1016/j.biopsycho.2011.06.012

Knott, V., McIntosh, J., Millar, A., Fisher, D., Villeneuve, C., Ilivitsky, V., & Horn, E. (2006). Nicotine and smoker status moderate brain electric and mood activation induced by ketamine, an N-methyl-D-aspartate (NMDA) receptor antagonist. *Pharmacology, Biochemistry, and Behavior*, *85*(1), 228–242. https://doi.org/10.1016/j.pbb.2006.08.005

Koob, G. F. (2013). Negative reinforcement in drug addiction: The darkness within. *Current Opinion in Neurobiology*, *23*(4), 559–563. https://doi.org/10.1016/j.conb.2013.03.011

Koob, G. F., & Volkow, N. D. (2016). Neurobiology of addiction: A neurocircuitry analysis. *The Lancet Psychiatry*, *3*(8), 760–773. https://doi.org/10.1016/S2215-0366(16)00104-8

Kryst, J., Kawalec, P., Mitoraj, A. M., Pilc, A., Lasoń, W., & Brzostek, T. (2020). Efficacy of single and repeated administration of ketamine in unipolar and bipolar depression: A meta-analysis of randomized clinical trials. *Pharmacological Reports: PR*, *72*(3), 543–562. https://doi.org/10.1007/s43440-020-00097-z

Kushner, M. (2000). The relationship between anxiety disorders and alcohol use disorders A review of major perspectives and findings. *Clinical Psychology Review*, *20*(2), 149–171. https://doi.org/10.1016/S0272-7358(99)00027-6

Lai, M.-C., Lombardo, M. V., Chakrabarti, B., Sadek, S. A., Pasco, G., Wheelwright, S. J., Bullmore, E. T., Baron-Cohen, S., MRC AIMS Consortium, & Suckling, J. (2010). A shift to randomness of brain oscillations in people with autism. *Biological Psychiatry*, *68*(12), 1092–1099. https://doi.org/10.1016/j.biopsych.2010.06.027

Lakatos, P., Karmos, G., Mehta, A. D., Ulbert, I., & Schroeder, C. E. (2008). Entrainment of Neuronal Oscillations as a Mechanism of Attentional Selection. *Science*, *320*(5872), 110–113. https://doi.org/10.1126/science.1154735

Lakatos, P., Shah, A. S., Knuth, K. H., Ulbert, I., Karmos, G., & Schroeder, C. E. (2005). An Oscillatory Hierarchy Controlling Neuronal Excitability and Stimulus Processing in the Auditory Cortex. *Journal of Neurophysiology*, *94*(3), 1904–1911. https://doi.org/10.1152/jn.00263.2005

Lally, N., Mullins, P. G., Roberts, M. V., Price, D., Gruber, T., & Haenschel, C. (2014). Glutamatergic correlates

of gamma-band oscillatory activity during cognition: A concurrent ER-MRS and EEG study. *NeuroImage*, *85*, 823–833. https://doi.org/10.1016/j.neuroimage.2013.07.049

Large, E. W., & Kolen, J. F. (1994). Resonance and the Perception of Musical Meter. *Connection Science*, *6*(2–3), 177–208. https://doi.org/10.1080/09540099408915723

Lau, Z. J., Pham, T., Chen, S. H. A., & Makowski, D. (2022). Brain entropy, fractal dimensions and predictability: A review of complexity measures for EEG in healthy and neuropsychiatric populations. *European Journal of Neuroscience*, *56*(7), 5047–5069. https://doi.org/10.1111/ejn.15800

Lavender, E., Hirasawa-Fujita, M., & Domino, E. F. (2020). Ketamine's dose related multiple mechanisms of actions: Dissociative anesthetic to rapid antidepressant. *Behavioural Brain Research*, *390*, 112631. https://doi.org/10.1016/j.bbr.2020.112631

Lejuez, C. W., Read, J. P., Kahler, C. W., Richards, J. B., Ramsey, S. E., Stuart, G. L., Strong, D. R., & Brown, R. A. (2002). Evaluation of a behavioral measure of risk taking: The Balloon Analogue Risk Task (BART). *Journal of Experimental Psychology: Applied*, *8*(2), 75–84. https://doi.org/10.1037/1076-898X.8.2.75

Lendner, J. D., Helfrich, R. F., Mander, B. A., Romundstad, L., Lin, J. J., Walker, M. P., Larsson, P. G., & Knight, R. T. (2020). An electrophysiological marker of arousal level in humans. *eLife*, *9*, e55092. https://doi.org/10.7554/eLife.55092

Li, D., & Mashour, G. A. (2019). Cortical dynamics during psychedelic and anesthetized states induced by ketamine. *NeuroImage*, *196*, 32–40. https://doi.org/10.1016/j.neuroimage.2019.03.076

Li, Y., Kang, C., Wei, Z., Qu, X., Liu, T., Zhou, Y., & Hu, Y. (2017). Beta oscillations in major depression – signalling a new cortical circuit for central executive function. *Scientific Reports*, *7*, 18021. https://doi.org/10.1038/s41598-017-18306-w

Li, Z., Ruan, M., Chen, J., & Fang, Y. (2021). Major Depressive Disorder: Advances in Neuroscience Research and Translational Applications. *Neuroscience Bulletin*, *37*(6), 863–880. https://doi.org/10.1007/s12264-021-00638-3

Lijffijt, M., Murphy, N., Iqbal, S., Green, C. E., Iqbal, T., Chang, L. C., Haile, C. N., Hirsch, L. C., Ramakrishnan, N., Fall, D. A., Swann, A. C., Al Jurdi, R. K., & Mathew, S. J. (2022). Identification of an optimal dose of intravenous ketamine for late-life treatment-resistant depression: A Bayesian adaptive randomization trial. *Neuropsychopharmacology: Official Publication of the American College of Neuropsychopharmacology*, *47*(5), 1088–1095. https://doi.org/10.1038/s41386-021-01242-9

Liu, B., Liu, J., Wang, M., Zhang, Y., & Li, L. (2017). From Serotonin to Neuroplasticity: Evolvement of Theories for Major Depressive Disorder. *Frontiers in Cellular Neuroscience*, *11*, 305. https://doi.org/10.3389/fncel.2017.00305

Liu, M., Ma, J., Fu, C.-Y., Yeo, J., Xiao, S.-S., Xiao, W.-X., Li, R.-R., Zhang, W., Xie, Z.-M., Li, Y.-J., & Li, Y.-X. (2022). Dysfunction of Emotion Regulation in Mild Cognitive Impairment Individuals Combined With Depressive Disorder: A Neural Mechanism Study. *Frontiers in Aging Neuroscience*, *14*, 884741. https://doi.org/10.3389/fnagi.2022.884741

Liu, W., Ge, T., Leng, Y., Pan, Z., Fan, J., Yang, W., & Cui, R. (2017). The Role of Neural Plasticity in Depression: From Hippocampus to Prefrontal Cortex. *Neural Plasticity*, *2017*(1), 6871089.

https://doi.org/10.1155/2017/6871089

Liu, X., Liu, S., Li, M., Su, F., Chen, S., Ke, Y., & Ming, D. (2022a). Altered gamma oscillations and beta–gamma coupling in drug-naive first-episode major depressive disorder: Association with sleep and cognitive disturbance. *Journal of Affective Disorders*, *316*, 99–108. https://doi.org/10.1016/j.jad.2022.08.022

Liu, X., Liu, S., Li, M., Su, F., Chen, S., Ke, Y., & Ming, D. (2022b). Altered gamma oscillations and beta–gamma coupling in drug-naive first-episode major depressive disorder: Association with sleep and cognitive disturbance. *Journal of Affective Disorders*, *316*, 99–108. https://doi.org/10.1016/j.jad.2022.08.022

Luijten, M., Kleinjan, M., & Franken, I. H. A. (2016). Event-related potentials reflecting smoking cue reactivity and cognitive control as predictors of smoking relapse and resumption. *Psychopharmacology*, *233*(15–16), 2857–2868. https://doi.org/10.1007/s00213-016-4332-8

Ma, J., & Leung, L. S. (2007). The supramammillo-septal-hippocampal pathway mediates sensorimotor gating impairment and hyperlocomotion induced by MK-801 and ketamine in rats. *Psychopharmacology*, *191*(4), 961–974. https://doi.org/10.1007/s00213-006-0667-x

Maris, E., & Oostenveld, R. (2007a). Nonparametric statistical testing of EEG- and MEG-data. *Journal of Neuroscience Methods*, *164*(1), 177–190. https://doi.org/10.1016/j.jneumeth.2007.03.024

Maris, E., & Oostenveld, R. (2007b). Nonparametric statistical testing of EEG- and MEG-data. *Journal of Neuroscience Methods*, *164*(1), 177–190. https://doi.org/10.1016/j.jneumeth.2007.03.024

Martinotti, G., Vita, A., Fagiolini, A., Maina, G., Bertolino, A., Dell'Osso, B., Siracusano, A., Clerici, M., Bellomo, A., Sani, G., d'Andrea, G., Chiaie, R. D., Conca, A., Barlati, S., Di Lorenzo, G., De Fazio, P., De Filippis, S., Nicolò, G., Rosso, G., … REAL-ESK Study Group. (2022). Real-world experience of esketamine use to manage treatment-resistant depression: A multicentric study on safety and effectiveness (REAL-ESK study). *Journal of Affective Disorders*, *319*, 646–654. https://doi.org/10.1016/j.jad.2022.09.043

Mas-Herrero, E., Ripollés, P., HajiHosseini, A., Rodríguez-Fornells, A., & Marco-Pallarés, J. (2015a). Beta oscillations and reward processing: Coupling oscillatory activity and hemodynamic responses. *NeuroImage*, *119*, 13–19. https://doi.org/10.1016/j.neuroimage.2015.05.095

Mas-Herrero, E., Ripollés, P., HajiHosseini, A., Rodríguez-Fornells, A., & Marco-Pallarés, J. (2015b). Beta oscillations and reward processing: Coupling oscillatory activity and hemodynamic responses. *NeuroImage*, *119*, 13–19. https://doi.org/10.1016/j.neuroimage.2015.05.095

Massar, S. A. A., Rossi, V., Schutter, D. J. L. G., & Kenemans, J. L. (2012). Baseline EEG theta/beta ratio and punishment sensitivity as biomarkers for feedback-related negativity (FRN) and risk-taking. *Clinical Neurophysiology*, *123*(10), 1958–1965. https://doi.org/10.1016/j.clinph.2012.03.005

Masuyama, A., Kubo, T., Shinkawa, H., & Sugawara, D. (2022). The roles of trait and process resilience in relation of BIS/BAS and depressive symptoms among adolescents. *PeerJ*, *10*, e13687. https://doi.org/10.7717/peerj.13687

Maxim, V., Sendur, L., Fadili, J., Suckling, J., Gould, R., Howard, R., & Bullmore, E. (2005). Fractional Gaussian noise, functional MRI and Alzheimer's disease. *NeuroImage*, *25*(1), 141–158. https://doi.org/10.1016/j.neuroimage.2004.10.044

McMillan, R., Forsyth, A., Campbell, D., Malpas, G., Maxwell, E., Dukart, J., Hipp, J. F., & Muthukumaraswamy,

S. (2019). Temporal dynamics of the pharmacological MRI response to subanaesthetic ketamine in healthy volunteers: A simultaneous EEG/fMRI study. *Journal of Psychopharmacology (Oxford, England)*, *33*(2), 219–229. https://doi.org/10.1177/0269881118822263

McMillan, R., & Muthukumaraswamy, S. D. (2020). The neurophysiology of ketamine: An integrative review. *Reviews in the Neurosciences*, *31*(5), 457–503. https://doi.org/10.1515/revneuro-2019-0090

McMillan, R., Sumner, R., Forsyth, A., Campbell, D., Malpas, G., Maxwell, E., Deng, C., Hay, J., Ponton, R., Sundram, F., & Muthukumaraswamy, S. (2020). Simultaneous EEG/fMRI recorded during ketamine infusion in patients with major depressive disorder. *Progress in Neuro-Psychopharmacology and Biological Psychiatry*, *99*, 109838. https://doi.org/10.1016/j.pnpbp.2019.109838

Medeiros, G. C., Matheson, M., Demo, I., Reid, M. J., Matheson, S., Twose, C., Smith, G. S., Gould, T. D., Zarate, C. A., Barrett, F. S., & Goes, F. S. (2023). Brain-based correlates of antidepressant response to ketamine: A comprehensive systematic review of neuroimaging studies. *The Lancet Psychiatry*, *10*(10), 790–800. https://doi.org/10.1016/S2215-0366(23)00183-9

Mediano, P. A. M., Rosas, F. E., Luppi, A. I., Noreika, V., Seth, A. K., Carhart-Harris, R. L., Barnett, L., & Bor, D. (2023). Spectrally and temporally resolved estimation of neural signal diversity. *eLife*, *12*. https://doi.org/10.7554/eLife.88683

Méndez, M. A., Zuluaga, P., Hornero, R., Gómez, C., Escudero, J., Rodríguez-Palancas, A., Ortiz, T., & Fernández, A. (2012). Complexity analysis of spontaneous brain activity: Effects of depression and antidepressant treatment. *Journal of Psychopharmacology (Oxford, England)*, *26*(5), 636–643. https://doi.org/10.1177/0269881111408966

*Mental Health Atlas 2020* (1st ed). (2021). World Health Organization.

Missale, C., Nash, S. R., Robinson, S. W., Jaber, M., & Caron, M. G. (1998). Dopamine Receptors: From Structure to Function. *Physiological Reviews*, *78*(1), 189–225. https://doi.org/10.1152/physrev.1998.78.1.189

Moitra, M., Santomauro, D., Collins, P. Y., Vos, T., Whiteford, H., Saxena, S., & Ferrari, A. J. (2022). The global gap in treatment coverage for major depressive disorder in 84 countries from 2000–2019: A systematic review and Bayesian meta-regression analysis. *PLOS Medicine*, *19*(2), e1003901. https://doi.org/10.1371/journal.pmed.1003901

Moreno-López, L., Catena, A., Fernández-Serrano, M. J., Delgado-Rico, E., Stamatakis, E. A., Pérez-García, M., & Verdejo-García, A. (2012). Trait impulsivity and prefrontal gray matter reductions in cocaine dependent individuals. *Drug and Alcohol Dependence*, *125*(3), 208–214. https://doi.org/10.1016/j.drugalcdep.2012.02.012

Morillas-Romero, A., Tortella-Feliu, M., Bornas, X., & Putman, P. (2015). Spontaneous EEG theta/beta ratio and delta–beta coupling in relation to attentional network functioning and self-reported attentional control. *Cognitive, Affective, & Behavioral Neuroscience*, *15*(3), 598–606. https://doi.org/10.3758/s13415-015-0351-x

Murphy, N., Tamman, A. J. F., Lijffijt, M., Amarneh, D., Iqbal, S., Swann, A., Averill, L. A., O'Brien, B., & Mathew, S. J. (2023). Neural complexity EEG biomarkers of rapid and post-rapid ketamine effects in late-life treatment-resistant depression: A randomized control trial. *Neuropsychopharmacology*, *48*(11), Article 11. https://doi.org/10.1038/s41386-023-01586-4

Muthukumaraswamy, S. D., & Liley, D. TJ. (2018a). 1/f electrophysiological spectra in resting and drug-induced states can be explained by the dynamics of multiple oscillatory relaxation processes. *NeuroImage*, *179*, 582–595. https://doi.org/10.1016/j.neuroimage.2018.06.068

Muthukumaraswamy, S. D., & Liley, D. TJ. (2018b). 1/f electrophysiological spectra in resting and drug-induced states can be explained by the dynamics of multiple oscillatory relaxation processes. *NeuroImage*, *179*, 582–595. https://doi.org/10.1016/j.neuroimage.2018.06.068

Muthukumaraswamy, S. D., Shaw, A. D., Jackson, L. E., Hall, J., Moran, R., & Saxena, N. (2015). Evidence that Subanesthetic Doses of Ketamine Cause Sustained Disruptions of NMDA and AMPA-Mediated Frontoparietal Connectivity in Humans. *The Journal of Neuroscience: The Official Journal of the Society for Neuroscience*, *35*(33), 11694–11706. https://doi.org/10.1523/JNEUROSCI.0903-15.2015

Narayan, G. A., Hill, K. R., Wengler, K., He, X., Wang, J., Yang, J., Parsey, R. V., & DeLorenzo, C. (2022). Does the change in glutamate to GABA ratio correlate with change in depression severity? A randomized, double-blind clinical trial. *Molecular Psychiatry*, *27*(9), 3833–3841. https://doi.org/10.1038/s41380-022-01730-4

Nelson, A. B., Moisello, C., Lin, J., Panday, P., Ricci, S., Canessa, A., Di Rocco, A., Quartarone, A., Frazzitta, G., Isaias, I. U., Tononi, G., Cirelli, C., & Ghilardi, M. F. (2017). Beta Oscillatory Changes and Retention of Motor Skills during Practice in Healthy Subjects and in Patients with Parkinson's Disease. *Frontiers in Human Neuroscience*, *11*, 104. https://doi.org/10.3389/fnhum.2017.00104

Nelson, A. B., Ricci, S., Tatti, E., Panday, P., Girau, E., Lin, J., Thomson, B. O., Chen, H., Marshall, W., Tononi, G., Cirelli, C., & Ghilardi, M. F. (2021). Neural fatigue due to intensive learning is reversed by a nap but not by quiet waking. *Sleep*, *44*(1), zsaa143. https://doi.org/10.1093/sleep/zsaa143

Newson, J. J., & Thiagarajan, T. C. (2019). EEG Frequency Bands in Psychiatric Disorders: A Review of Resting State Studies. *Frontiers in Human Neuroscience*, *12*, 521. https://doi.org/10.3389/fnhum.2018.00521

Noda, Y., Zomorrodi, R., Saeki, T., Rajji, T. K., Blumberger, D. M., Daskalakis, Z. J., & Nakamura, M. (2017). Resting-state EEG gamma power and theta–gamma coupling enhancement following high-frequency left dorsolateral prefrontal rTMS in patients with depression. *Clinical Neurophysiology*, *128*(3), 424–432. https://doi.org/10.1016/j.clinph.2016.12.023

Olbrich, S., & Arns, M. (2013). EEG biomarkers in major depressive disorder: Discriminative power and prediction of treatment response. *International Review of Psychiatry*, *25*(5), 604–618. https://doi.org/10.3109/09540261.2013.816269

Olbrich, S., Van Dinteren, R., & Arns, M. (2015). Personalized Medicine: Review and Perspectives of Promising Baseline EEG Biomarkers in Major Depressive Disorder and Attention Deficit Hyperactivity Disorder. *Neuropsychobiology*, *72*(3–4), 229–240. https://doi.org/10.1159/000437435

Olguın, D. O., Bouchereau, F., & Martınez, S. (n.d.). *Adaptive Notch Filter for EEG Signals Based on the LMS Algorithm with Variable Step-Size Parameter*.

Oostenveld, R., Fries, P., Maris, E., & Schoffelen, J.-M. (2011a). FieldTrip: Open source software for advanced analysis of MEG, EEG, and invasive electrophysiological data. *Computational Intelligence and*

*Neuroscience*, *2011*, 156869. https://doi.org/10.1155/2011/156869

Oostenveld, R., Fries, P., Maris, E., & Schoffelen, J.-M. (2011b). FieldTrip: Open source software for advanced analysis of MEG, EEG, and invasive electrophysiological data. *Computational Intelligence and Neuroscience*, *2011*, 156869. https://doi.org/10.1155/2011/156869

Oostenveld, R., Fries, P., Maris, E., & Schoffelen, J.-M. (2011c). FieldTrip: Open Source Software for Advanced Analysis of MEG, EEG, and Invasive Electrophysiological Data. *Computational Intelligence and Neuroscience*, *2011*, 1–9. https://doi.org/10.1155/2011/156869

Østergaard, L., Jørgensen, M. B., & Knudsen, G. M. (2018). Low on energy? An energy supply-demand perspective on stress and depression. *Neuroscience & Biobehavioral Reviews*, *94*, 248–270. https://doi.org/10.1016/j.neubiorev.2018.08.007

Page, C. E., & Coutellier, L. (2019). Prefrontal excitatory/inhibitory balance in stress and emotional disorders: Evidence for over-inhibition. *Neuroscience & Biobehavioral Reviews*, *105*, 39–51. https://doi.org/10.1016/j.neubiorev.2019.07.024

Palacios-García, I., Silva, J., Villena-González, M., Campos-Arteaga, G., Artigas-Vergara, C., Luarte, N., Rodríguez, E., & Bosman, C. A. (2021). Increase in Beta Power Reflects Attentional Top-Down Modulation After Psychosocial Stress Induction. *Frontiers in Human Neuroscience*, *15*, 630813. https://doi.org/10.3389/fnhum.2021.630813

Palmiero, M., & Piccardi, L. (2017). Frontal EEG Asymmetry of Mood: A Mini-Review. *Frontiers in Behavioral Neuroscience*, *11*, 224. https://doi.org/10.3389/fnbeh.2017.00224

Palmisano, A., Pandit, S., Smeralda, C. L., Demchenko, I., Rossi, S., Battelli, L., Rivolta, D., Bhat, V., & Santarnecchi, E. (2024). The Pathophysiological Underpinnings of Gamma-Band Alterations in Psychiatric Disorders. *Life*, *14*(5), 578. https://doi.org/10.3390/life14050578

Patton, J. H., Stanford, M. S., & Barratt, E. S. (1995). Factor structure of the Barratt impulsiveness scale. *Journal of Clinical Psychology*, *51*(6), 768–774. https://doi.org/10.1002/1097-4679(199511)51:6<768::aid-jclp2270510607>3.0.co;2-1

Peschard, V., & Philippot, P. (2016). Social anxiety and information processing biases: An integrated theoretical perspective. *Cognition and Emotion*, *30*(4), 762–777. https://doi.org/10.1080/02699931.2015.1028335

Pinault, D. (2008). N-methyl d-aspartate receptor antagonists ketamine and MK-801 induce wake-related aberrant gamma oscillations in the rat neocortex. *Biological Psychiatry*, *63*(8), 730–735. https://doi.org/10.1016/j.biopsych.2007.10.006

Pion-Tonachini, L., Kreutz-Delgado, K., & Makeig, S. (2019). ICLabel: An automated electroencephalographic independent component classifier, dataset, and website. *NeuroImage*, *198*, 181–197. https://doi.org/10.1016/j.neuroimage.2019.05.026

Pizzagalli, D. A. (2011). Frontocingulate Dysfunction in Depression: Toward Biomarkers of Treatment Response. *Neuropsychopharmacology*, *36*(1), 183–206. https://doi.org/10.1038/npp.2010.166

Plöchl, M., Ossandón, J. P., & König, P. (2012). Combining EEG and eye tracking: Identification, characterization, and correction of eye movement artifacts in electroencephalographic data. *Frontiers in Human Neuroscience*, *6*. https://doi.org/10.3389/fnhum.2012.00278

Pontes, H. M., & Griffiths, M. D. (2016). Portuguese Validation of the Internet Gaming Disorder Scale–Short-

Form. *Cyberpsychology, Behavior, and Social Networking*, *19*(4), 288–293. https://doi.org/10.1089/cyber.2015.0605

Quello, S. B., Brady, K. T., & Sonne, S. C. (2005). Mood disorders and substance use disorder: A complex comorbidity. *Science & Practice Perspectives*, *3*(1), 13–21. https://doi.org/10.1151/spp053113

Quilty, L. C., Mackew, L., & Bagby, R. M. (2014). Distinct profiles of behavioral inhibition and activation system sensitivity in unipolar vs. Bipolar mood disorders. *Psychiatry Research*, *219*(1), 228–231. https://doi.org/10.1016/j.psychres.2014.05.007

Ramey, T., & Regier, P. S. (2019). Cognitive impairment in substance use disorders. *CNS Spectrums*, *24*(1), 102–113. https://doi.org/10.1017/S1092852918001426

Ramirez-Mahaluf, J. P., Roxin, A., Mayberg, H. S., & Compte, A. (2015). A Computational Model of Major Depression: The Role of Glutamate Dysfunction on Cingulo-Frontal Network Dynamics. *Cerebral Cortex*, bhv249. https://doi.org/10.1093/cercor/bhv249

Ramirez-Mahaluf, J. P., Roxin, A., Mayberg, H. S., & Compte, A. (2017). A Computational Model of Major Depression: The Role of Glutamate Dysfunction on Cingulo-Frontal Network Dynamics. *Cerebral Cortex*, *27*(1), 660–679. https://doi.org/10.1093/cercor/bhv249

Raza, H., John, A., & Howarth, F. C. (2015). Increased Oxidative Stress and Mitochondrial Dysfunction in Zucker Diabetic Rat Liver and Brain. *Cellular Physiology and Biochemistry*, *35*(3), 1241–1251. https://doi.org/10.1159/000373947

Rezin, G. T., Amboni, G., Zugno, A. I., Quevedo, J., & Streck, E. L. (2009). Mitochondrial dysfunction and psychiatric disorders. *Neurochemical Research*, *34*(6), 1021–1029. https://doi.org/10.1007/s11064-008-9865-8

Reznik, S. J., & Allen, J. J. B. (2018). Frontal asymmetry as a mediator and moderator of emotion: An updated review. *Psychophysiology*, *55*(1). https://doi.org/10.1111/psyp.12965

Ricci, S., Tatti, E., Nelson, A. B., Panday, P., Chen, H., Tononi, G., Cirelli, C., & Ghilardi, M. F. (2021). Extended Visual Sequence Learning Leaves a Local Trace in the Spontaneous EEG. *Frontiers in Neuroscience*, *15*. https://www.frontiersin.org/articles/10.3389/fnins.2021.707828

Rivolta, D., Heidegger, T., Scheller, B., Sauer, A., Schaum, M., Birkner, K., Singer, W., Wibral, M., & Uhlhaas, P. J. (2015). Ketamine Dysregulates the Amplitude and Connectivity of High-Frequency Oscillations in Cortical-Subcortical Networks in Humans: Evidence From Resting-State Magnetoencephalography-Recordings. *Schizophrenia Bulletin*, *41*(5), 1105–1114. https://doi.org/10.1093/schbul/sbv051

Roh, S.-C., Park, E.-J., Shim, M., & Lee, S.-H. (2016). EEG beta and low gamma power correlates with inattention in patients with major depressive disorder. *Journal of Affective Disorders*, *204*, 124–130. https://doi.org/10.1016/j.jad.2016.06.033

Rose, E. J., Simonotto, E., & Ebmeier, K. P. (2006). Limbic over-activity in depression during preserved performance on the n-back task. *NeuroImage*, *29*(1), 203–215. https://doi.org/10.1016/j.neuroimage.2005.07.002

Russo, S. J., & Nestler, E. J. (2013). The brain reward circuitry in mood disorders. *Nature Reviews Neuroscience*, *14*(9), 609–625. https://doi.org/10.1038/nrn3381

Ryu, V., Ha, R. Y., & Cho, H. (2021). Altered behavioral and electrophysiological responses to social fairness in manic and euthymic patients with bipolar disorder. *Brain and Behavior*, *11*(8), e2289.

https://doi.org/10.1002/brb3.2289

Sanacora, G., Gueorguieva, R., Epperson, C. N., Wu, Y.-T., Appel, M., Rothman, D. L., Krystal, J. H., & Mason, G. F. (2004). Subtype-specific alterations of gamma-aminobutyric acid and glutamate in patients with major depression. *Archives of General Psychiatry*, *61*(7), 705–713. https://doi.org/10.1001/archpsyc.61.7.705

Sanacora, G., Treccani, G., & Popoli, M. (2012). Towards a glutamate hypothesis of depression. *Neuropharmacology*, *62*(1), 63–77. https://doi.org/10.1016/j.neuropharm.2011.07.036

Sarasso, S., Boly, M., Napolitani, M., Gosseries, O., Charland-Verville, V., Casarotto, S., Rosanova, M., Casali, A. G., Brichant, J.-F., Boveroux, P., Rex, S., Tononi, G., Laureys, S., & Massimini, M. (2015). Consciousness and Complexity during Unresponsiveness Induced by Propofol, Xenon, and Ketamine. *Current Biology: CB*, *25*(23), 3099–3105. https://doi.org/10.1016/j.cub.2015.10.014

Sarawagi, A., Soni, N. D., & Patel, A. B. (2021). Glutamate and GABA Homeostasis and Neurometabolism in Major Depressive Disorder. *Frontiers in Psychiatry*, *12*, 637863. https://doi.org/10.3389/fpsyt.2021.637863

Sassenhagen, J., & Draschkow, D. (2019). Cluster-based permutation tests of MEG/EEG data do not establish significance of effect latency or location. *Psychophysiology*, *56*(6), e13335. https://doi.org/10.1111/psyp.13335

Saunders, J. B., Aasland, O. G., Babor, T. F., De La Fuente, J. R., & Grant, M. (1993). Development of the Alcohol Use Disorders Identification Test (AUDIT): WHO Collaborative Project on Early Detection of Persons with Harmful Alcohol Consumption-II. *Addiction*, *88*(6), 791–804. https://doi.org/10.1111/j.1360-0443.1993.tb02093.x

Scaglia, F. (2010a). The role of mitochondrial dysfunction in psychiatric disease. *Developmental Disabilities Research Reviews*, *16*(2), 136–143. https://doi.org/10.1002/ddrr.115

Scaglia, F. (2010b). The role of mitochondrial dysfunction in psychiatric disease. *Developmental Disabilities Research Reviews*, *16*(2), 136–143. https://doi.org/10.1002/ddrr.115

Schaffer, C. E., Davidson, R. J., & Saron, C. (1983). Frontal and parietal electroencephalogram asymmetry in depressed and nondepressed subjects. *Biological Psychiatry*, *18*(7), 753–762.

Schartner, M. M., Carhart-Harris, R. L., Barrett, A. B., Seth, A. K., & Muthukumaraswamy, S. D. (2017a). Increased spontaneous MEG signal diversity for psychoactive doses of ketamine, LSD and psilocybin. *Scientific Reports*, *7*(1), 46421. https://doi.org/10.1038/srep46421

Schartner, M. M., Carhart-Harris, R. L., Barrett, A. B., Seth, A. K., & Muthukumaraswamy, S. D. (2017b). Increased spontaneous MEG signal diversity for psychoactive doses of ketamine, LSD and psilocybin. *Scientific Reports*, *7*, 46421. https://doi.org/10.1038/srep46421

Schartner, M., Seth, A., Noirhomme, Q., Boly, M., Bruno, M.-A., Laureys, S., & Barrett, A. (2015). Complexity of Multi-Dimensional Spontaneous EEG Decreases during Propofol Induced General Anaesthesia. *PloS One*, *10*(8), e0133532. https://doi.org/10.1371/journal.pone.0133532

Schmidt, R., Ruiz, M. H., Kilavik, B. E., Lundqvist, M., Starr, P. A., & Aron, A. R. (2019). Beta Oscillations in Working Memory, Executive Control of Movement and Thought, and Sensorimotor Function. *Journal of Neuroscience*, *39*(42), 8231–8238. https://doi.org/10.1523/JNEUROSCI.1163-19.2019

Schutte, I., Deschamps, P. K. H., Van Harten, P. N., & Kenemans, J. L. (2020). Dopaminergic and noradrenergic

manipulation of anticipatory reward and probability event-related potentials. *Psychopharmacology*, *237*(7), 2019–2030. https://doi.org/10.1007/s00213-020-05515-x

Shaffer, C., Westlin, C., Quigley, K. S., Whitfield-Gabrieli, S., & Barrett, L. F. (2022). Allostasis, Action, and Affect in Depression: Insights from the Theory of Constructed Emotion. *Annual Review of Clinical Psychology*, *18*, 553–580. https://doi.org/10.1146/annurev-clinpsy-081219-115627

Shaw, A. D., Saxena, N., E Jackson, L., Hall, J. E., Singh, K. D., & Muthukumaraswamy, S. D. (2015). Ketamine amplifies induced gamma frequency oscillations in the human cerebral cortex. *European Neuropsychopharmacology: The Journal of the European College of Neuropsychopharmacology*, *25*(8), 1136–1146. https://doi.org/10.1016/j.euroneuro.2015.04.012

Shungu, D. C., Weiduschat, N., Murrough, J. W., Mao, X., Pillemer, S., Dyke, J. P., Medow, M. S., Natelson, B. H., Stewart, J. M., & Mathew, S. J. (2012). Increased ventricular lactate in chronic fatigue syndrome. III. Relationships to cortical glutathione and clinical symptoms implicate oxidative stress in disorder pathophysiology. *NMR in Biomedicine*, *25*(9), 1073–1087. https://doi.org/10.1002/nbm.2772

Sinha, R. (2008). Chronic Stress, Drug Use, and Vulnerability to Addiction. *Annals of the New York Academy of Sciences*, *1141*(1), 105–130. https://doi.org/10.1196/annals.1441.030

Smits, F. M., Porcaro, C., Cottone, C., Cancelli, A., Rossini, P. M., & Tecchio, F. (2016). Electroencephalographic Fractal Dimension in Healthy Ageing and Alzheimer's Disease. *PLOS ONE*, *11*(2), e0149587. https://doi.org/10.1371/journal.pone.0149587

Snyder, H. R. (2013). Major depressive disorder is associated with broad impairments on neuropsychological measures of executive function: A meta-analysis and review. *Psychological Bulletin*, *139*(1), 81–132. https://doi.org/10.1037/a0028727

Spielberger, C. D. (1983). *State-trait anxiety inventory for adults*. https://psycnet.apa.org/doiLanding?doi=10.1037%2Ft06496-000

Spitzer, B., & Haegens, S. (2017). Beyond the Status Quo: A Role for Beta Oscillations in Endogenous Content (Re)Activation. *eNeuro*, *4*(4). https://doi.org/10.1523/ENEURO.0170-17.2017

Sporn, S., Hein, T., & Herrojo Ruiz, M. (n.d.). Alterations in the amplitude and burst rate of beta oscillations impair reward-dependent motor learning in anxiety. *eLife*, *9*, e50654. https://doi.org/10.7554/eLife.50654

Stam, C. J. (2005a). Nonlinear dynamical analysis of EEG and MEG: Review of an emerging field. *Clinical Neurophysiology*, *116*(10), 2266–2301. https://doi.org/10.1016/j.clinph.2005.06.011

Stam, C. J. (2005b). Nonlinear dynamical analysis of EEG and MEG: Review of an emerging field. *Clinical Neurophysiology: Official Journal of the International Federation of Clinical Neurophysiology*, *116*(10), 2266–2301. https://doi.org/10.1016/j.clinph.2005.06.011

Stordal, K. I., Lundervold, A. J., Egeland, J., Mykletun, A., Asbjørnsen, A., Landrø, N. I., Roness, A., Rund, B. R., Sundet, K., Oedegaard, K. J., & Lund, A. (2004). Impairment across executive functions in recurrent major depression. *Nordic Journal of Psychiatry*, *58*(1), 41–47. https://doi.org/10.1080/08039480310000789

Stork, C., & Renshaw, P. F. (2005). Mitochondrial dysfunction in bipolar disorder: Evidence from magnetic resonance spectroscopy research. *Molecular Psychiatry*, *10*(10), 900–919. https://doi.org/10.1038/sj.mp.4001711

Stroop, J. R. (1935). Studies of interference in serial verbal reactions. *Journal of Experimental Psychology*, *18*(6), 643–662. https://doi.org/10.1037/h0054651

Studerus, E., Kometer, M., Hasler, F., & Vollenweider, F. X. (2011). Acute, subacute and long-term subjective effects of psilocybin in healthy humans: A pooled analysis of experimental studies. *Journal of Psychopharmacology*, *25*(11), 1434–1452. https://doi.org/10.1177/0269881110382466

Sumner, R. L., Chacko, E., McMillan, R., Spriggs, M. J., Anderson, C., Chen, J., French, A., Jung, S., Rajan, A., Malpas, G., Hay, J., Ponton, R., Muthukumaraswamy, S. D., & Sundram, F. (2021). A qualitative and quantitative account of patient's experiences of ketamine and its antidepressant properties. *Journal of Psychopharmacology (Oxford, England)*, *35*(8), 946–961. https://doi.org/10.1177/0269881121998321

Sun, J., Luo, Y., Chang, H., Zhang, R., Liu, R., Jiang, Y., & Xi, H. (2020). The Mediating Role of Cognitive Emotion Regulation in BIS/BAS Sensitivities, Depression, and Anxiety Among Community-Dwelling Older Adults in China. *Psychology Research and Behavior Management*, *13*, 939. https://doi.org/10.2147/PRBM.S269874

Susin, E., & Destexhe, A. (2023). A Network Model of the Modulation of γ Oscillations by NMDA Receptors in Cerebral Cortex. *eNeuro*, *10*(11), ENEURO.0157-23.2023. https://doi.org/10.1523/ENEURO.0157-23.2023

Sutherland, M. T., McHugh, M. J., Pariyadath, V., & Stein, E. A. (2012). Resting state functional connectivity in addiction: Lessons learned and a road ahead. *NeuroImage*, *62*(4), 2281–2295. https://doi.org/10.1016/j.neuroimage.2012.01.117

Takahashi, Y., Yamagata, S., Ritchie, S. J., Barker, E. D., & Ando, J. (2021). Etiological pathways of depressive and anxiety symptoms linked to personality traits: A genetically-informative longitudinal study. *Journal of Affective Disorders*, *291*, 261–269. https://doi.org/10.1016/j.jad.2021.05.004

Tatti, E., Cinti, A., Serbina, A., Luciani, A., D'Urso, G., Cacciola, A., Quartarone, A., & Ghilardi, M. F. (2024a). Resting-State EEG Alterations of Practice-Related Spectral Activity and Connectivity Patterns in Depression. *Biomedicines*, *12*(9), 2054. https://doi.org/10.3390/biomedicines12092054

Tatti, E., Cinti, A., Serbina, A., Luciani, A., D'Urso, G., Cacciola, A., Quartarone, A., & Ghilardi, M. F. (2024b). Resting-State EEG Alterations of Practice-Related Spectral Activity and Connectivity Patterns in Depression. *Biomedicines*, *12*(9), 2054. https://doi.org/10.3390/biomedicines12092054

Tatti, E., Ricci, S., Nelson, A. B., Mathew, D., Chen, H., Quartarone, A., Cirelli, C., Tononi, G., & Ghilardi, M. F. (2020). Prior Practice Affects Movement-Related Beta Modulation and Quiet Wake Restores It to Baseline. *Frontiers in Systems Neuroscience*, *14*. https://www.frontiersin.org/articles/10.3389/fnsys.2020.00061

The South Oaks Gambling Screen (SOGS): A new instrument for the identification of pathological gamblers. (1987). *American Journal of Psychiatry*, *144*(9), 1184–1188. https://doi.org/10.1176/ajp.144.9.1184

Thibodeau, R., Jorgensen, R. S., & Kim, S. (2006a). Depression, anxiety, and resting frontal EEG asymmetry: A meta-analytic review. *Journal of Abnormal Psychology*, *115*(4), 715–729. https://doi.org/10.1037/0021-843X.115.4.715

Thibodeau, R., Jorgensen, R. S., & Kim, S. (2006b). Depression, anxiety, and resting frontal EEG asymmetry:

A meta-analytic review. *Journal of Abnormal Psychology*, *115*(4), 715–729. https://doi.org/10.1037/0021-843X.115.4.715

Tian, H., Hu, Z., Xu, J., & Wang, C. (2022). The molecular pathophysiology of depression and the new therapeutics. *MedComm*, *3*(3), e156. https://doi.org/10.1002/mco2.156

Timmermann, C., Bauer, P. R., Gosseries, O., Vanhaudenhuyse, A., Vollenweider, F., Laureys, S., Singer, T., Antonova, E., & Lutz, A. (2023). A neurophenomenological approach to non-ordinary states of consciousness: Hypnosis, meditation, and psychedelics. *Trends in Cognitive Sciences*, *27*(2), 139–159. https://doi.org/10.1016/j.tics.2022.11.006

Tobe, E. (2013). Mitochondrial dysfunction, oxidative stress, and major depressive disorder. *Neuropsychiatric Disease and Treatment*, 567. https://doi.org/10.2147/NDT.S44282

Tolkunov, D., Rubin, D., & Mujica-Parodi, L. (2010). Power spectrum scale invariance quantifies limbic dysregulation in trait anxious adults using fMRI: Adapting methods optimized for characterizing autonomic dysregulation to neural dynamic time series. *NeuroImage*, *50*(1), 72–80. https://doi.org/10.1016/j.neuroimage.2009.12.021

Tort, A. B. L., Komorowski, R., Eichenbaum, H., & Kopell, N. (2010). Measuring phase-amplitude coupling between neuronal oscillations of different frequencies. *Journal of Neurophysiology*, *104*(2), 1195–1210. https://doi.org/10.1152/jn.00106.2010

Toyoshima, K., Masuya, J., Ono, M., Honyashiki, M., Hashimoto, S., Kusumi, I., & Inoue, T. (2022). Effects of the Interaction between Affective Temperaments and BIS/BAS on Depressive Symptoms in Individuals with Major Depressive Disorder. *International Journal of Environmental Research and Public Health*, *19*(23), 15841. https://doi.org/10.3390/ijerph192315841

Trivedi, M. H., Rush, A. J., Wisniewski, S. R., Nierenberg, A. A., Warden, D., Ritz, L., Norquist, G., Howland, R. H., Lebowitz, B., McGrath, P. J., Shores-Wilson, K., Biggs, M. M., Balasubramani, G. K., Fava, M., & STAR*D Study Team. (2006). Evaluation of outcomes with citalopram for depression using measurement-based care in STAR*D: Implications for clinical practice. *The American Journal of Psychiatry*, *163*(1), 28–40. https://doi.org/10.1176/appi.ajp.163.1.28

Tukey, J. W. (1977). Some thoughts on clinical trials, especially problems of multiplicity. *Science (New York, N.Y.)*, *198*(4318), 679–684. https://doi.org/10.1126/science.333584

Van Der Meij, R., Kahana, M., & Maris, E. (2012). Phase–Amplitude Coupling in Human Electrocorticography Is Spatially Distributed and Phase Diverse. *The Journal of Neuroscience*, *32*(1), 111–123. https://doi.org/10.1523/JNEUROSCI.4816-11.2012

van der Vinne, N., Vollebregt, M. A., van Putten, M. J. A. M., & Arns, M. (2019). Stability of frontal alpha asymmetry in depressed patients during antidepressant treatment. *NeuroImage: Clinical*, *24*, 102056. https://doi.org/10.1016/j.nicl.2019.102056

van Schalkwyk, G. I., Wilkinson, S. T., Davidson, L., Silverman, W. K., & Sanacora, G. (2018). Acute psychoactive effects of intravenous ketamine during treatment of mood disorders: Analysis of the Clinician Administered Dissociative State Scale. *Journal of Affective Disorders*, *227*, 11–16. https://doi.org/10.1016/j.jad.2017.09.023

Verdejo-García, A., Betanzos-Espinosa, P., Lozano, O. M., Vergara-Moragues, E., González-Saiz, F., Fernández-Calderón, F., Bilbao-Acedos, I., & Pérez-García, M. (2012). Self-regulation and treatment

retention in cocaine dependent individuals: A longitudinal study. *Drug and Alcohol Dependence*, *122*(1–2), 142–148. https://doi.org/10.1016/j.drugalcdep.2011.09.025

Vlisides, P. E., Bel-Bahar, T., Lee, U., Li, D., Kim, H., Janke, E., Tarnal, V., Pichurko, A. B., McKinney, A. M., Kunkler, B. S., Picton, P., & Mashour, G. A. (2017). Neurophysiologic Correlates of Ketamine Sedation and Anesthesia: A High-density Electroencephalography Study in Healthy Volunteers. *Anesthesiology*, *127*(1), 58–69. https://doi.org/10.1097/ALN.0000000000001671

Vlisides, P. E., Bel-Bahar, T., Nelson, A., Chilton, K., Smith, E., Janke, E., Tarnal, V., Picton, P., Harris, R. E., & Mashour, G. A. (2018). Subanaesthetic ketamine and altered states of consciousness in humans. *British Journal of Anaesthesia*, *121*(1), 249–259. https://doi.org/10.1016/j.bja.2018.03.011

Volkow, N. D., Fowler, J. S., Wang, G. J., Baler, R., & Telang, F. (2009). Imaging dopamine's role in drug abuse and addiction. *Neuropharmacology*, *56*, 3–8. https://doi.org/10.1016/j.neuropharm.2008.05.022

Volkow, N. D., & Morales, M. (2015). The Brain on Drugs: From Reward to Addiction. *Cell*, *162*(4), 712–725. https://doi.org/10.1016/j.cell.2015.07.046

Vollenweider, F. X., & Kometer, M. (2010). The neurobiology of psychedelic drugs: Implications for the treatment of mood disorders. *Nature Reviews Neuroscience*, *11*(9), 642–651. https://doi.org/10.1038/nrn2884

Voytek, B., & Knight, R. T. (2015). Dynamic Network Communication as a Unifying Neural Basis for Cognition, Development, Aging, and Disease. *Biological Psychiatry*, *77*(12), 1089–1097. https://doi.org/10.1016/j.biopsych.2015.04.016

Wei, M., Qin, J., Yan, R., Li, H., Yao, Z., & Lu, Q. (2013). Identifying major depressive disorder using Hurst exponent of resting-state brain networks. *Psychiatry Research*, *214*(3), 306–312. https://doi.org/10.1016/j.pscychresns.2013.09.008

Wen, H., & Liu, Z. (2016a). Separating Fractal and Oscillatory Components in the Power Spectrum of Neurophysiological Signal. *Brain Topography*, *29*(1), 13–26. https://doi.org/10.1007/s10548-015-0448-0

Wen, H., & Liu, Z. (2016b). Separating Fractal and Oscillatory Components in the Power Spectrum of Neurophysiological Signal. *Brain Topography*, *29*(1), 13–26. https://doi.org/10.1007/s10548-015-0448-0

Werner, G. (2010). Fractals in the Nervous System: Conceptual Implications for Theoretical Neuroscience. *Frontiers in Physiology*, *1*, 15. https://doi.org/10.3389/fphys.2010.00015

Widmann, A., Schröger, E., & Maess, B. (2015). Digital filter design for electrophysiological data – a practical approach. *Journal of Neuroscience Methods*, *250*, 34–46. https://doi.org/10.1016/j.jneumeth.2014.08.002

Wilkinson, S. T., Toprak, M., Turner, M. S., Levine, S. P., Katz, R. B., & Sanacora, G. (2017). A Survey of the Clinical, Off-Label Use of Ketamine as a Treatment for Psychiatric Disorders. *The American Journal of Psychiatry*, *174*(7), 695–696. https://doi.org/10.1176/appi.ajp.2017.17020239

Wolff, A., Di Giovanni, D. A., Gómez-Pilar, J., Nakao, T., Huang, Z., Longtin, A., & Northoff, G. (2019). The temporal signature of self: Temporal measures of resting-state EEG predict self-consciousness. *Human Brain Mapping*, *40*(3), 789–803. https://doi.org/10.1002/hbm.24412

Yaple, Z., Martinez-Saito, M., Novikov, N., Altukhov, D., Shestakova, A., & Klucharev, V. (2018). Power of

Feedback-Induced Beta Oscillations Reflect Omission of Rewards: Evidence From an EEG Gambling Study. *Frontiers in Neuroscience*, *12*, 776. https://doi.org/10.3389/fnins.2018.00776

Yau, Y. H. C., & Potenza, M. N. (2015). Gambling Disorder and Other Behavioral Addictions: Recognition and Treatment. *Harvard Review of Psychiatry*, *23*(2), 134–146. https://doi.org/10.1097/HRP.0000000000000051

Young, J. J., Chan, A. H. W., Jette, N., Bender, H. A., Saad, A. E., Saez, I., Panov, F., Ghatan, S., Yoo, J. Y., Singh, A., Fields, M. C., Marcuse, L. V., & Mayberg, H. S. (2024a). Elevated phase amplitude coupling as a depression biomarker in epilepsy. *Epilepsy & Behavior*, *152*, 109659. https://doi.org/10.1016/j.yebeh.2024.109659

Young, J. J., Chan, A. H. W., Jette, N., Bender, H. A., Saad, A. E., Saez, I., Panov, F., Ghatan, S., Yoo, J. Y., Singh, A., Fields, M. C., Marcuse, L. V., & Mayberg, H. S. (2024b). Elevated phase amplitude coupling as a depression biomarker in epilepsy. *Epilepsy & Behavior*, *152*, 109659. https://doi.org/10.1016/j.yebeh.2024.109659

Zacharias, N., Musso, F., Müller, F., Lammers, F., Saleh, A., London, M., de Boer, P., & Winterer, G. (2020a). Ketamine effects on default mode network activity and vigilance: A randomized, placebo-controlled crossover simultaneous fMRI/EEG study. *Human Brain Mapping*, *41*(1), 107–119. https://doi.org/10.1002/hbm.24791

Zacharias, N., Musso, F., Müller, F., Lammers, F., Saleh, A., London, M., de Boer, P., & Winterer, G. (2020b). Ketamine effects on default mode network activity and vigilance: A randomized, placebo-controlled crossover simultaneous fMRI/EEG study. *Human Brain Mapping*, *41*(1), 107–119. https://doi.org/10.1002/hbm.24791

Zakiniaeiz, Y., Hillmer, A. T., Matuskey, D., Nabulsi, N., Ropchan, J., Mazure, C. M., Picciotto, M. R., Huang, Y., McKee, S. A., Morris, E. D., & Cosgrove, K. P. (2019). Sex differences in amphetamine-induced dopamine release in the dorsolateral prefrontal cortex of tobacco smokers. *Neuropsychopharmacology*, *44*(13), 2205–2211. https://doi.org/10.1038/s41386-019-0456-y

Zanos, P., & Gould, T. D. (2018). Mechanisms of Ketamine Action as an Antidepressant. *Molecular Psychiatry*, *23*(4), 801–811. https://doi.org/10.1038/mp.2017.255

Zarate, C. A., Singh, J. B., Carlson, P. J., Brutsche, N. E., Ameli, R., Luckenbaugh, D. A., Charney, D. S., & Manji, H. K. (2006). A randomized trial of an N-methyl-D-aspartate antagonist in treatment-resistant major depression. *Archives of General Psychiatry*, *63*(8), 856–864. https://doi.org/10.1001/archpsyc.63.8.856

Zhang, W., Liu, W., Liu, S., Su, F., Kang, X., Ke, Y., & Ming, D. (2023a). Altered fronto-central theta-gamma coupling in major depressive disorder during auditory steady-state responses. *Clinical Neurophysiology*, *146*, 65–76. https://doi.org/10.1016/j.clinph.2022.11.013

Zhang, W., Liu, W., Liu, S., Su, F., Kang, X., Ke, Y., & Ming, D. (2023b). Altered fronto-central theta-gamma coupling in major depressive disorder during auditory steady-state responses. *Clinical Neurophysiology*, *146*, 65–76. https://doi.org/10.1016/j.clinph.2022.11.013

Zheng, C., & Zhang, T. (2015). Synaptic plasticity-related neural oscillations on hippocampus–prefrontal cortex pathway in depression. *Neuroscience*, *292*, 170–180. https://doi.org/10.1016/j.neuroscience.2015.01.071

Zhou, Y., Cao, Z., Yang, M., Xi, X., Guo, Y., Fang, M., Cheng, L., & Du, Y. (2017). Comorbid generalized anxiety disorder and its association with quality of life in patients with major depressive disorder. *Scientific Reports*, *7*(1), 40511. https://doi.org/10.1038/srep40511

Zilverstand, A., Huang, A. S., Alia-Klein, N., & Goldstein, R. Z. (2018a). Neuroimaging Impaired Response Inhibition and Salience Attribution in Human Drug Addiction: A Systematic Review. *Neuron*, *98*(5), 886–903. https://doi.org/10.1016/j.neuron.2018.03.048

Zilverstand, A., Huang, A. S., Alia-Klein, N., & Goldstein, R. Z. (2018b). Neuroimaging Impaired Response Inhibition and Salience Attribution in Human Drug Addiction: A Systematic Review. *Neuron*, *98*(5), 886–903. https://doi.org/10.1016/j.neuron.2018.03.048

# Glossary of Acronyms

ACC: Anterior Cingulate Cortex
ADD: Individuals with Addictive Behaviors
ADD-T: Individuals with Addictive Behaviors who are Receiving Treatment
ADD-NT: Individuals with Addictive Behaviors who are Not Receiving Treatment
AFF: Affective Symptoms (subscale of BDI)
ASCQ: Altered States of Consciousness Questionnaire
Att_Imp: Attentional Impulsivity (subscale of BIS-11)
AUC: Area Under Curve
AUDIT: Alcohol Use Disorders Identification Test
BART: Balloon Analogue Risk Task
BAS: Behavioral Activation System
BD: Bipolar Disorder
BDI: Beck Depression Inventory
BIS: Behavioral Inhibition System
BIS-11: Barratt Impulsiveness Scale
BPRS: Brief Psychotic Rating Scale
CADSS: Clinician-Administered Dissociative States Scale
CoCo: Cognitive Complexity (subscale of BIS-11)
COG: Cognitive Symptoms (subscale of BDI)
CoIn: Cognitive Instability (subscale of BIS-11)
CSD: Current Source Density
CSER: Complexity via State-space Entropy Rate
CTL: Control Group
CUDIT: Cannabis Use Disorders Identification Test
DBS: Deep Brain Stimulation
DLPFC: Dorsolateral Prefrontal Cortex
DMN: Default Mode Network
DSM-5: Diagnostic and Statistical Manual of Mental Disorders, Fifth Edition
DUDIT: Drug Use Disorders Identification Test
EC: Eyes Closed
ECN: Executive Control Network
EEG: Electroencephalography
E/I: Excitatory/Inhibitory Balance
EN: Executive Network
EO: Eyes Open
ER: Early Responders
ERP: Event-Related Potential
ERSP: Event-Related Spectral Perturbation
FDR: False Discovery Rate
FFT: Fast Fourier Transform
FIR: Finite Impulse Response
fMRI: Functional Magnetic Resonance Imaging
FTND: Fagerstrom Test for Nicotine Dependence
FRACT: Fractal Component
GLMM: Generalized Linear Mixed Model
GRCS: Gaming-related Cognition Scale
hBDI: individuals with high scores on the Beck Depression Inventory
HMS: Hood Mysticism Scale
ICA: Independent Component Analysis
IGDS9-SF: Internet Gaming Disorder Scale-Short Form
IGT: Iowa Gambling Task
IRASA: Irregular-Resampling Auto-Spectral Analysis
LPP: Late Positive Potential
LR: Late Responders
LTP: Long-Term Potentiation
LZc: Lempel-Ziv complexity
MADRS: Montgomery–Åsberg Depression Rating Scale
MDD: Major Depressive Disorder
MGT: Monetary Gambling Task
MI: Modulation Index
mIGT: Modified Iowa Gambling Task
Mot_Imp: Motor Impulsivity (subscale of BIS-11)
MRS: Magnetic Resonance Spectroscopy
NMDA receptors: N-methyl-D-aspartate receptors
No_Plan_Imp: Non-Planning Impulsivity (subscale of BIS-11)
ORIG: Original Spectral Component
OSCIL: Pure Oscillatory Component
PAC: Phase-Amplitude Coupling
PE: Points Earned (BART)
PET - Positron Emission Tomography
PFC: Prefrontal Cortex
PING: Pyramidal Interneuron Network Gamma
PLE: Power Law Exponent
PLEhf: Power Law Exponent high frequencies
PLEhf: Power Law Exponent low frequencies
REM: Rapid Eye Movement
RTS: Risk-Taking Score (BART).
SOGS: South Oaks Gambling Screen
SN: Salience Network
SNRI: Serotonin-Norepinephrine Reuptake Inhibitor
SOM: Somatic Symptoms (subscale of BDI)
PSD: Power Spectral Density
SSRI: Selective Serotonin Reuptake Inhibitor
STAI: State-Trait Anxiety Inventory
STAI-I: State Anxiety (subscale of STAI)
STAI-II: Trait Anxiety (subscale of STAI)
SUDs: Substance Use Disorders
tACS: Transcranial Alternating Current Stimulation
TMS: Transcranial Magnetic Stimulation
TRD: Treatment-Resistant Depression
TR-BP: Treatment-Resistant Bipolar Disorder
UDP: User Datagram Protocol
vmPFC: Ventromedial Prefrontal Cortex
WCST: Wisconsin Card Sorting Test

# Acknowledgment

I would like to express my sincere gratitude to Professor Simone Rossi for his invaluable guidance and mentorship throughout my doctoral studies. His unwavering support and dedication to this research project have been instrumental in its success.

I am also deeply grateful to Professor Lice Ghilardi for welcoming me into her laboratory during my research period at the CUNY School of Medicine and for her indispensable contributions to this work. Additionally, I extend my heartfelt thanks to Professor Elisa Tatti for imparting her extensive knowledge and expertise in EEG and neural activity and for her kind and supportive presence during my time in New York City.

My appreciation also goes to my colleagues at SibinLab—Alberto, Francesco, Carmelo, Francesco, and Adriano—and to Claudio and Giovanni at the Department of Psychiatry in Siena. I am grateful to have shared this scientific and personal growth journey with such talented individuals.

Finally, I would like to thank my family for their unwavering support and encouragement, and I thank Giacomo for being there just as he is. Their belief in me has been essential to reaching each of my milestones, and I am profoundly grateful for their presence at every step of this journey.